**Zeitschrift:** IABSE congress report = Rapport du congrès AIPC = IVBH Kongressbericht

**Band:** 2 (1936)

**Rubrik:** VIII. Research concerning building ground

# VIII

# Research concerning building ground.

## Baugrundforschung.

## Etude des terrains.

Leere Seite
Blank page
Page vide

# VIII 1

# Soil Studies for the Storstrøm Bridge, Denmark.

## Bodenuntersuchungen für den Bau der Storstrøm-Brücke in Dänemark.

## L'auscultation du terrain pour la construction du pont Storstrøm, Danemark.

A. E. Bretting,
Chief Engineer, Christiani & Nielsen, Copenhagen.

*Introduction.*

In this paper are to be mentioned the soil studies carried out in connection with the construction of the Storstrømsbridge, Denmark, built in the years 1933—37 for the Danish State Railways.

The substructure now nearly completed has been carried out by Messrs. Christiani & Nielsen, Copenhagen. Messrs. Dorman, Long & Co., Middlesbrough, England, have carried out the superstructure.

The Storstrømsbridge will carry a single track railway, an automobile road and a foot-path over the Sound "Storstrømmen", thus providing a connection between the islands of Zealand and Falster.

The bridge will be abt. 3200 m long and have 51 piers. In "Storstrømmen" the average depth of water is abt. 8 m; the piers are generally founded at a depth of 2—3 m below bottom, directly on clay. Maximum foundation depth at level + 16 m.

The soil consists of glacial clay of varying consistency, under which the chalk is found in greater depths as seen on the longitudinal section. Fig. 1.

On account of the great number of piers and the relatively small variations in the depth of water in the bridgeline it has been possible to standardize the methods of construction for the greater part of the piers.

Where the clay on which the piers are founded, is of sufficient resistance. the pit was pumped dry, and the foundation slab and the pier shaft concreted in the ordinary way. Where the bottom was weaker the foundation slab was concreted under water, whereupon the water was pumped out, and the pier shaft concreted in the dry.

Only the first method of construction will here be discussed in details, as it imposed the greatest stresses on the clay of the bottom and on the steel sheet piling which served as a cofferdam for the lower part of the pit. Further this

method has been of special interest on account of the rapid execution of the work (one pier generally completed up to level + 3 m in less than a month) and the possibility of measuring during the execution of the work the stresses set up in the steel sheet piling.

This method has heretofore been employed for 24 piers and without exception with satisfactory results.

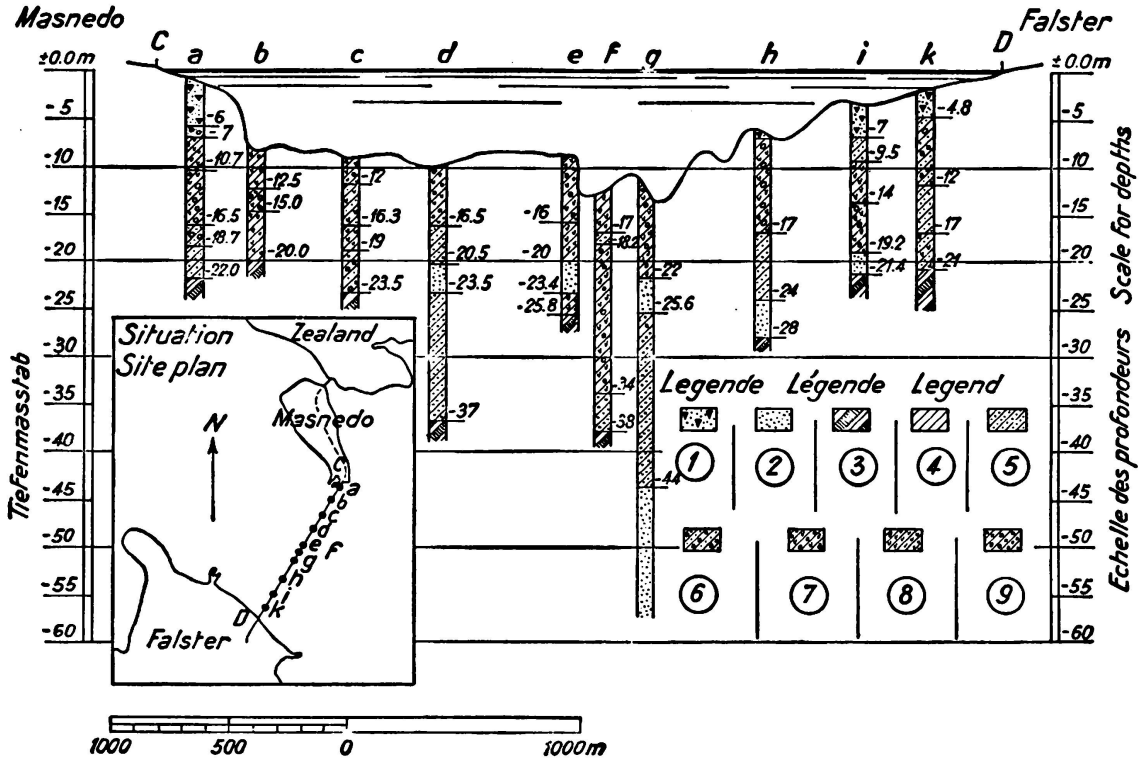


Fig. 1.

Geological Section.
1) mud.
2) sand and gravel.
3) chalk.
4) clay.
5) clay w. sand.
6) clay with sand and stones.
7) clay with limestone and stones.
8) clay with limestone.
9) clay with stones.

Fig. 2 shows how a floating ring-shaped steel cofferdam, a so-called unit, is used for the upper part of the pit. The unit has been towed to the site of the pier in question and lowered by means of water ballast on short wooden piles driven in advance along the contour of the unit.

The outside wall of the unit corresponds to the elliptical contour of the foundation slab. A steel sheet piling has been hung in advance along the outer circumference of the unit, and this sheet piling is driven under water by means of a Mac Kiernan Terry hammer till the upper end of it is just above the lower edge of the unit. The wedge shaped joint between the outside of the unit and the steel sheet piling is tightened by means of a continuous hemp rope, water is pumped out, the joint automatically tightening itself, sometimes helped by divers, and the bottom is laid dry so that excavation of the foundation can take

place. During excavation one had the opportunity to check the stresses in the steel sheet piling and the resistance of the clay in the bottom of the pit.

No bracing at all was employed. The unit itself was designed to take the entire water pressure on its outside and also the reaction from the top of the steel sheet piling.

The lower end of the piling was solely supported on the clay bottom.

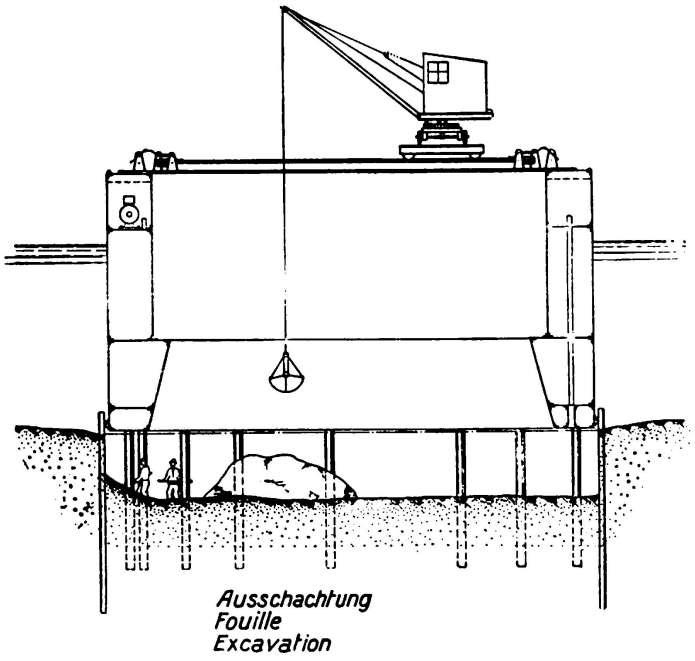


Fig. 2.

Foundation by use of Unit.

When the excavation was finished the foundation slab was concreted against the steel sheet piling, which remained in the pier as a protection against scour.

The inside wall of the unit served as a form for the bottom part of the pier shaft, which was concreted only up to 3 m below water level. When the concrete had hardened the unit was removed and re-employed for another pier of the same type.

That part of the pier shaft which was between 3 m below water and 3 m above water was constructed on a slipway as a reinforced concrete caisson, without bottom, covered with granite ashlar on the outside.

This caisson was lowered in the water by a carriage running on the slipway and suspended between two barges and thus towed to the pier site and lowered in exact position. Previously an asphaltic tightening material had been placed on the top of the pier at level + 3 m; the water could immediately thereafter be pumped out and the caisson filled with concrete.

The upper part of the pier shaft was concreted in the normal way inside steel forms.

The statical conditions of the sheet piling were as described above extraordinarily clear, especially as the deflection of the sheeting caused an open joint

to be formed on the outside between the piling and the clay, so that the water pressure must at the time of failure be reckoned to act right down to the bottom end of the sheeting.

This condition was considered at the breaking limit of the structure, and the steel sheet piling was designed to resist this water pressure, including a certain margin to allow for high water conditions, at stresses near the yield point of the steel.

The resistance of the clay could of course not be ascertained with so much accuracy as that of the steel sheet piling and a factor of safety of abt. 1,5, therefore, was introduced in the values found for the shearing strength of the clay on the basis of laboratory tests with the cone-apparatus described below.

*Borings and Sampling Operations.*

Before the type of foundation was decided upon and the steel sheet piling was designed more than a hundred borings were made at the site of the piers and several samples of the soil were taken at each boring for testing in the laboratory.

The boring operations themselves were executed in the ordinary manner as wash borings from a large barge carrying a set of boring apparatus at each end, so that two borings were made at the same time.

A detailed record of all the boring operations were made, stating the boring velocity under different conditions, exact depth of samples taken etc.

In order to get the samples, which were taken at short intervals, as undisturbed as possible a special hydraulic clay sampler was designed. Fig. 4 shows this clay sampler in details, while the general arrangement for the sampling operations is seen on Fig. 3.

The clay sampler is designed to take samples of abt 48 mm diameter.

It consists of a steel cutting tube lined with a thin brass tube in which the sample is introduced during the operations. This cutting tube is connected to a piston moving in a cylinder of abt. 76 mm inside diameter. In the centre of the cylinder is a fixed guiding rod ending in a bottom plug, which acts as a piston in the brass tube, when this tube, together with the steel cutting tube and the main piston, is moved downwards in the cylinder by means of water pressure acting on the upper side of the main piston. The water under the main piston will escape through the centre bore in the guiding rod.

To operate the sampler it is connected to pressure pipes as shown on Fig. 5, screwed tight together by means of conical threads, and lowered in the casing tube seen on Fig. 3, with piston locked in its top position and the lower end of the cutting tube flush with the bottom plug, until this reaches the bottom. Soft material left on the bottom is thus displaced.

Then a clamping piece is bolted on to the pressure pipe and connected to the loading beams bolted to the casing tube. These beams are loaded by sand boxes or pig iron supplying the reaction to the pressure needed for the cutting out of the sample.

Now water from the pressure pump is led through the pipe into the cylinder and causes the piston to move so that the cutting tube will penetrate into the ground and cut out a sample of clay.

When the piston reaches its bottom position, which is observed on the manometer of the pump by a sudden increase in the pressure, the piston is automati-

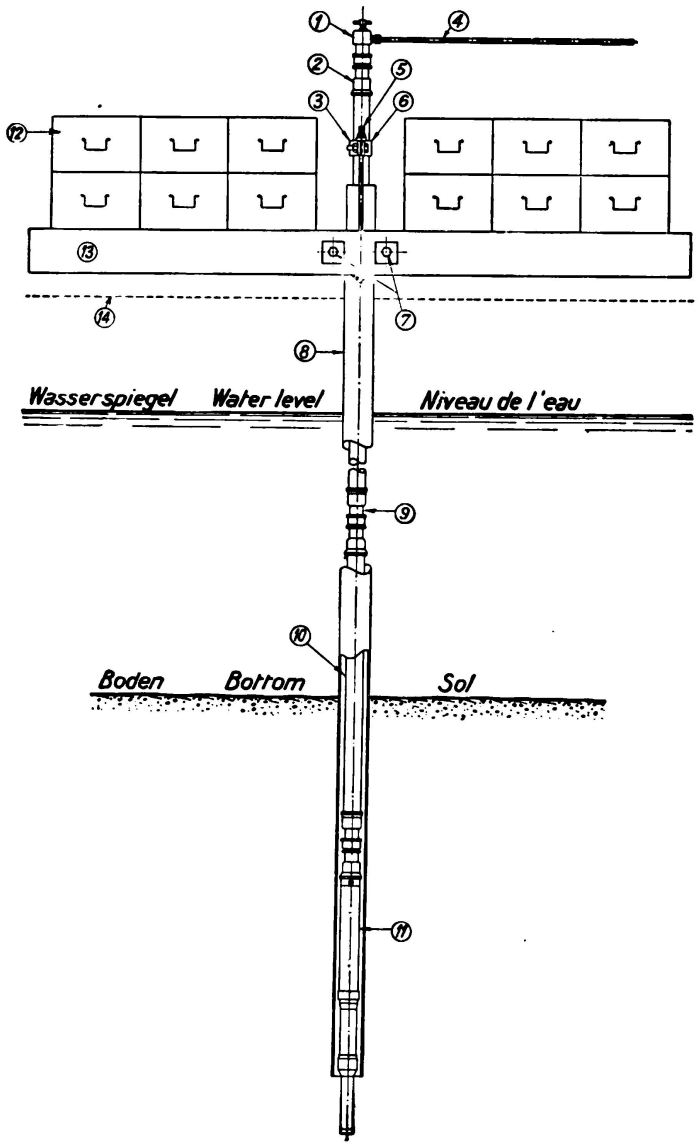


Fig. 3.

Sampling operation with hydraulic clay sampler.

1) Cap with air valve.
2) socket.
3) clamping piece.
4) from force pump.
5) 2 — 5/8" bolts.
6) 2 — 3/4" bolts.
7) 2 — 1" bolts.
8) casing pipe.
9) coupling.
10) hydraulic pressure pipe.
11) hydraulic clay sampler.
12) sand boxes (or pig iron).
13) loading beams.
14) floor level of barge.

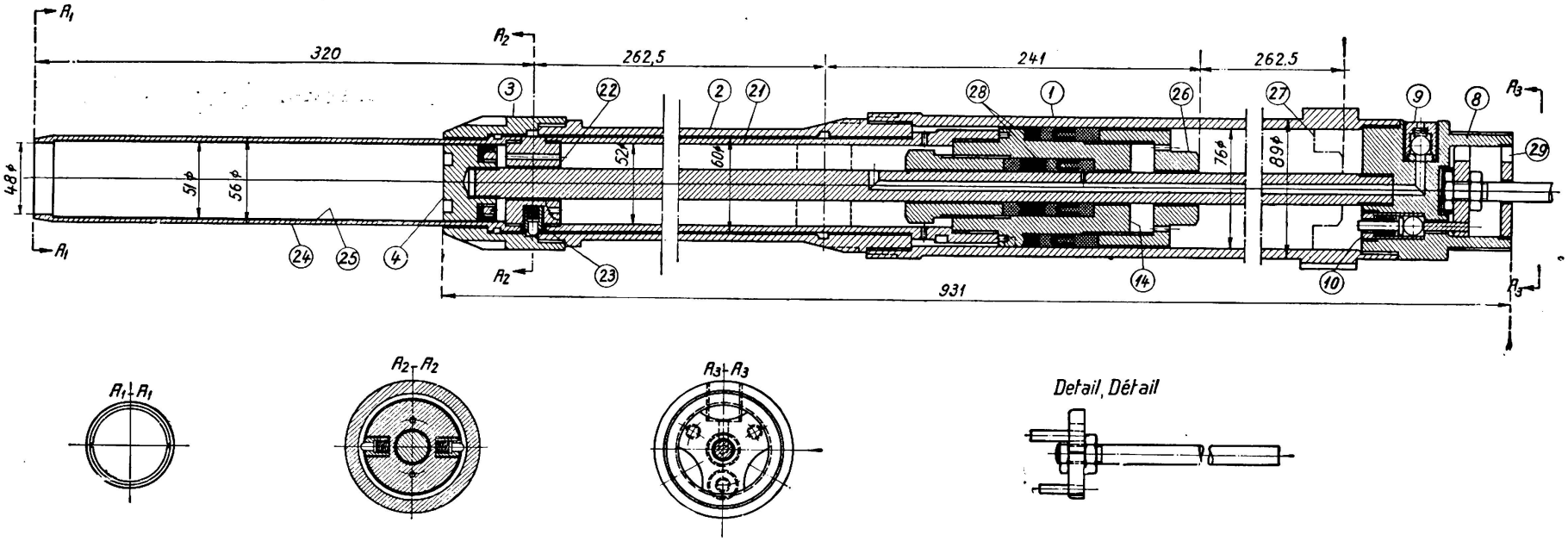


Fig. 4.

Hydraulic clay sampler.

Hydraulic clay sampler, Detail.

Note: Piston shown in bottom position.

Explanations:

1) Main cylinder.
2) Cylinder extension.
3) Screw cap.
4) Central tightening plug.
8) Cylinder head.
9) Escape valve.
10) Non-return valve.
14) Piston top.
21) Force piston body.
22) Piston bottom.
23) Spring loaded lockingbolts.
24) Clay sample cutting tube.
25) Detachable clay sample container.
26) Hexagonal head.
27) Top position of piston.
28) Hemp packings.
29) Entrance for pressure water.

cally locked in its position and the sampler is lifted to the deck of the barge, the screw cap is removed and the tube containing the sample detached.

The consistency of the sample is determined immediately on the site by means of a simple cone-apparatus called spring-scale-cone, whereafter the brass-tube is sealed with caps and adhesive tape at both ends and sent to the laboratory for further testing.

The clay sampler is designed for a normal working pressure of max. 50 atm. corresponding to a total pressure on the cutting tube of abt. 2 ts.

It was found that the samples taken by this device were considerably less disturbed than samples taken by instruments of more simple design, intended to be driven into the ground by blows with a hammer.

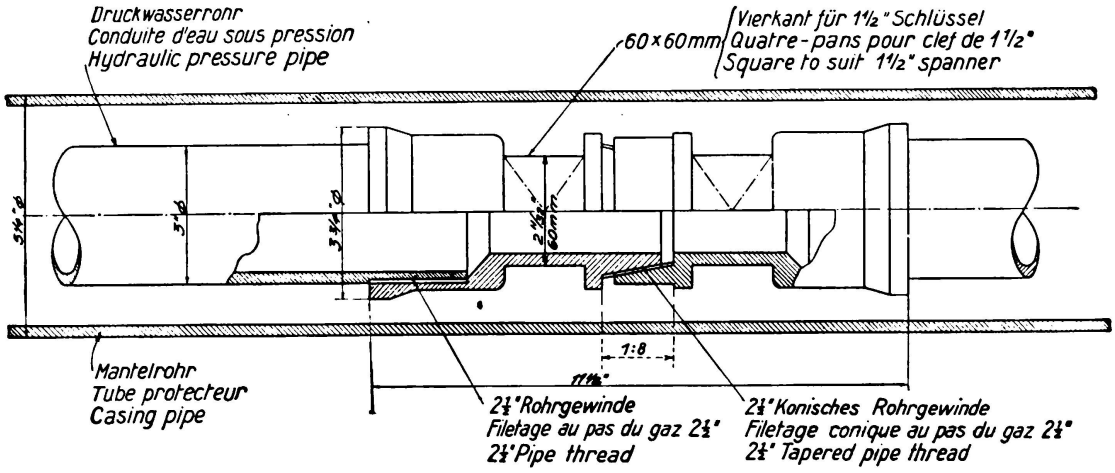


Fig. 5.

Joint in hydraulic pressure pipe.

*Laboratory Test.*

The samples were tested by the author at the Structural Research Laboratory, Royal Technical College, Copenhagen.

In the laboratory were made the ordinary tests of water content, plasticity, shrinkage and liquid limit, specific gravity, granulometric composition, compressibility, permeability, and resistance of cylinders. An apparatus for direct shearing test was not available, but some direct shearing tests were made for a check at the "Laboratorium für Schiffbau und Wasserbau" in Berlin.

The main tests of the consistence of the samples were made by a cone-apparatus devised by the author in 1930, as will be described in detail below.

Further all samples were examined geologically by Mrs. E. L. Mertz of the Danish Geological Survey.

The clay at Storstrømmen is a glacial boulder clay with a considerable content of chalk, as much as abt. 50%.

At greater depths is often found diluvial clay and diluvial sand with varying content of clay. These diluvial strata are less resistant than the boulder clay and are characterized by the extreme sensibility against disturbance.

By remolding of the diluvial clay the resistance generally will be reduced to 15—25% of the resistance of the undisturbed sample.

The water content of the boulder clay ranges from 10—15% of the weight of the dry substance and for the diluvial clay from 18—26%.

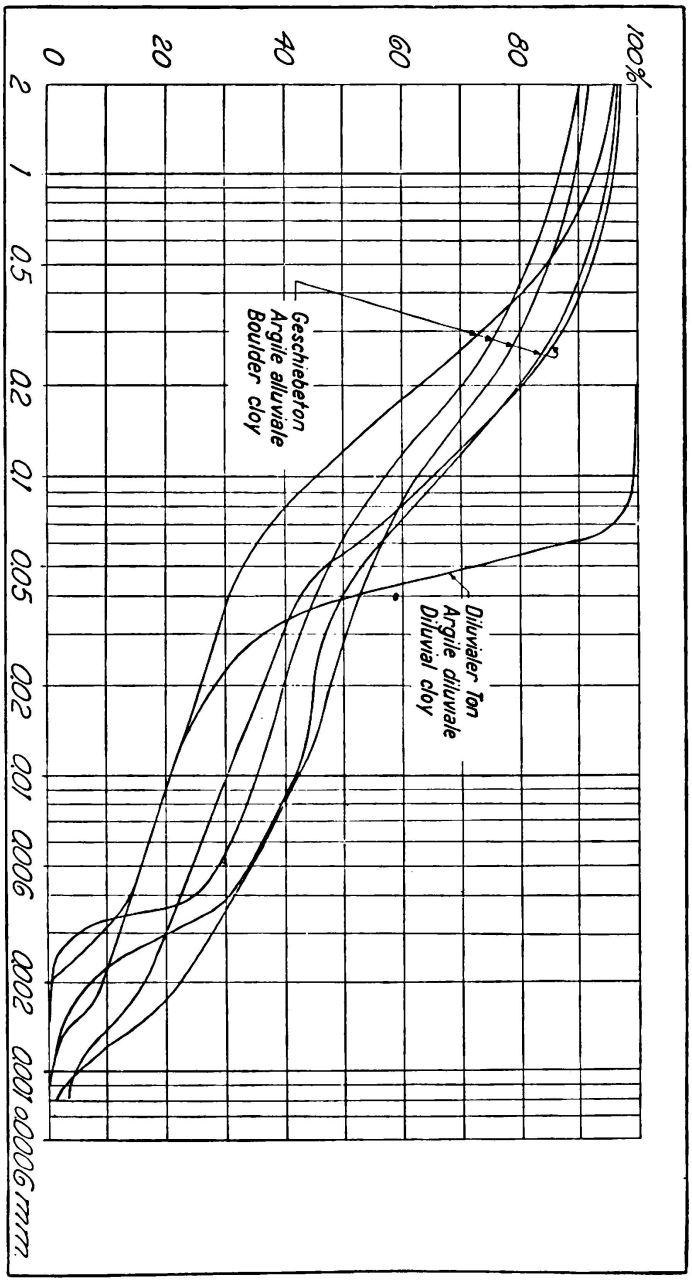


Fig. 6. Some typical grain-size curves.

For boulder clay the shrinkage limit is found at 8—10%,
the plasticity limit at 10—13%, and
the liquid limit at 20—22%.

Characteristic curves of granulometric composition are shown on Fig. 6.

Also a number of compression tests were made. One example is shown on Fig. 7.

On account of the small water content of the boulder clay on which most of

the piers are founded, the settlements of the piers were expected to be very small, which has been confirmed by levelling of some of the piers.

The cone-apparatus employed for testing the consistency of the clay is shown on Figs. 8 and 9.

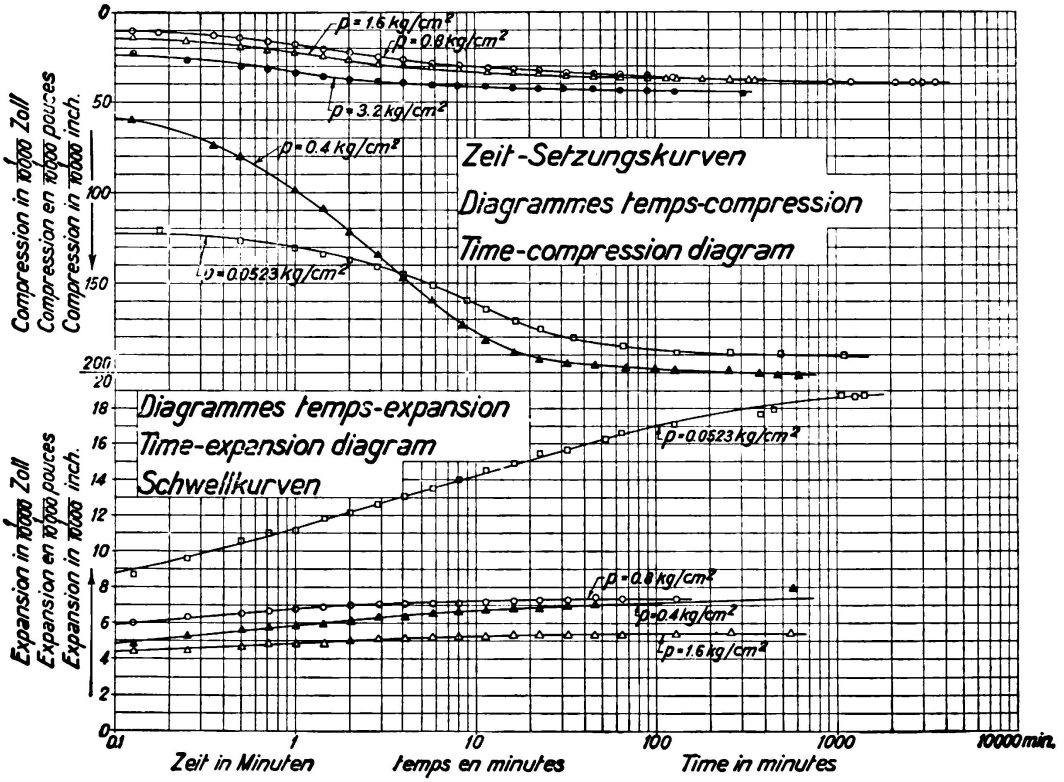


Fig. 7.

Time-compression and -expansion diagrams.

The 60° cone fixed on a vertical rod is loaded with various acts of weights, from 0,3 kilos to 12 kilos, and screwed down until the point just touches the surface of the clay.

The brass tube containing the sample is cut with a saw, so that the sample during the testing operation is surrounded by the brass-ring.

The micrometer screw on the top end of the apparatus is adjusted, the cone with its weight released and the penetration measured by the screw.

The test is made with different weights on the cone and several readings for each weight. The average penetrations y in mm are plotted against the weight G on double logarithmic paper, the weights as abscissas and the penetrations as ordinates, as shown on Fig. 10. The results closely approximate a straight line, and for the same type of clay the inclination of this line against the axis is found to be nearly constant.

The consistency K of the clay is defined as the weight of the cone which gives a penetration of 10 mm.

The results follow the law

$$G = K \cdot \left(\frac{y}{10}^{n}\right)$$

For the boulder clay of Storstrømmen n is on an average = 1,75. The consistency K can be expressed as

$$K = G \cdot \left(\frac{10}{y}\right)^{1,75}.$$

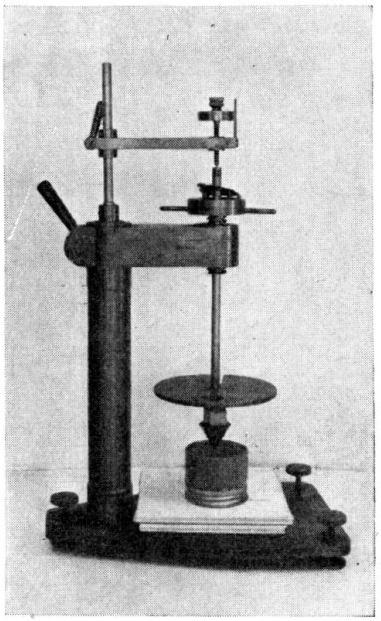

Fig. 8.
Cone test apparatus (Photo).

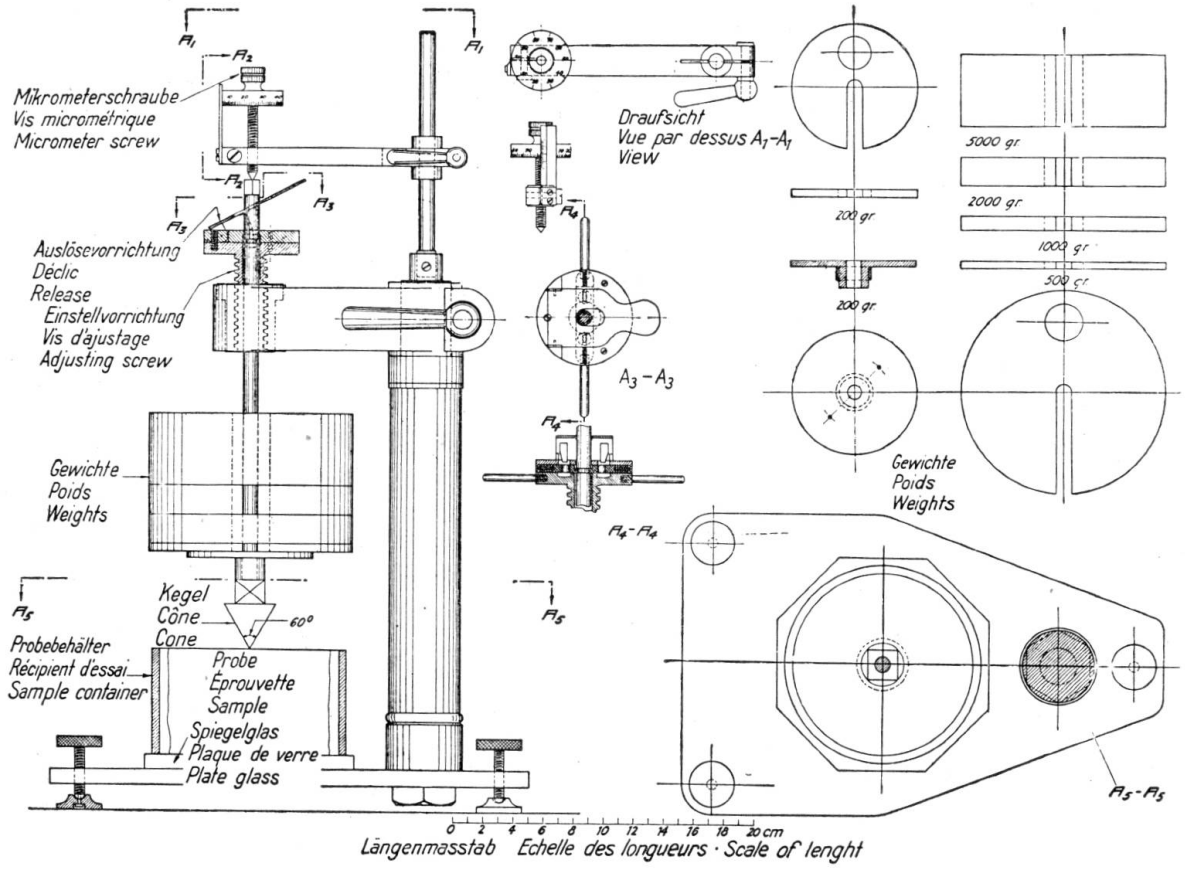


Fig. 9.
Cone test apparatus. Details.

The advantage of this apparatus is that the great weights give penetrations easy to measure with the necessary accuracy, and that errors caused by the existence of small stones in the samples are easily eliminated, when a greater number of observations is taken.

The observations were plotted as shown in a few examples on Fig. 11.

Tests were made with undisturbed clay as well as with remolded clay.

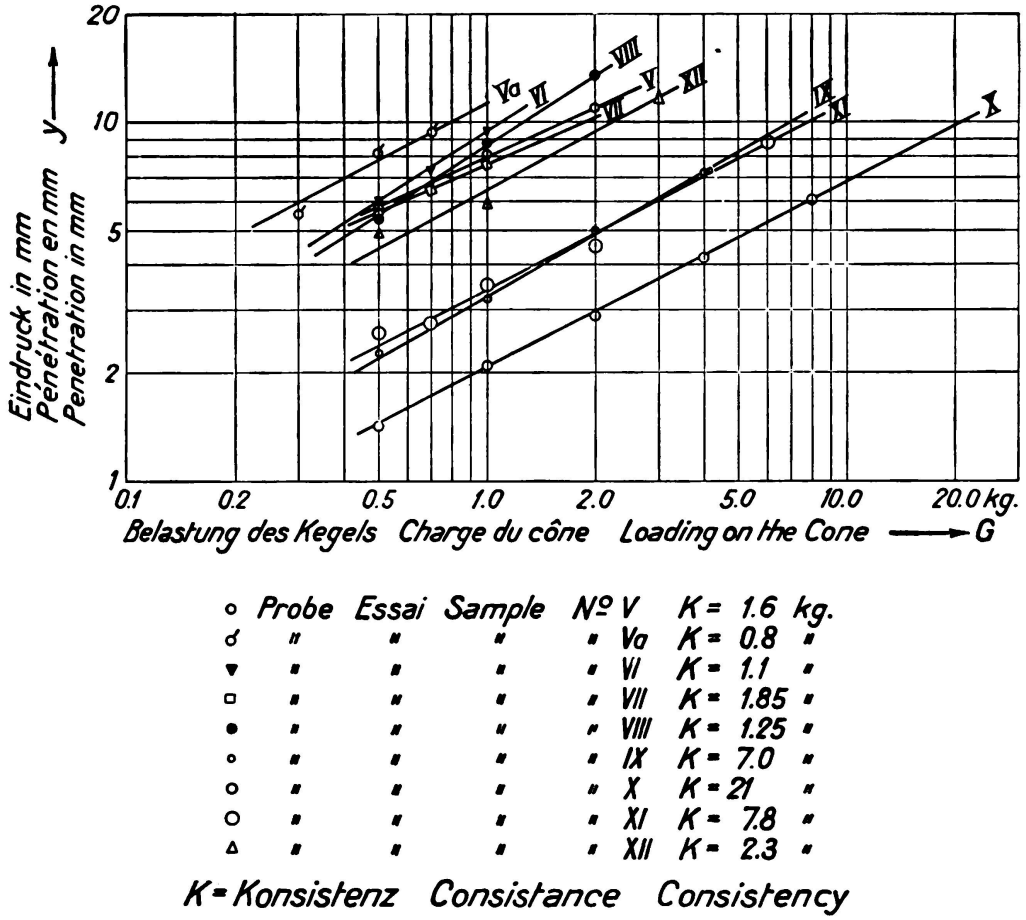


Fig. 10.

Results from tests with cone apparatus.

On the diagrams are further shown the results obtained with the spring-scale-cone on the site. This apparatus is designed by Mr. O. Godskesen, C. E. By comparing the results obtained by the spring-scale-cone with those obtained by the above mentioned cone-apparatus, it was found that the spring-scale-cone on an average gave consistencies abt. 40% higher.

It seems that the samples tested immediately after the extraction had a higher consistency than that found later on by the same method in the laboratory, probably on account of internal swelling.

During the practical execution of the piers the author was, however, not under the impression that the results found in the laboratory were too unfavourable such as was supposed at the start.

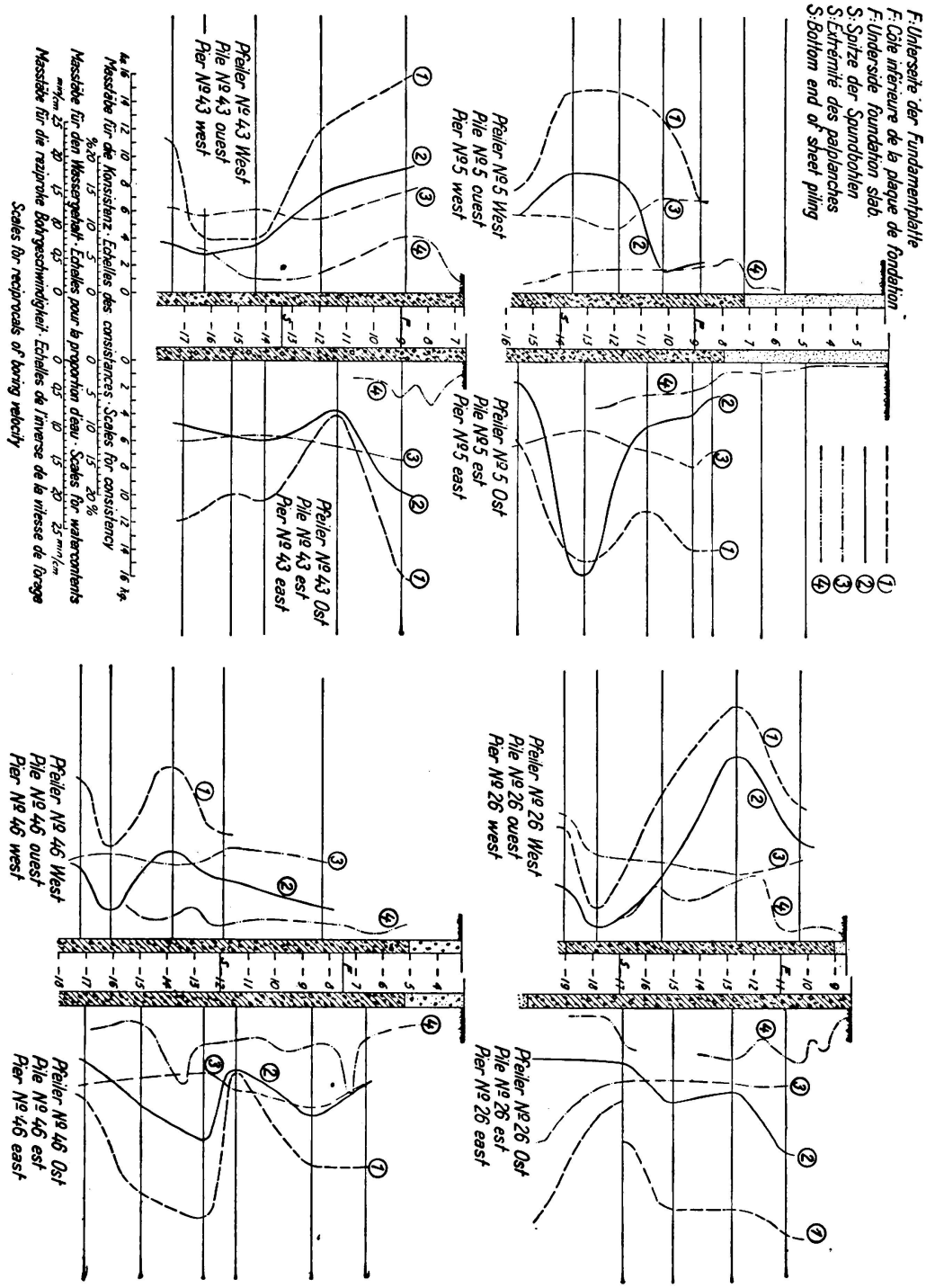


Fig. 11.

Typical consistency diagrams.

1) Consistency determined at the site (Spring scale cone).
2) Consistency determined in the laboratory.
3) Watercontent in per cent of dry substance.
4) Reciprocals of boring velocity.

It therefore seems that a similar swelling must have taken place in the clay of the bottom, when the pit was pumped out and the clay relieved of the water pressure. It appears that the speed of the work was of importance, and that the resistance of the clay decreased when the pit by some reason or other was kept dry longer than usual.

A series of comparative tests was made in the laboratory to determine the relation between the cone-consistency and the cylinder-resistance. The number of these tests can hardly be considered sufficient for this purpose, and further investigations are considered desirable.

The cylinder tests were, however, carried out with a slow increase of the load, so that it must be supposed that the internal friction has been more or less effective.

In the structure, where the pit was kept dry only for a short period, this can hardly have been the case, and it was assumed by the calculations that only the cohesion of the clay determined its resistance, and that internal friction could be neglected.

According to the above mentioned cylinder tests the breaking strength d in kilos/cm$^2$ of the cylinders was found on an average to be about:

$d = 0.5 \cdot K$ (K consistency in kilos).

Neglecting the friction, the shearing strength of the clay ought to be

$e = 0.5 \cdot d$

and consequently

$c = 0.25 \cdot K$.

Practical experience showed, however, that this value of the shearing strength was too high. This can be explained partly by the slow speed of the cylinder tests, and partly by the fact that the clay in the pit probably will be more or less disturbed during the pumping out of the pit.

The deformations of the steel sheet piling were considerable, so that at least the upper part of the clay supporting the wall was disturbed during the pumping out.

Tests with completely remolded samples showed that the consistency was reduced to abt. 45% of the consistency of undisturbed samples.

By the practical calculations the shearing strength of the clay was therefore only taken at

$c = 0.1 \cdot K$,

which value was proved by the check measurements of the sheet piling to be fairly close to the actual resistance.

In the opinion of the author the cone test employed on impermeable clay will express the cohesion of the clay. On account of the great speed of the test the effect of internal friction can be neglected, so that results agreeing with the shearing strength observed in actual practice will be obtained.

The ratio between cohesion and consistency can, however, not be considered constant, but must be determined for each special type of clay.

*Statical Calculation of steel sheet piling.*

A simple method of calculation was sought for determining the necessary driving depth of the steel sheet piling under the foundation level, so that the

shearing resistance of the clay was not exceeded, and for finding the corresponding bending moments in the sheet piles.

According to what is mentioned in the introduction the dimensioning was done under the assumption that the sheet piling was curved inwards just to the bottom end, and that the full water pressure, including a margin of 1 m for high water conditions, was acting from the outside in the full height (fig. 12a).

Under these circumstances the limit of the resistance of the clay must be supposed to be reached, and the bending moments in the sheeting to be a maximum. In the calculations were introduced a shearing resistance (cohesion) $c = 2/3 \cdot 0.1\ K$; a safety factor for the clay of 1.5 was thus intended.

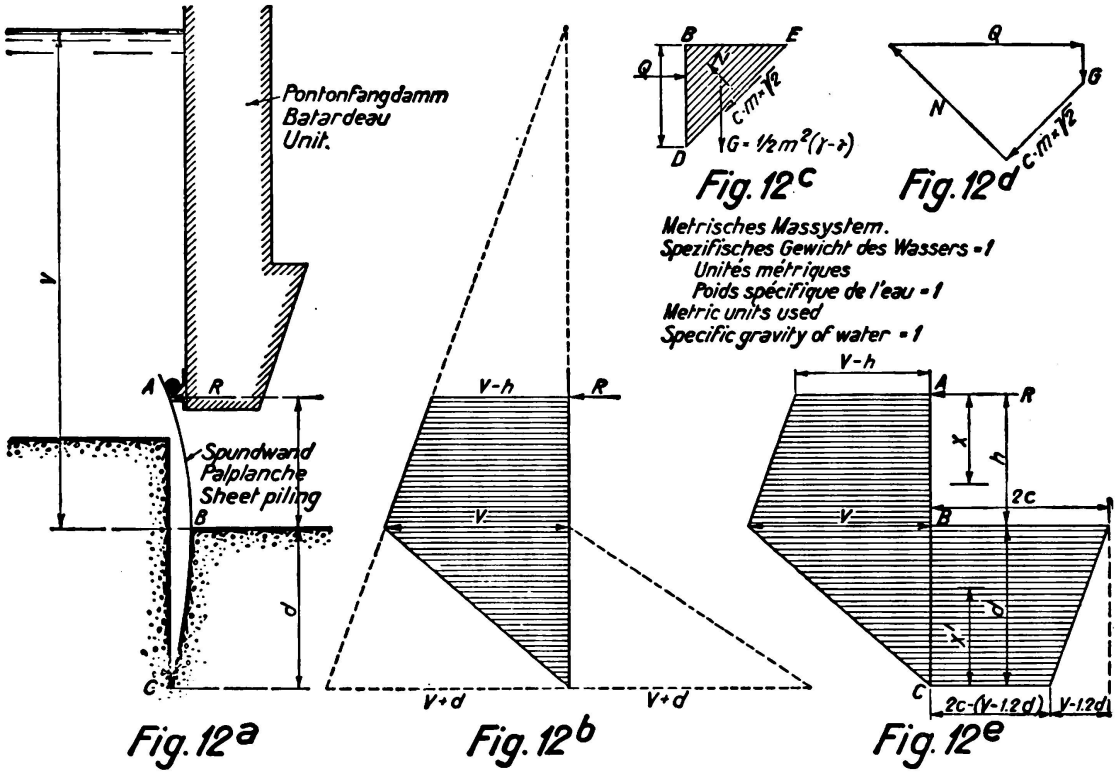


Fig. 12.
Calculation of steel sheet piling.

Inside the sheeting, the water pressure in the voids of the clay must decrease from the full value existing at the bottom end on the outside to zero at the foundation level. For the sake of simplicity this variation is taken according to a straight line, as indicated in Fig. 12b, which shows the pressure exerted on both sides of the wall, and the difference between them.

The gradient of pressure will be:

$$\alpha = \frac{v + d}{d} = 1 + \frac{v}{d}$$

i. e. the interior buoyancy in the clay is equal to the ordinary statical buoyancy multiplied by $\left(1 + \frac{v}{d}\right)$.

Under the resultant water pressure the sheeting will press against the clay. Sliding is supposed to take place along planes of rupture under $45^0$. Considering a sliding wedge, B D E in Fig. 12 c, this is seen to be subjected to the following external forces: The horizontal reaction Q from the sheeting; a vertical force G = weight of wedge minus buoyancy; the cohesion $c\,m\,\sqrt{2}$ acting along the plane of rupture DE and an unknown reaction N perpendicular to the same plane DE.

As the specific gravity $\gamma$ of the clay in the actual state of moisture can be taken as 2.2 (specific gravity of water = 1), it is found that

$$G = \frac{m^2}{2}\left[2.2 - \left(1 + \frac{v}{d}\right)\right] = m^2\left(0.6 - \frac{v}{2d}\right).$$

Fig. 12 d shows the force polygon and by projection on a line parallel to the plane of rupture, it is seen that

$$\frac{Q}{\sqrt{2}} = \frac{m^2}{\sqrt{2}}\left(0.6 - \frac{v}{2d}\right) + cm\sqrt{2}$$

or

$$Q = 2cm + m^2\left(0.6 - \frac{v}{2d}\right).$$

The intensity of the pressure at the depth m is found by derivation:

$$q = \frac{dQ}{dm} = 2c + 2m\left(0.6 - \frac{v}{2d}\right)$$

hence for m = o, q = 2 c and for m = d, q = 2 c − v + 1.2 d.

Fig. 12 e represents the diagram of the resultant loading on the wall.

Taking moments about A:

$$\frac{1}{2}\frac{h^2}{3}(v-h) + \frac{h^2 v}{3} + \frac{1}{3}dv\left(h + \frac{d}{3}\right)$$

$$= 2cd\left(h + \frac{d}{2}\right) - \frac{1}{2}d(v - 1.2d)\left(h + \frac{2}{3}d\right), \text{ which gives}$$

$$c = \frac{v}{2} + \frac{h^2(3v-h) - 1.2d^2(3h+2d)}{6d(2h+d)} \qquad \text{(I)}$$

Projection on an horizontal line:

$$R = h\left(v - \frac{h}{2}\right) - d(2c - v + 0.6d). \qquad \text{(II)}$$

The bending moment at the depth $x \leqq h$ below A is

$$M_x = Rx - (v-h)\frac{x^2}{2} - \frac{1}{6}x^3 \text{ which is a maximum for}$$

$$x_0 = -(v-h) \pm \sqrt{(v-h)^2 + 2R} \text{ provided } x_0 \leqq h, \qquad \text{(III)}$$

in which case

$$M_{max} = R\,x_0 - (v-h)\frac{x_0^2}{2} - \frac{1}{6}x_0^3 \qquad \text{(IV)}$$

The bending moment at a distance $x' \leqq$ above C is found

$M'_x = -0.2\,x'^3 + x'^2\left(c - \frac{v}{2} + 0.6\,d\right)$ which is a maximum for

$$x'_0 = \frac{1}{0.3}\left(c - \frac{v}{2} + 0.6\,d\right), \text{ provided } x'_0 \leqq d. \tag{V}$$

This gives

$$M'_{max} = 0.1\,x'^3_0. \tag{VI}$$

The latter formula is to be used when $x'_0 \leqq d$ and this condition will be fulfilled when $\left(\frac{d}{h}\right)^3 \geqq 5\left(\frac{v}{h} - \frac{1}{3}\right)$.

The formulae (I)—(VI) may be represented graphically introducing the ratios $\frac{d}{h}, \frac{c}{h}, \frac{R}{h^2}, \frac{x_0}{h}$ and $\frac{M_{max}}{h^3}$ thus writing the formulae:

$$\frac{c}{h} = \frac{1}{2}\left(\frac{v}{h}\right) + \frac{3\left(\frac{v}{h}\right) - 1 - 1.2\left(\frac{d}{h}\right)^2\left[3 + 2\left(\frac{d}{h}\right)\right]}{6\left(\frac{d}{h}\right)\cdot\left[2 + \left(\frac{d}{h}\right)\right]} \tag{Ia}$$

$\left(\frac{c}{h}\right)$ rectilinear with $\left(\frac{v}{h}\right)$ for $\left(\frac{d}{h}\right)$ = constant.

$$\frac{R}{h^2} = \frac{v}{h} - \frac{1}{2} - \frac{d}{h}\left(2\frac{c}{h} - \frac{v}{h} + 0.6\,\frac{d}{h}\right) \tag{IIa}$$

$\frac{R}{h^2}$ rectilinear with $\frac{v}{h}$ for $\frac{d}{h}$ = constant.

For $\frac{x_0}{h} \leqq 1$ i. e. for $\left(\frac{d}{h}\right)^3 \leqq 5\left(\frac{v}{h} - \frac{1}{3}\right)$:

$$\frac{x_0}{h} = -\left(\frac{v}{h} - 1\right) + \sqrt{\left(\frac{v}{h} - 1\right)^2 + 2\frac{R}{h^2}} \tag{IIIa}$$

$$\frac{M_{max}}{h^3} = \frac{R}{h^2}\frac{x_0}{h} - \frac{1}{2}\left(\frac{v}{h} - 1\right)\left(\frac{x_0}{h}\right)^2 - \frac{1}{6}\left(\frac{x_0}{h}\right)^3 \tag{IVa}$$

For $\frac{x'_0}{h} \leqq \frac{d}{h}$ i. e. for $\left(\frac{d}{h}\right)^3 \geqq 5\left(\frac{v}{h} - \frac{1}{3}\right)$

$$\frac{x'_0}{h} = \frac{1}{0.3}\left(\frac{c}{h} - \frac{1}{2}\frac{v}{h} + 0.6\,\frac{d}{h}\right) \tag{Va}$$

Rectilinear for $\frac{d}{h}$ = constant.

$$\frac{M'_{max}}{h^3} = 0.1\left(\frac{x'_0}{h}\right)^3. \tag{VIa}$$

In Fig. 13 are plotted the curves or lines expressed by the formulae $I^a$—$VI^a$.

These curves have been used for designing the sheet piling for the various piers.

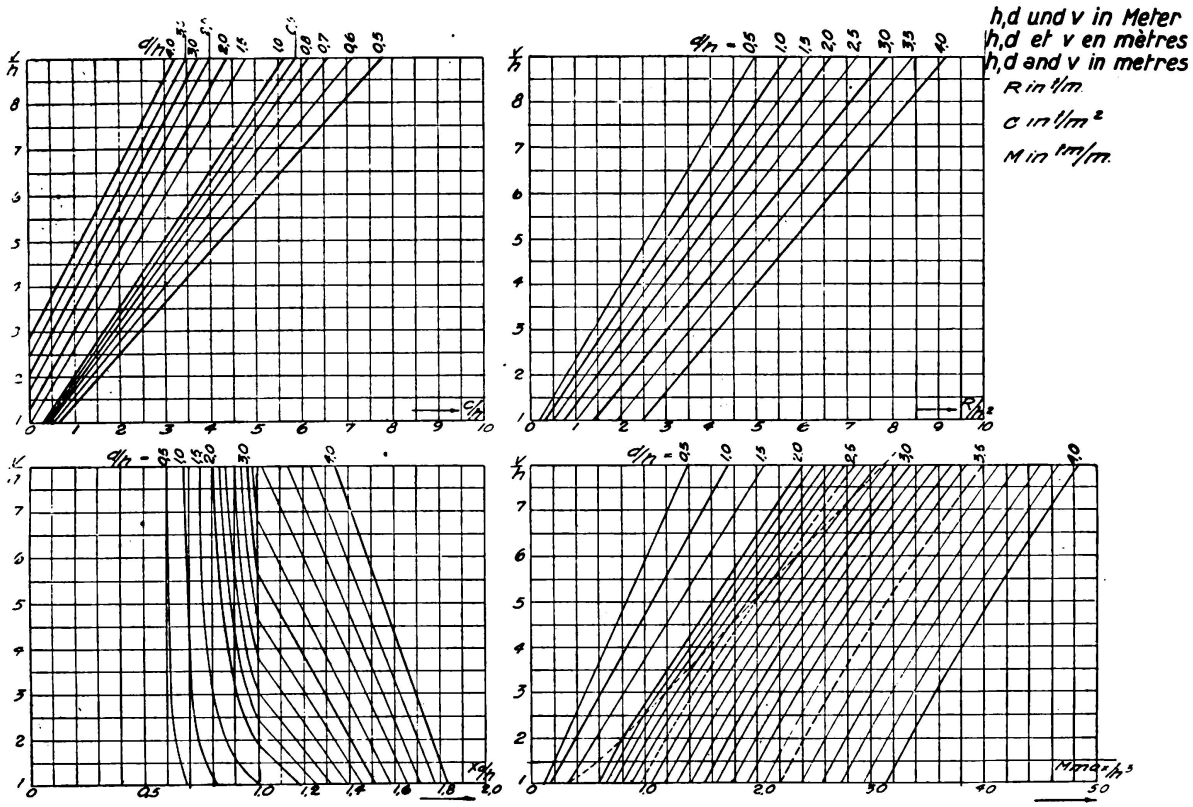


Fig. 13.
Diagram for design of steel sheet piling.

*Measurement of Actual Stresses in Steel Sheet Piling.*

The cross section of the steel sheet piling was in all cases that of Krupp No. III, generally fabricated from ordinary mild steel. Where long piles were needed and the bending moments were high Chromador steel with an ultimate tensile strength of 5800 kg/cm² and a yield point of 3600/cm² was employed.

During the excavation of the pit the bending stresses were ascertained to get an idea of the exactitude of the assumptions made regarding the resistance of the clay and the basis upon which the statical calculations were made.

As some of the sheet piles might be bent during driving, it would have been useless to employ gauge lines laid out on the piles before driving.

As an expedient the curvature of a great number of the piles was measured and the mean value of these curvatures was assumed to express the stresses produced by water pressure etc.

Further the inclinations of the piles were measured by a clinometer.

The apparatus employed is illustrated on Fig. 14, which probably is self-explanatory. When held against a pile the gauge dial will show the rise f of the pile on a length L equal to 1.50 m.

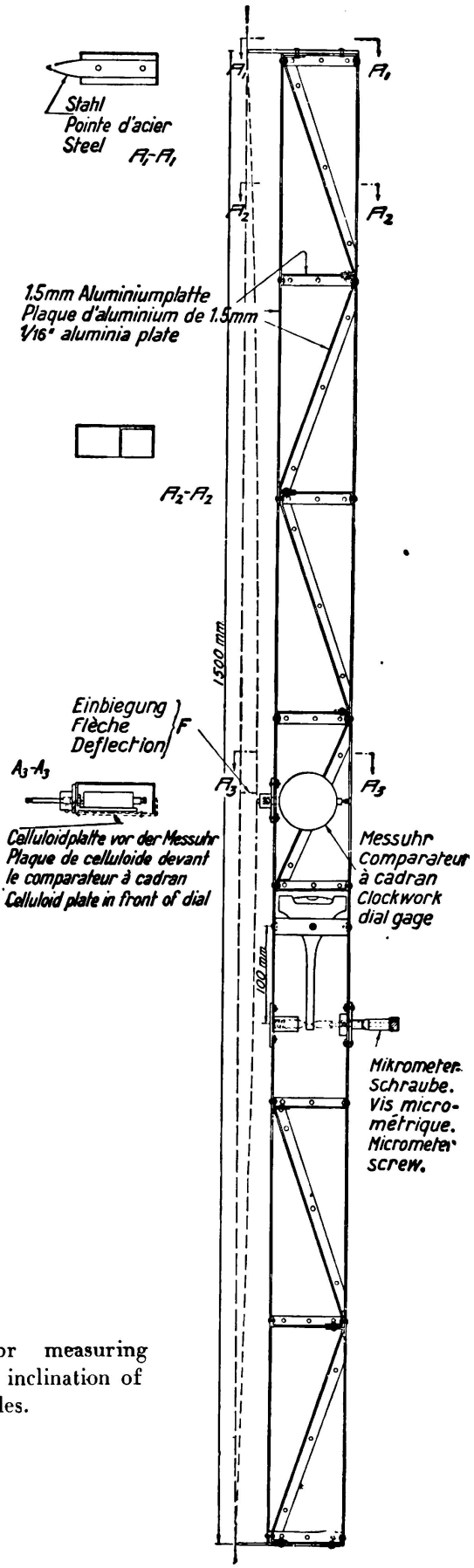


Fig. 14.

Apparatus for measuring curvature and inclination of steel sheet piles.

$$\text{The radius of curvature } \rho = \frac{L^2}{8\,f.}$$

$$\text{The bending moment } \quad M = \frac{EI}{\rho} \text{ where}$$

E = elastic modulus and I = moment of inertia.

Substituting the values for L, E and I and eliminating $\rho$, we find $M = 12.8 \cdot f$, where M is expressed in tm and f in mm.

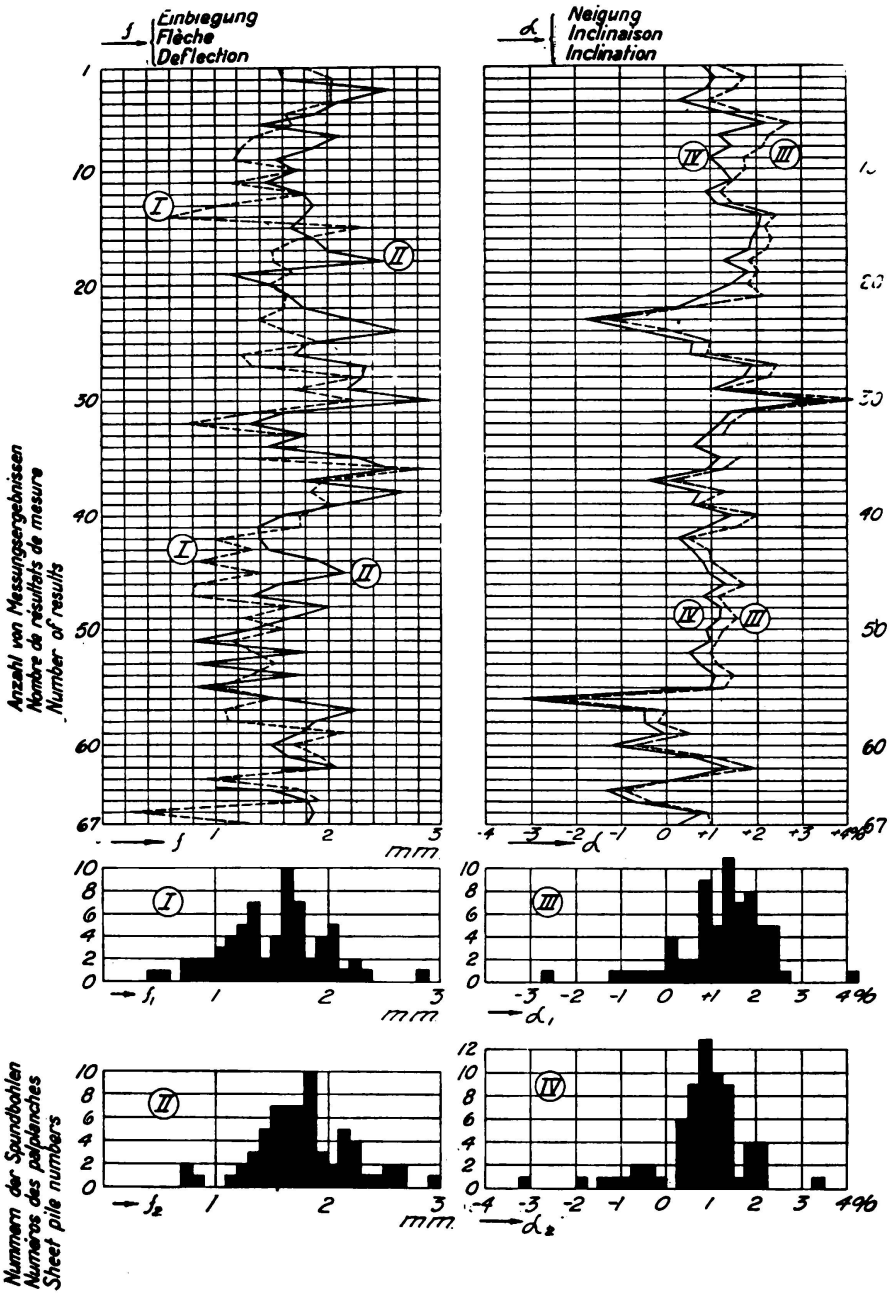


Fig. 15.

Results from check measurements in pier Nr. 39.

I and III are results from measurings betwn. El. — 6.90 m and El. — 8.40 m.

II and IV are results from measurings betwn. El. — 7.65 m and El. — 9.15 m.

The results of a complete observation are shown on Fig. 15. Even in case the individual observations deviate considerably from each other, it is thought that the average will give a fairly good idea of the stresses in the sheet piles.

| PIER Nº PFEILER Nº | PART OF SHEET PILING CHECKED. MESSUNGSSTELLEN | | DATE DATUM. | TOTAL LENGTH OF SHEET PILES TOTALE LÄNGE DER SPUNDBOHLEN | MATERIAL | MEAN CONSISTENCY MITTELKONSISTENZ. | THEORETICAL STRESSES THEORETISCHE SPANNUNGEN. $\sigma_{max}$ | $\sigma_2$ AT POINT OF MEASUREMENT $\sigma_2$ IM PUNKTE DER MESSUNGEN | OBSERVED STRESS BEOBACHTETE SPANNUNG $\sigma_2$ |
|---|---|---|---|---|---|---|---|---|---|
| 13 | Total circumference. | Jedes Doppeleisen | 11-5-34 | 8.5 | Mild Steel | 5.0 Kg. | 1815 Kg/cm² | 1700 Kg/cm² | 1880 Kg/cm² |
| 39 | " " " " | | 12-6-34 | 7.5 " | " | 10.7 " | 1960 " | 1900 " | 1600 " |
| 9 | " " " " | | 27-6-34 | 7.5 " | " | 7.2 " | 1600 " | 1590 " | 2080 " |
| 14 | " " " " | | 10-8-34 | 8.5 " | " | 6.3 " | 2050 " | 1970 " | 2340 " |
| 8 | " " " " | | 10-9-34 | 11.0 " | Chromador. | 5.6 " | 2860 " | 2660 " | 2290 " |
| 5 | Eastern half. | Östliche Hälfte | 26-10-34 | 8.5 " | Mild Steel | 8.8 " | 1650 " | " | 1450 " |
| | Western half. | Westliche " | 27-10-34 | | | 6.1 " | | 1640 " | 1510 " |
| 40 | Every other double pile | Jedes zweite Doppeleisen | 26-11-34 | 7.0 " | " " | 8.2 " | 910 " | 890 " | 830 " |
| 7 | Western half. | Westliche Hälfte. | 21-12-34 | 12.0 " | Chromador. | 3.5 " | 3610 " | 3150 " | 2110 " |
| 43 | " " " " | | 21-12-34 | 8.0 " | Mild Steel | 7.5 " | 1520 " | 1500 " | 1720 " |
| 26 | Northwestern half. | Nordwestliche Hälfte | 27-2-35 | 9.5 " | " " | 6.1 " | 2340 " | 2250 " | 2290 " |
| 42 | " " two thirds | 2/3 d. Umfanges N.W. | 23-3-35 | 9.5 " | " " | 5.0 " | 2050 " | 1950 " | 1440 " |
| 17 | Western half | Westliche Hälfte. | 27-4-35 | 10.0 " | " " | 6.1 " | 2670 " | 2550 " | 1030 " |
| 41 | " " " " | | 3-5-35 | 12.0 " | Chromador. | 2.6 " | 3390 " | 2760 " | 1290 " |
| 16 | " " " " | | 28-5-35 | 12.0 " | " | 2.7 " | 3700 " | 3250 " | 1080 " |
| 44 | " " " " | | 3-6-35 | 9.0 " | Mild Steel | 5.1 " | 1810 " | 1660 " | 1400 " |
| 11 | " " " " | | 26-6-35 | 11.5 " | Chromador. | 5.9 " | 3260 | 2900 " | 1810 " |
| 46 | " " " " | | 16-7-35 | 8.0 " | Mild Steel | 3.3 " | 1290 | 1270 " | 1480 " |
| 10 | Eastern end | Östliches Ende | 1-8-35 | 12.0 " | Chromador. | 7.3 " | 3590 | 3150 " | 1920 " |
| | Southern side | Südliche Seite | 3-8-35 | | | | | | 1560 " |
| | Northern side | Nördliche Seite | 3-8-35 | | | | | | 1440 " |
| 45 | Western half. | Westliche Hälfte | 8-8-35 | 8.0 " | Mild Steel | 6.8 " | 1390 | 1370 " | 1760 " |
| 25 | Eastern half | Östliche Hälfte | 26-8-35 | 10.0 " | " " | 7.5 " | 2590 | 2420 " | 1910 " |
| 47 | Western half. | Westliche Hälfte | 30-6-35 | 7.5 " | " " | 5.9 " | 1160 | 1150 " | 920 " |
| 49 | " " " " | | 21-9-35 | 9.5 " | " " | 3.8 " | 1770 | 1650 " | 1500 " |
| 37 | Western end. | Westliches Ende. | 12-10-35 | 12.0 " | " " | 4.7 " | 3620 | 3180 " | 2370 " |
| | Eastern end. | Östliches Ende. | 19-10-35 | | | 3.0 " | | | 2150 " |
| 48 | Western half. | Westliche Hälfte. | 17-10-35 | 10.5 | " " | 3.2 " | 2220 | 1940 " | 1440 " |

Fig. 16.

Schedule of check measurements.

All the results from the 24 piers where measurements have been taken are compiled in the table below (Fig. 16).

It should be noted that the theoretical $\sigma_{max}$ and the corresponding $\sigma_2$ at the point where measurements were taken are worked out with the correct water pressure but under the same conditions of support as was employed when calculating the dimensions of the sheeting. As a safety factor of abt. 1.5 has been used in fixing the shearing resistance of the clay it is likely that the bottom end of the sheeting to a certain degree will have been fixed during the measurements and that the assumptions for the calculations will not be quite correct.

As a rule the actual stresses should be expected to be less than the theoretical ones. It would certainly be of interest to figure out more accurately the theoretical stresses under conditions of support more similar to the actual ones, in which case a better accordance would without doubt be found. This can be done without difficulty, and the author has the intention later to carry through such calculations.

It is, however, supposed that the results found will nevertheless be of interest as similar measurements have probably heretofore very seldom been carried out.

In some cases the stresses found by the check measurements were considerably lower than expected. This, of course, may be explained thereby that the bottom conditions were really better than supposed on the basis of the laboratory tests, but it may be mentioned that some of the piers where this has taken place had unusually long sheet piles, and the excavation at the same time was carried out with extraordinary speed, for which reason the plastic deformation of the clay had hardly had time to reach their maximum value. In several cases the author received the impression that the stresses ran higher when the work was, for some reason or other, extended over a longer time.

## Summary.

The standardized method of construction for the foundations of the Storstrømsbridge in Denmark is described.

New hydraulic clay sampler for the extraction of undisturbed samples of the subsoil described.

Method of testing consistency of clay by new cone-apparatus described. Consistency in kilos K, weight of cone G in kilos, penetration of cone y in mm depend on equation

$$K = G \cdot \left(\frac{10}{y}\right)^n.$$

For clay of Storstrømmen $n = 1.75$.

The cone consistency of fat clays is thought to express the cohesion of the soil without regard to the internal friction.

For the clay in question practical experience makes probable the following relation:

$c = 0.1 \cdot K$ (c in kg/cm², K in kg).

Statical calculation of steel sheet piling is explained. The clay is supposed to be frictionless during the short period where pit was laid dry. Diagrams for finding driving depth and maximum moments of steel sheet piling established.

Measurement of actual stresses in sheet piling carried out during excavation of pit.

Results compared with theoretical stresses.

# VIII 2

## Subsidence in Bridge Constructions on the German State Arterial Roads.

## Setzungsbeobachtungen an Brückenbauten der Reichsautobahnen.

## Observations d'affaissement sur les ouvrages d'art du réseau allemand d'autostrades.

Dr. Ing. L. Casagrande,*
Berlin.

*I. Introduction.*

Early recognising the importance of examining the character of the soil, the General Inspector of the German highways board, soon after taking up his post, ordered that the soil was to be rested with respect to its carrying capacity according to the most modern views of earthwork mechanics, before any new sections of the state motorcar highways were started. In the course of 1934, each of the separate head offices entrusted with the work of constructing the state motorcar highways received its own testing station for the purpose not only of investigating the condition of the ground under the highways, but also of allowing, from suitable tests of the soil conditions under the intended structures, a decision to be made regarding the most suitable type of foundations or bridge systems. Accordingly, the soil testing stations are equipped with apparatus which allow the compressibility and permeability of soil samples in their original state to be determined, and consequently the probable amount of settling to be expected. Apart from the convenience of being able to form an approximate idea of the magnitude of the probable settling, the purpose of such an investigation of the soil, in consequence of the great number of works of all kinds which are to be erected in the future for the state motorcar highways on similar soil, consisted mainly in:

1. classifying the upper strata in the whole of Germany, with regard to its carrying capacity and compressibility,
2. checking the theory of settling used in calculations, by comparing the theoretical settling with the settling actually occurring,
3. the possibility of obtaining greater economy when designing new bridge structures.

The second and third points depend closely on each other, since the obtaining of greater economy in construction is necessarily conditioned by the figures used when calculating the amount of settling.

* Vocabulary for illustration texts at end of article.

The engineers and geologists employed in the soil testing stations of the state motorcar highways have had only slight opportunity to attend courses on "earthwork mechanics" in their student days, since hitherto only a few technical colleges include this subject in their curriculum. This circumstance, also the great difficulty in obtaining assistants, and last but not least the speed at which the work had to be carried out, make it easy to understand that the investigations on settling for the works hitherto completed are to a certain extent incomplete. In spite of that,

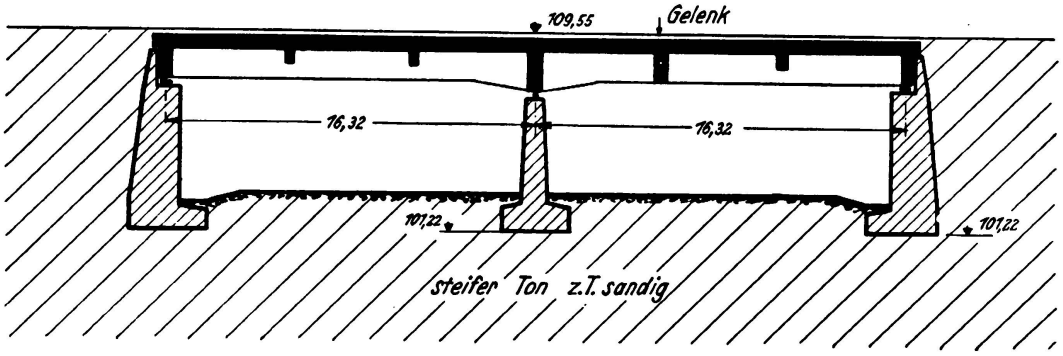


Fig. 1.

the amount of information now available has already allowed interesting conclusions to be drawn, and the purpose of the present report is to mention them and to evaluate them.

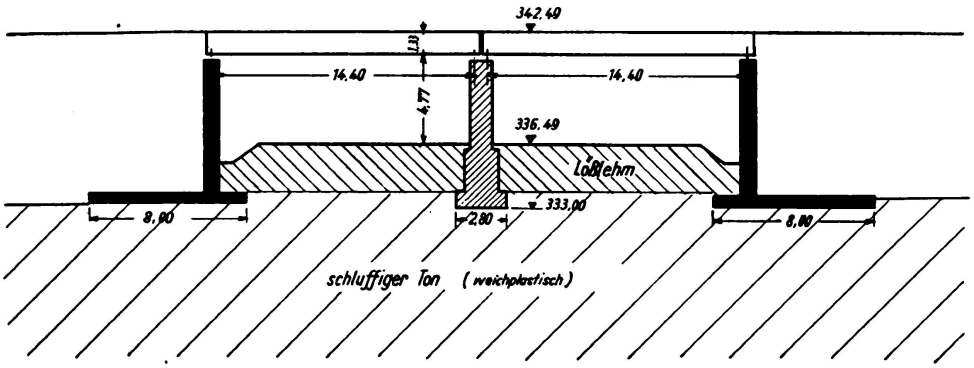


Fig. 2.

## *II. Theory of the prediction of the amount of settling through pure compression of the subsoil.*

Compactness of a soil is conditioned by its porosity. It is thereby assumed that the separate particles of the soil and also the water, may be regarded as comparatively incompressible. Reduction of porosity and the squeezing of water out of the voids, go hand in hand. The more permeable the soil, the quicker can the moisture contained in it be expelled, i. e. the quicker will it be compressed by a superimposed load. In the case of sands, this process takes place almost immediately, but in the case of more compact soils (clay, loam, etc.) it may last even for years, depending on the permeability and thickness of the layers. Between the two extremes of sand and compact clay, the number of different kinds of soil is very great and consequently also the number of different rates of settling to be expected.

A further important factor is the degree of compressibility of the soil. Sands possess little compressibility; clays, in consequence of their much greater volume of voids, possess great compressibility. If, therefore, a sand sample and a clay sample are loaded to the same extent, the clay will generally be compressed more than the sand. Thorough investigations have been made by *Terzaghi*[1] concerning the influence of the shape of the particles, as well as of the structure of the ground.

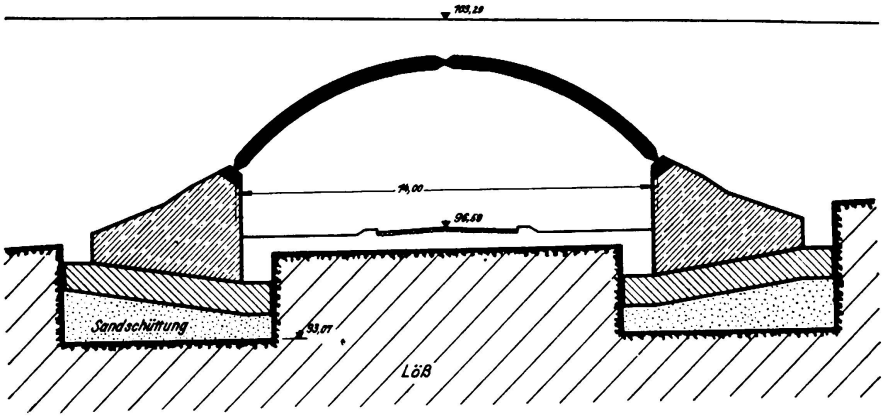


Fig. 3.

The compression test gives answers to two questions:

1. to what degree the soil sample could be compressed under a given load, and
2. at what rate the compression takes place.

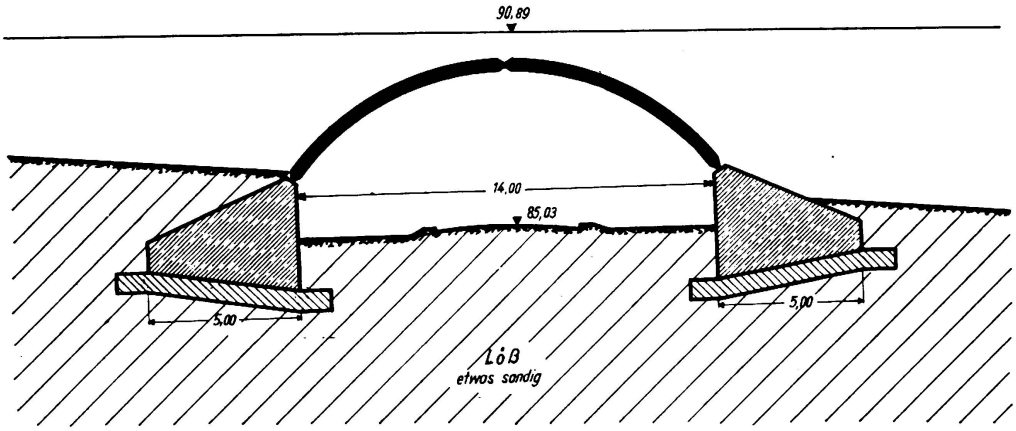


Fig. 4.

It would lead us too far to enter more into detail concerning the question of predicting the amount of settling. *Terzaghi* and *Fröhlich* have dealt thoroughly with the question of compression of clay soils in a recently published work[2], where they give simple formulae and tables for the degree and rate of compression.

[1] *K. v. Terzaghi:* „Erdbaumechanik", Vienna 1925; „Festigkeitseigenschaften der Schüttungen, Sedimente und Gele", *Auerbach* und *Hort*, Handbuch der Mechanik, Vol. IV, Leipzig 1931; „Ingenieurgeologie", *Redlich-Terzaghi-Kampe*, Vienna and Berlin 1929.

[2] *K. v. Terzaghi* and *O. K. Fröhlich:* „Theorie der Setzung von Tonschichten", Leipzig and Vienna 1936.

*III. Observations made on the settling of a number of bridge structures on the German motorcar highways.*

Although, in consequence of the circumstances mentioned above, only a comparatively small number of predictions of settling could be calculated from the laboratory tests carried out on corresponding soil samples, the not yet complete analyses of the settlings show, however, a certain agreement between the calculated

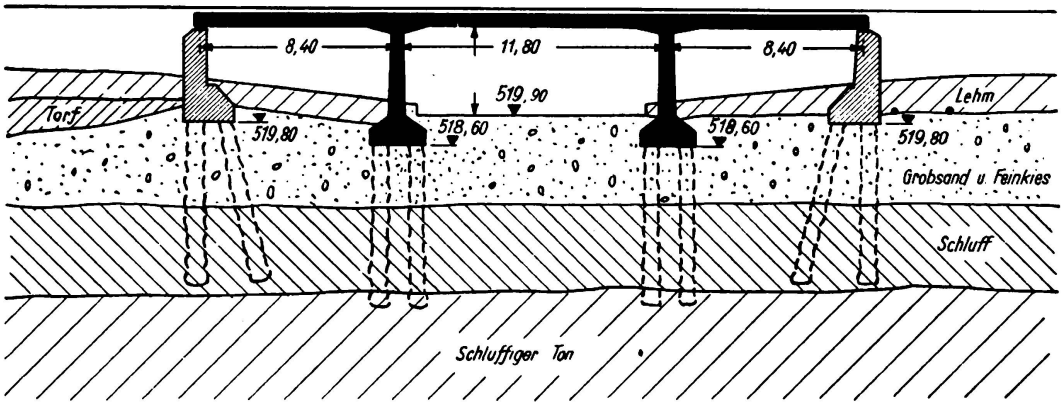


Fig. 5.

and the observed values, which is exact enough for practical purposes. In this connection it is remarkable that the predicted amount of settling based on theory is always greater than the amount actually observed. In some cases the difference attained a maximum of 100%, i. e. instead of 100 mm as calculated, the actual settling was only about 50 mm.

The following examples contain only the most essential data required to allow the examples to be understood and compared. Diagrammatic sectional sketches of structures and subsoil, as well as graphic representations of the measured settlings, have, owing to the space available, been given for only the most interesting cases.

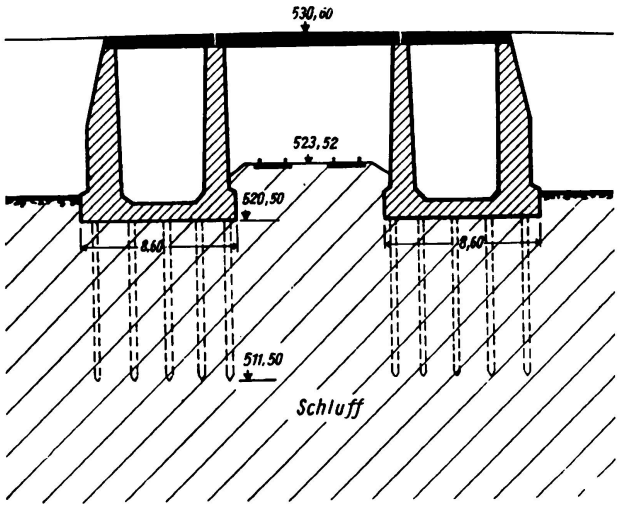


Fig. 6.

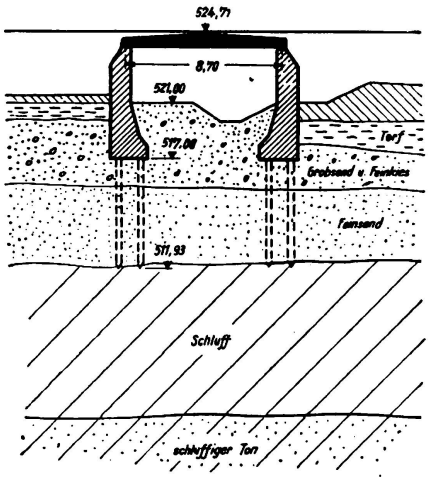


Fig. 7.

1. Work No. 128, km 265.885, Hanover Office. Reinforced concrete two-bay cantilever girder with suspended girders (Fig. 1). Spread footings on deep compact

clay (40% < 0,002 mm, natural water content about 31%), mean foundation pressure 1.4 kg/cm² below abutments and piers. Completed June 1935, settlings in April 1936 were maximum 54 mm for the abutments and 56 mm for the pier. Calculated settling 100—150 mm total. Settling still continues, no damage.

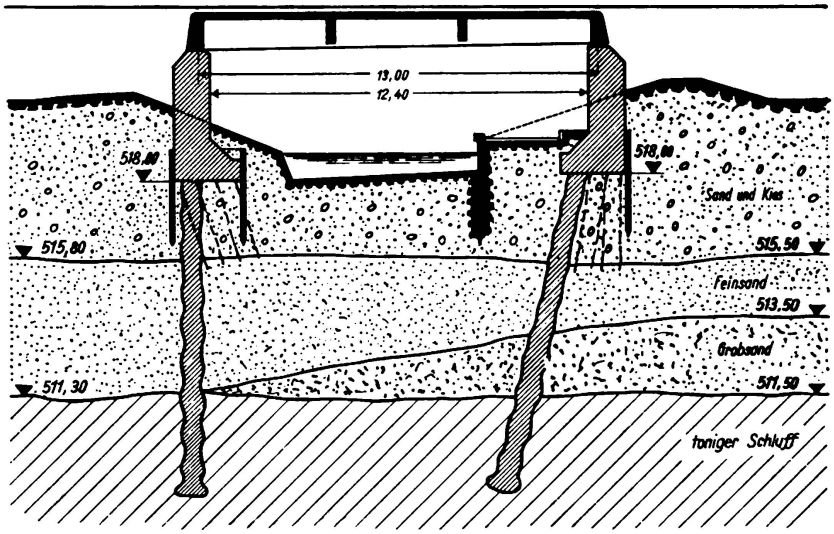


Fig. 8.

2. Work at km 28.5, Cologne Office. Two steel plate continous girders each of 6 bays on reinforced concrete piers, total length 540 m, bay lengths each 45 m. Spread footings on stiff clay up to 6 m thick, under which irregularly deposited beds of gravel and marl, also rock. Completed December 1935, maximum settling of the piers 52 mm, last measurement in March 1936. Settling still continues, no damage.

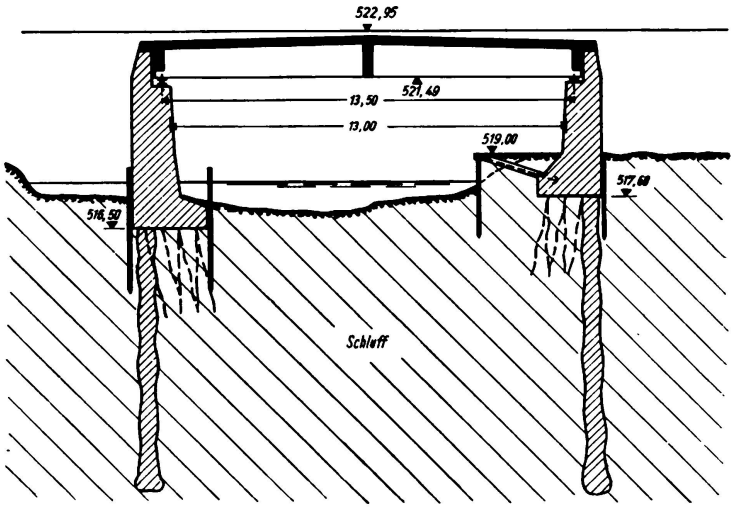


Fig. 9.

3. Work at km 38.982, Dresden Office (Fig. 2). Reinforced concrete deck girders, 2 bays each 14,4 m span. Spread footings on very plastic siltlike clay up to 12 m thick, natural water content 16.0—21.3%, flow limit 29.9—56.3%, rolling limit 15,7—18.8%. Foundation pressure about 1.5 kg/cm² for abutments and 1.0 kg/m² for piers. Completed August 1935. Predicted settlings about 150 mm for abutments and 60 mm for piers, actual settlings about 46 mm for abutments and 25 mm for piers, last measurement August 1935. Settling has stopped, no damage.

4. Work W 26, km 48.425, Halle Office. Fixed arch (vaulted culvert), Spread foundations on soft clayey silt about 1.50 m thick, under which sand. Foundation pressure 2.75 kg/cm². Completed February 1936, predicted settling about 95 mm, actual settling 50 mm. Settling has stopped.

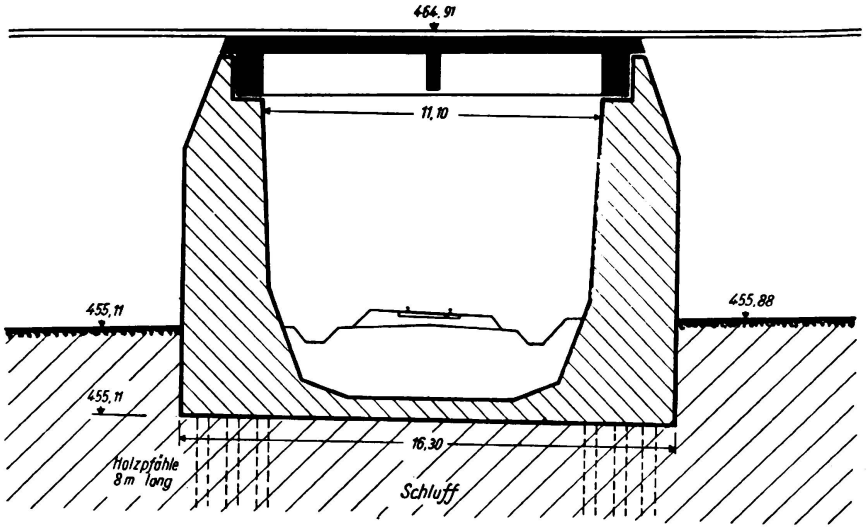


Fig. 10.

5. Work No. W 45a, km 15.135, Halle Office. Closed reinforced concrete frames, spread foundations, foundation pressure about 1.1 kg/cm², subsoil 8—10 m sandy clay, under which sand. Completed November 1935, predicted settling about 220 mm, actual settling 140 mm. Settling still continues, no damage.

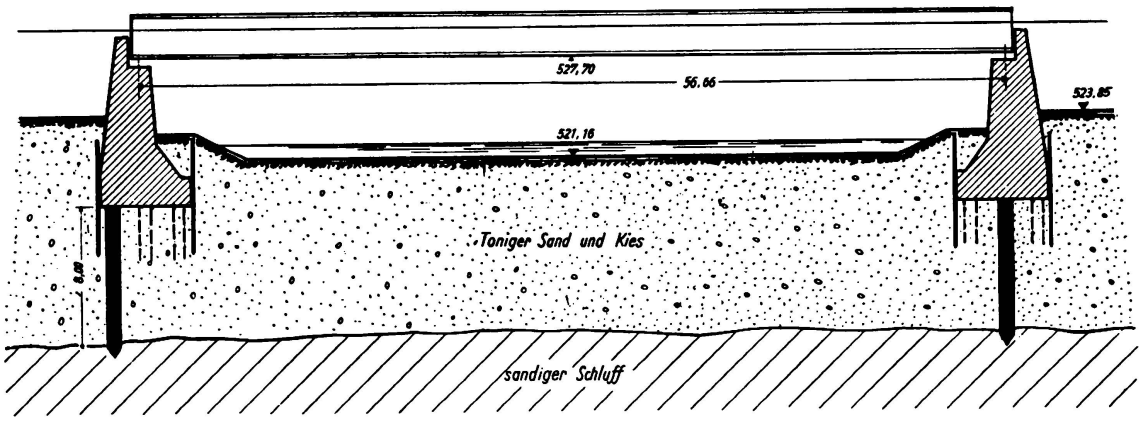


Fig. 11.

6. Work at km 40.584, Stuttgart Office. Vaulted culvert, spread foundations on 1.30 m sand, under which soft clayey silt (valley loam), natural water content 43%, flow limit 54%, rolling limit 31%. Foundation pressure about 1.5 kg/cm². Completed December 1935, actual settling to April 1936 about 280 mm. Settling still continues.

7. Work No. 66, km 89.515, Königsberg Office. Two plate girders, each 16 m span. Spread foundations 1.4 kg/cm² on alternating layers of compact and siltlike clay; compact clay: natural water content 35—37%, flow limit 57—67%, rolling limit 24—26%; siltlike clay: natural water content 25—30%, flow limit 35—38%,

rolling limit 13—23%. Completed July 1935, actual settlings about 35 mm for abutments, 70 mm for piers, last measurement August 1935. Settling still continues.

8. Work No. 228, km 323.030, Hanover Office. Three-hinged arch, 14 m span, spread foundations on deep loess (fig. 24), foundation pressure 2.6 kg/cm², completed June 1935, settling to April 1936 about 40 mm. Settling stopping, no damage (fig. 3).

9. Work No. 229, km 323.538, Hanover Office. Three-hinged arch, 14 m span (fig. 4), foundation pressure 2.6 kg/cm², spread foundations partly on sandy loess. Completed August 1935, settling to April 1936, about 23 mm. Settling stopping, no damage.

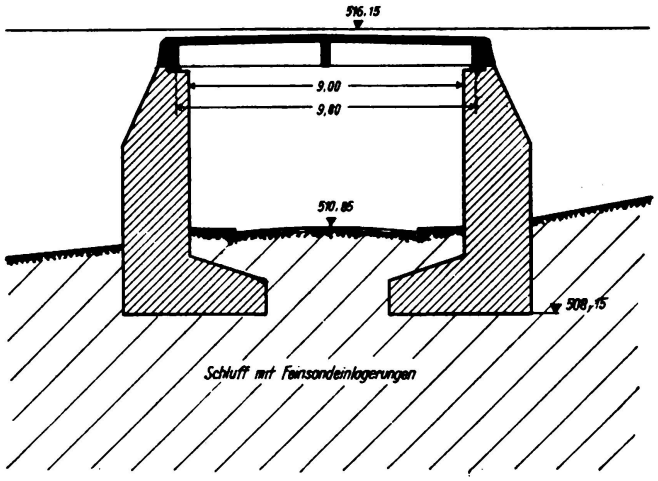


Fig. 12.

10. Work at km 89.255, Munich Office. Reinforced concrete 3-bay deck girder, central bay as Gerber girder, outer spans 8,40 m, inner 11.80 m (fig. 5). Floating pile foundation (Franki piles) about 10 m long, mean foundation pressure 1.1 kg/cm² below abutments, 1.4 kg/cm² below piers. Subsoil coarse sand and fine gravel, under which silt and siltlike clay (fig. 25). Silt: natural water content 33%, flow limit 36%, rolling limit 27%. Siltlike clay: natural water content 32%, flow limit 38%,

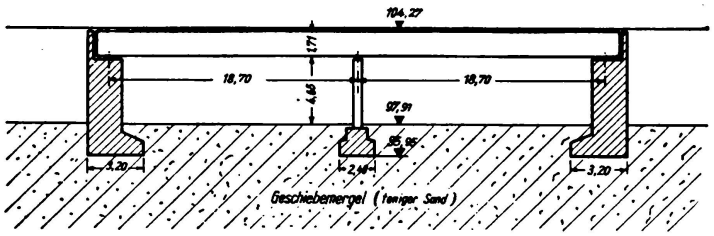


Fig. 13.

rolling limit 27%. Completed December 1935, predicted settling for abutments about 120 mm, for piers 90 mm, actual settlings to April 1936, for abutments about 125 mm, for piers about 60 mm. Settling still continues (fig. 33).

11. Work at km 77.695, Munich Office. Reinforced concrete 3-bay deck girder (fig. 6). Foundation: one abutment and one row of piers each on continous foundation slab, Franki piles 9 m long (floating pile foundation). Foundation pressure at its lowest edge about 1.1 kg/cm², subsoil consists of silt over 40 m deep, natural water content 34—64%, flow limit 35—72%, rolling limit 8—28%, permeability

$3.7 \times 10^{-5}$ to $1.3 \times 10^{-4}$ cm/min. (for distribution of particles see fig. 26). Completed May 1936, predicted settling about 470 mm, actual settling to May 1936 about 500 mm. Settling still continues and damage is apparent (fig. 34).

12. Work at km 89.213, Munich Office (fig. 7). Reinforced concrete slab, 8.70 span, mean foundation pressure about 1.50 kg/cm², subsoil coarse sand and fine

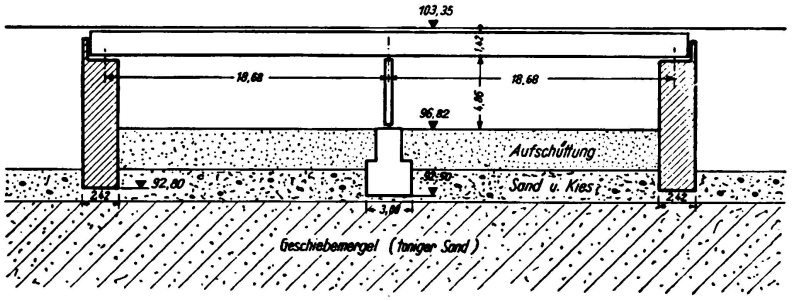


Fig. 14.

gravel, under which fine sand, under which silt and siltlike clay (fig. 27); pile fondations to upper edge of silt. Silt: natural water content 33—36%, flow limit 36%, rolling limit 27%, siltlike clay: natural water content 32%, flow limit 38%, rolling limit 27%. Completed December 1935, predicted settling about 200 mm, actual settling to May 1936 about 150 mm (fig. 35). No damage.

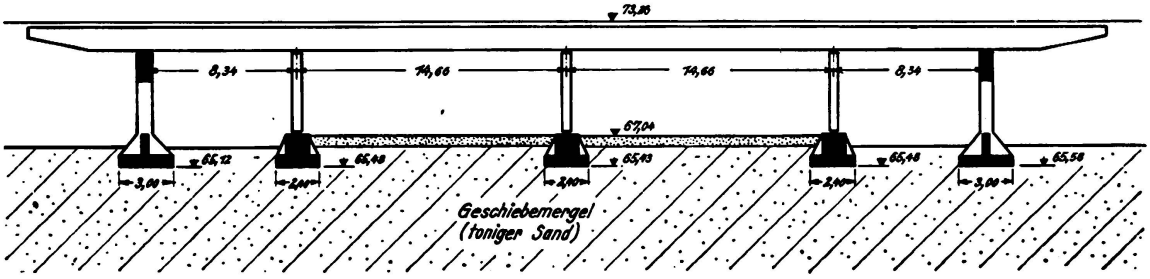


Fig. 15.

13. Work at km 78.246, Munich Office. Reinforced concrete deck girder, 13 m span (fig. 8), pile foundations (Franki) about 10 m long, mean foundation pressure 1.5 kg/cm², subsoil sand and gravel, under which fine and coarse sand, under which

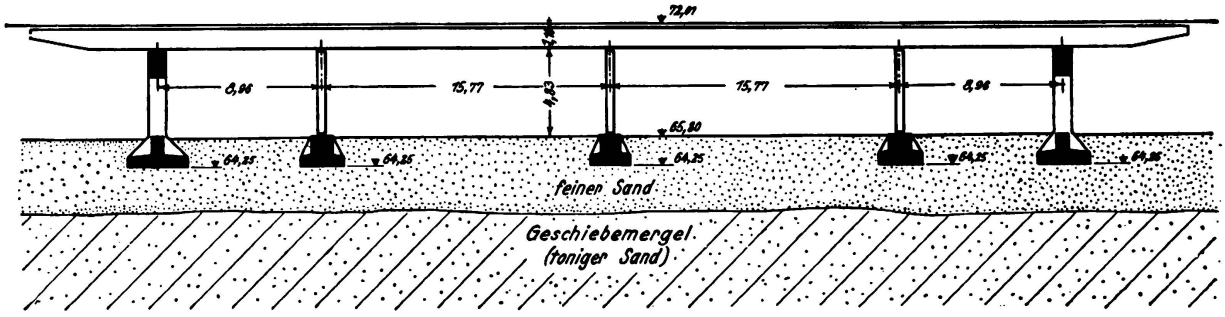


Fig. 16.

clayey silt (fig. 28): natural water content 19—32%, flow limit 31—39%, rolling limit 16—24%, permeability $2.6 \times 10^{-7}$ to $1.1 \times 10^{-6}$ cm/min. Completed August 1935, predicted settling about 250 mm, actual settling to end of March 1936 about 60 mm (fig. 36), no damage.

14. Work at km 86.455, Munich Office. Reinforced concrete deck girder with 13 m span (fig. 9). Abutments on Franki piles about 10 m long, mean foundation pressure 1.3 kg/cm², subsoil silt layers intercalated with fine sand to 20 m depth, under which compact marl (fig. 29). Silt: natural water content 32—54%, flow limit 32—51%, rolling limit 27—38%, permeability $1.1 \times 10^{-6}$ to $4.0 \times 10^{-5}$ cm/min. Completed October 1935, predicted settling about 350 mm, actual settling to May 1936 about 230 mm (fig. 37). Settling still continues, slight backward inclination of abutments (in consequence of embankment filling).

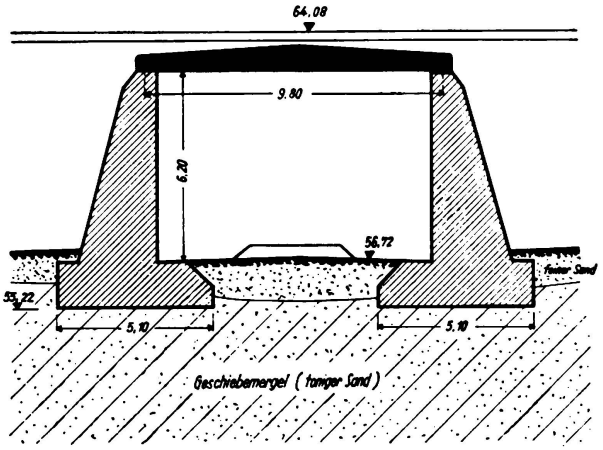


Fig. 17.

15. Work at km 61.863, Munich Office. Reinforced concrete deck girder with 11.1 m span (fig. 10), abutment foundations on common slab, pier foundation with wood piles about 8—11 m long, mean foundation pressure 1.0 kg/cm², subsoil silt with thin veins of sand, depth not ascertainable; silt: natural water content 24—32%, flow limit 30—33%, rolling limit 15—22%, permeability $2 \times 10^{-6}$ cm/min. (for distribution of particles see fig. 30). Completed November 1935, predicted settling about 350 mm, actual settling to May 1936 200 mm (fig. 38), settling still continues, no damage.

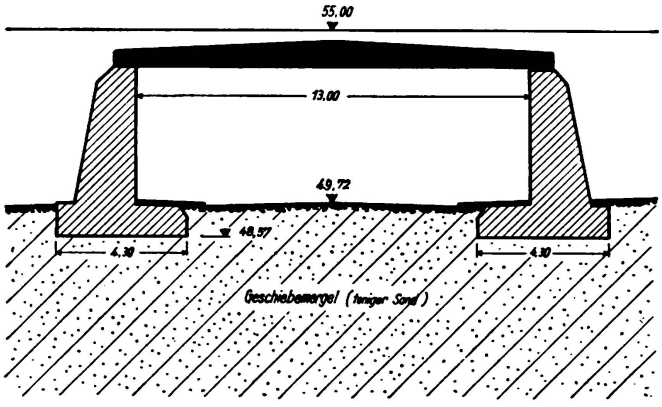


Fig. 18.

16. Work at km 88.695, Munich Office. Plate girder with 56.66 m span (fig. 11). Foundation of the abutments on wood piles about 8 m long, mean foundation pressure 2.0 kg/cm², subsoil clayey sand and gravel, under which sandy silt in parts very soft (fig. 31); natural water content 32—48%, flow limit 23—43%, rolling limit 22—41%, permeability $8 \times 10^{-7}$ to $4 \times 10^{-6}$ cm/min. Completed July 1936,

predicted settling of eastern abutment 900 mm of western abutment 500 mm, actual settlings average 300 mm (fig. 39), settling still continues, abutments have inclined backwards (in consequence of embankment filling).

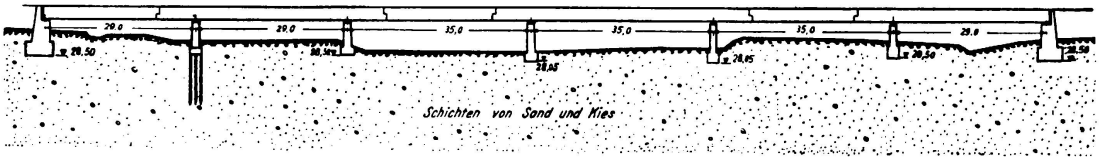


Fig. 19.

17. Work at km 65.179, Munich Office. Reinforced concrete deck girder of 9.80 m span (fig. 12), spread foundations on silt (fig. 32) intercalated with fine sand to a great depth, mean foundation pressure 1.8 kg/cm². Completed July 1935, predicted settling about 350 mm, actual settling 280 mm to May 1936 (fig. 40), sett-

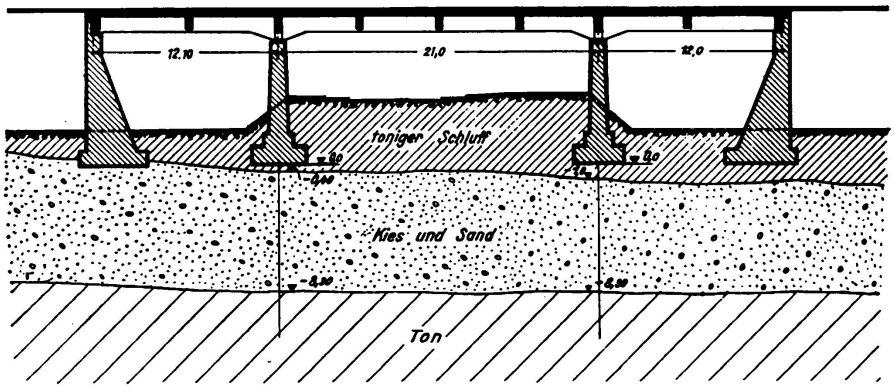


Fig. 20.

ling still continues, slight backward inclinations of the abutments and opening of the construction joints.

18. Work No. 32, km 43.8, Berlin Office. Two-bay girders of each 15.3 m span (fig. 13), spread foundations on drift-marl (sandy clay), natural water content 15%. Mean foundation pressure 2.5 kg/cm². Completed December 1935, predicted settling 80—100 mm, actual settling about 12 mm to December 1935, settling stopping, no damage.

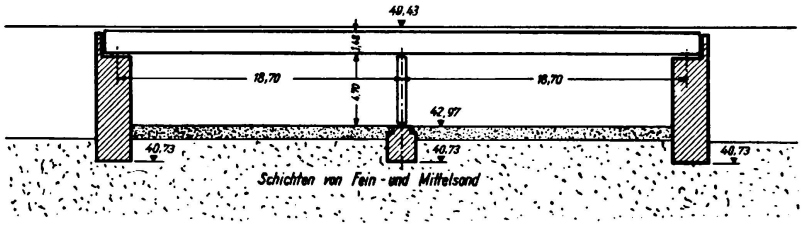


Fig. 21.

19. Work No. 33, km 44.6, Berlin Office. Two-bay girders of ecch 18.7 m span (fig. 14), spread foundations on thin sandy gravel bed, under which drift marl of great thickness. Mean foundation pressure 3.0 kg/cm². Completed March 1936, predicted settling about 10 mm, actual settling to March 1936 about 14 mm. Settling stopped, no damage.

20. Work No. 102, km 6.928, Berlin Office. Four-bay girder, total length 46 m (fig. 15). Spread foundations on drift marl: natural water content 12.4%. Mean foundation pressure 3.0 kg/cm². Completed November 1935, predicted settling about 20 mm, actual settling about 5 mm to January 1936. Settling stopped, no damage.

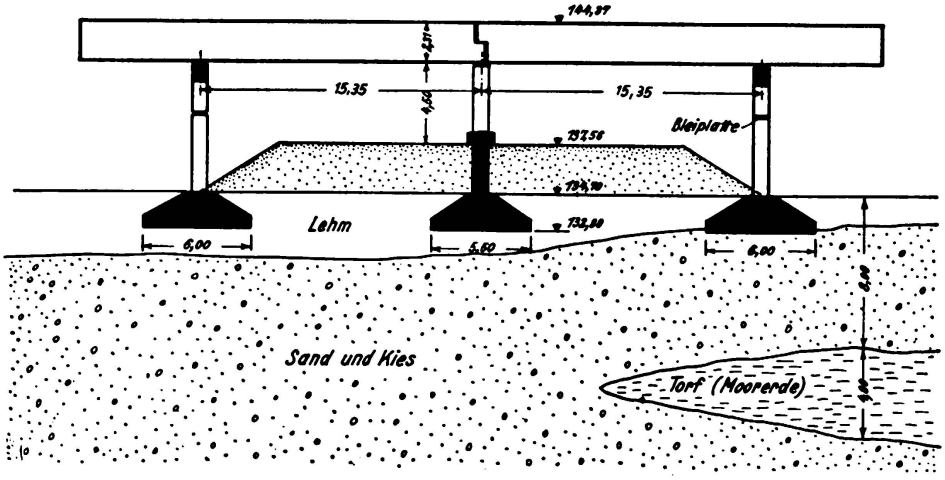


Fig. 22.

21. Work No. 104, km 9.628, Berlin Office. Four-bay girder, total length 49.5 m (fig. 16). Spread foundations on 3 m fine sand, under which drift marl: natural water content 12%, mean foundation pressure 3.0 kg/cm². Completed November 1935, predicted settling about 20 mm, actual settling to January 1936 about 5 mm, settling stopped, no damage.

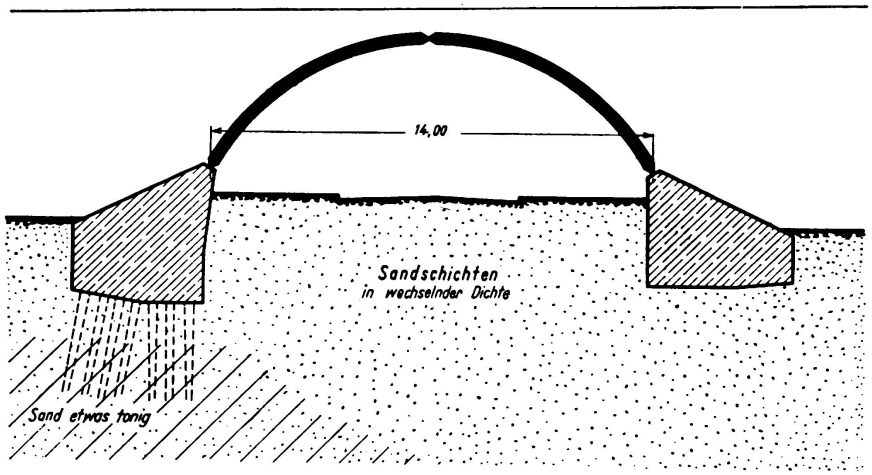


Fig. 23.

22. Work No. 111, km 16.553, Berlin Office. Deck girder of 9.8 m span (fig. 17). Spread foundations on drift marl: natural water content 10.7%, mean foundation pressure 3 kg/cm². Completed November 1935, predicted settling about 20 mm, actual settling to January 1936 about 15 mm. Settling stopped, no damage.

23. Work No. 115, km 20.560, Berlin Office. Girder bridge of 13 m span (fig. 18). Spread foundations on drift marl: natural water content 14.7%, mean foundation

pressure 2.5 kg/cm². Completed July 1935, predicted settling about 60—80 mm, actual settling to January 1936 about 16 mm. Settling stopped, no damage.

24. Work No. 15, km 19.942, Königsberg Office. Four-bay girder, total length 55.8 m, spread foundations on drift marl, mean foundation pressure 2.5 kg/cm² for abutments and 3.0 kg/cm² for piers. Completed January 1935, actual settling to August 1935 about 5 mm. Settling stopped, no damage.

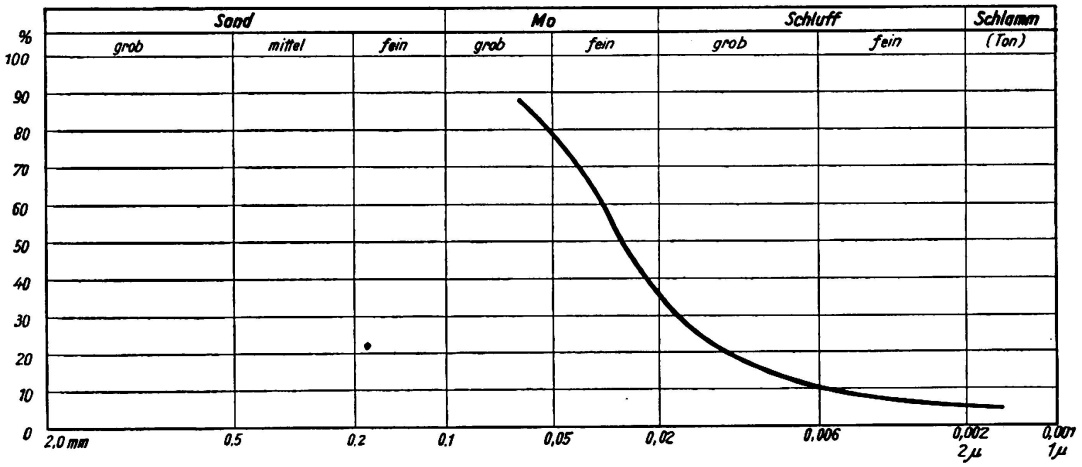


Fig. 24.

25. Work No. 16a, km 21.658, Königsberg Office. Girder bridge of 4.50 m span, spread foundations on drift marl, mean foundation pressure 2.5 kg/cm². Completed April 1935, actual settling about 15 mm. Settling stopped, no damage.

26. Work No. 157, km 52.555, Königsberg Office. Closed frames with 6.0 m span, spread foundation on 2—3 m sand layer, under which drift marl to very great depth: natural water content 15—27%, flow limit 27—34%, rolling limit 18—20%.

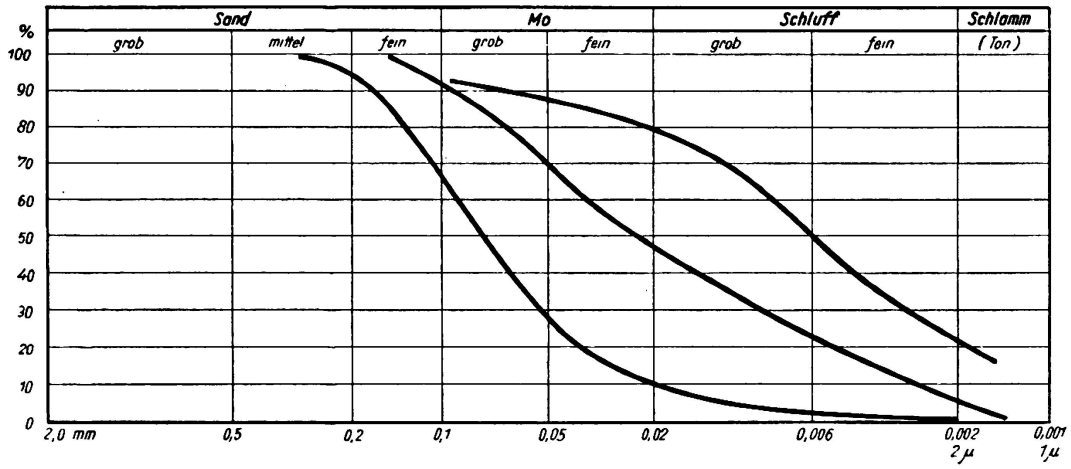


Fig. 25.

Mean foundation pressure 2 kg/cm². Completed August 1934, actual settling on average about 120 mm to August 1935. Settling stopped, steps formed at the construction joints (in consequence of inequalities in filling).

27. Work No. 14, km 19.400, Königsberg Office. Two-bay girder, spread foundations on drift marl with intercalations of clayey fine sand, mean foundation pressure

2.5 kg/cm² for abutments, 3 kg/cm² for piers. Completed November 1934, actual settling to August 1935 about 12 mm. Settling stopped, no damage.

28. Work No. 13, km 18.6, Königsberg Office. Two-bay girders with each 14.3 m span, spread foundations on 1.50 m clayey fine sand, under which alternating layers of clayey fine sand and drift marl. Mean foundation pressure 2.5 kg/cm² for abut-

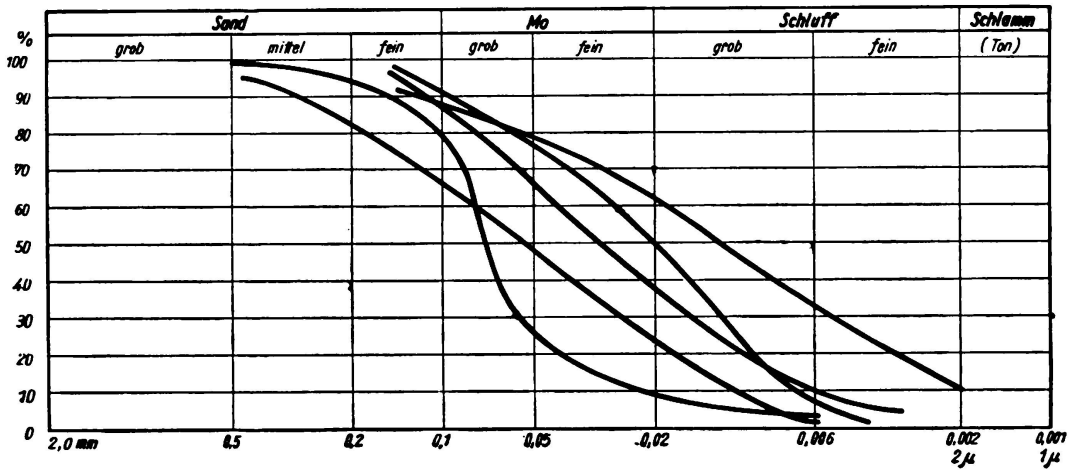


Fig. 26.

ments, 3.0 kg/cm² for piers. Completed November 1934, actual settling to August 1935 about 10 mm. Settling stopped, no damage.

29. 5 works without exact designation of position, Stettin Office. Spread foundations on drift marl, mean foundation pressure 2.8—3.0 kg/cm². No settling and no damage.

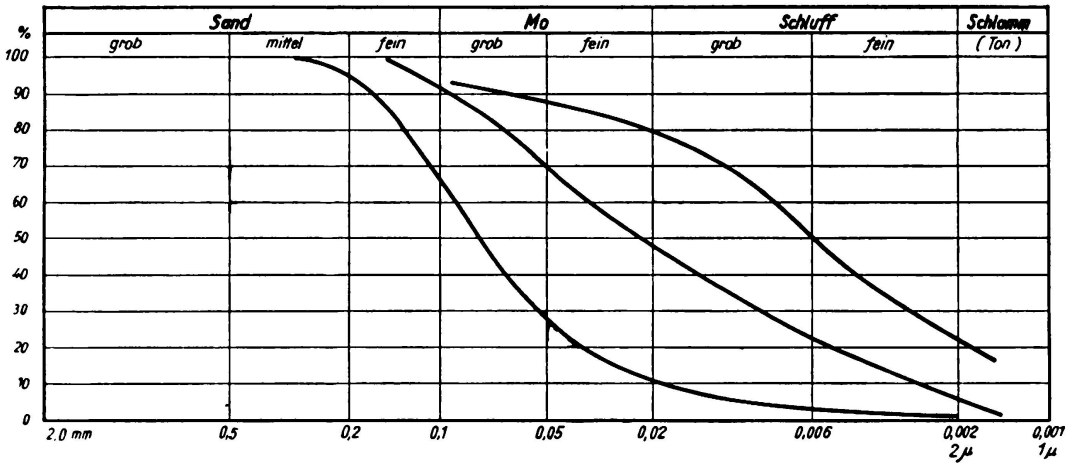


Fig. 27.

30. 9 two-bay deck girder bridges, Stettin Office. Spread foundations on drift marl, mean foundation pressure 2.5—4.0 kg/cm². No settling and no damage.

31. 3 two-bay deck girder bridges, Stettin Office. Spread foundations on 2—3 m clayey sand, under which drift marl mean foundation pressure 2.65 kg/cm²; no settling and no damage.

32. 3 two-bay deck girder bridges, Stettin Office. Spread foundations on 2—3 m

clayey sand, under which sand layers of great depth. Mean foundation pressure 2.2—2.5 kg/cm², actual settlings between 0 and 5 mm, no damage.

33. Work No. 8, km 12.63, Königsberg Office. Reinforced concrete frame of 15.4 m span on reinforced concrete piles 4—6 m long. Subsoil siltlike and clayey fine sand and gravel. Completed June 1935, actual settling to June 1935 about 10 mm. Settling stopped, no damage.

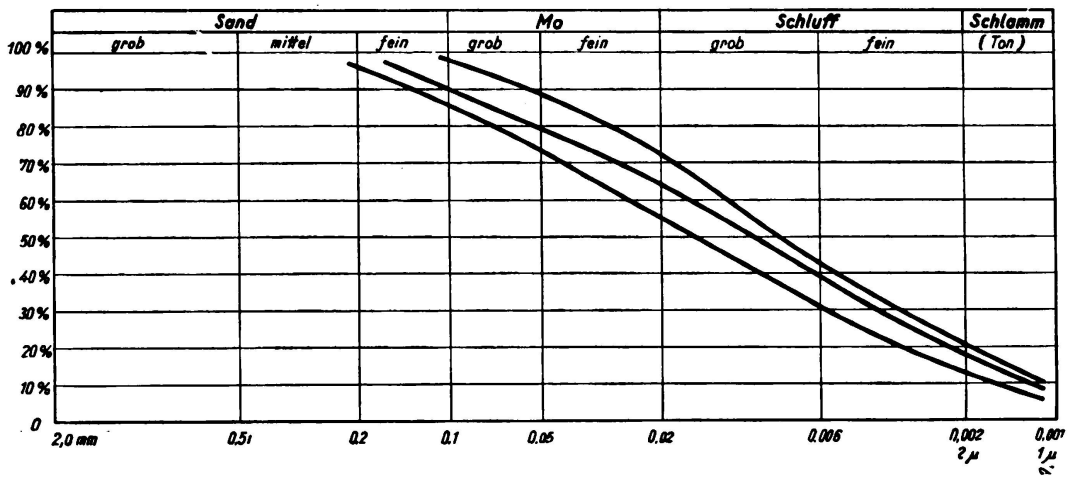


Fig. 28.

34. Work at km 69.122, Dresden Office. Continuous girder on 4 supports, spread foundations 2.5 kg/cm² on clayey sand: natural water content 21%, flow limit 35%, rolling limit 30%. Completed in August 1935, actual settling to August 1935, about 4 mm. Settling stopped, no damage.

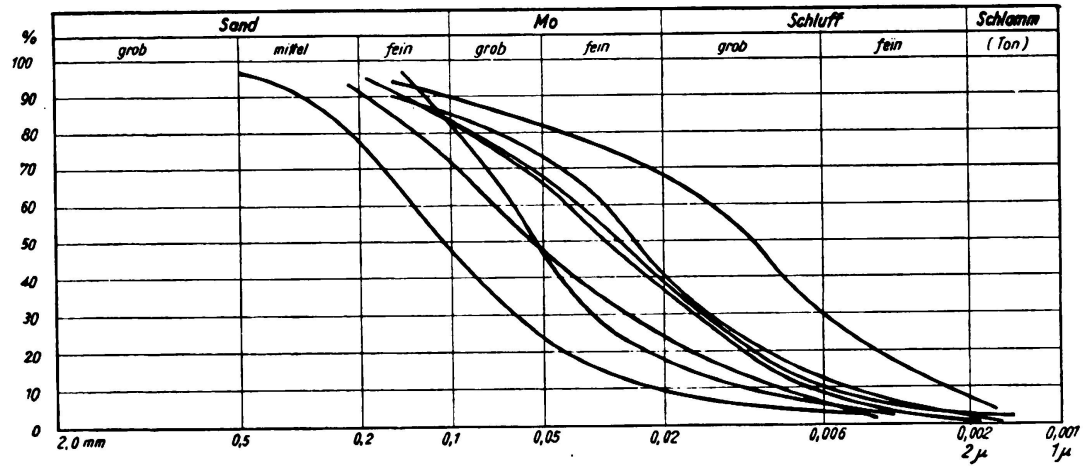


Fig. 29.

35. Work No. 155, km 48.262, Königsberg Office. Five-bay girder (plate-girder) 140 m long, 2 outer bays each 25 m and 3 central bays each 30 m span. Spread foundations, mean foundation pressure 2 kg/cm² for abutments and 3 kg/cm² for central piers. Foundations of central piers constructed between sheet iron piling. Subsoil sand layers, in parts slightly clayey, in 10—14 m depth drift marl. Completed September 1934, actual settling about 5 mm. Settling stopped, no damage.

36. Work No. 337, km 408.0, Hanover Office. Gerber girder over 6 bays, total length 190 m (fig. 19), spread foundations on layers of sand and gravel, first lefthand pier on pile foundation, as there is local appearance of clay and peat. Mean foundation pressure at abutments 1.5—1.7 kg/cm², at piers 1.5—3.0 kg/cm². Completed March 1936, actual settlings of abutments 16 mm, of piers 15 mm, of the first lefthand pier 19 mm. Settling stopped, no damage.

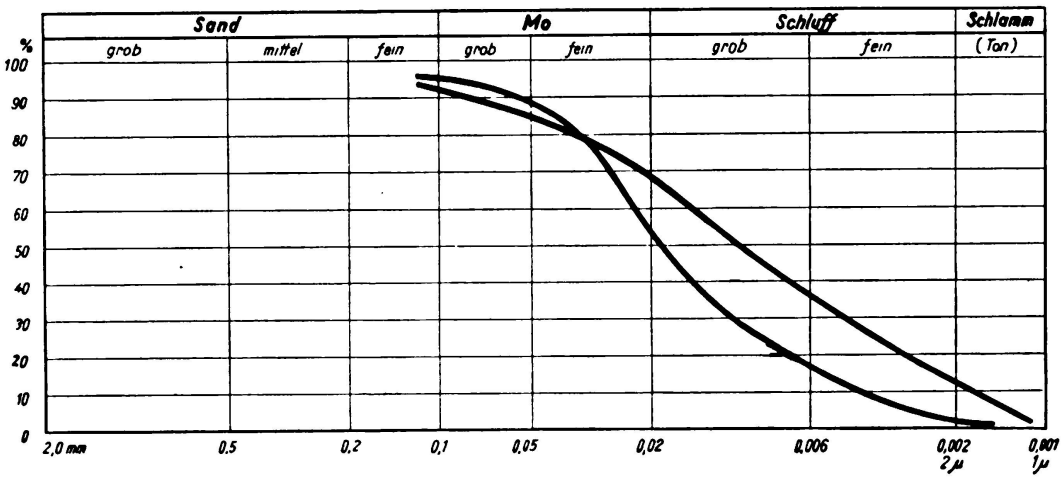


Fig. 30.

37. Work No. 252, km 334.7, Hanover Office. Three-bay deck girder, outer bays each 12 m, central bay 21 m span. Subsoil gravel and sand to a great depth, under which clay (fig. 20), mean foundation pressure at abutments 1.4 kg/cm², at piers 1.5 kg/cm². Completed August 1935, actual settlings at western abutment between

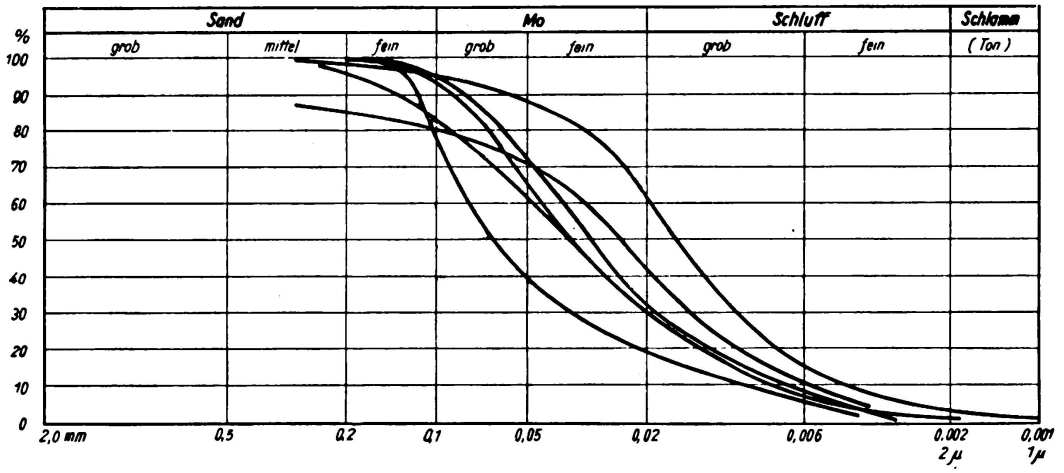


Fig. 31,

22 and 100 mm (roller bearing was lifted), at eastern abutment between 20 and 45 mm, at piers average 15 mm. Settling stopped, no damage (great settling of abutments conditioned by filling in behind the structures).

38. Work No. 18, km 19.431, Berlin Office. Two-bay girder with each 19.7 m span (fig. 21). Spread foundations on sand layers of various size of grain, mean foundation pressure 2.5 kg/cm². Completed February 1936, predicted settling about

10 mm, actual settling up to February 1936 about 10 mm. Settling stopped, no damage.

39. Work No. 7, km 4.863, Breslau Office. Two-bay girder with Gerber hinge over the central pier, each 15.35 m span (fig. 22), spread foundations on loam and deep sand and gravel, peat under the righthand outer pier at a great depth. Mean foundation pressure at outer piers 1.5 kg/cm², at central pier 2.0 kg/cm². Completed October 1934, outer piers turned outwardly on the average of 45 mm (March 1935), righthand outer pier also settled about 30 mm. Settling stopped, no damage.

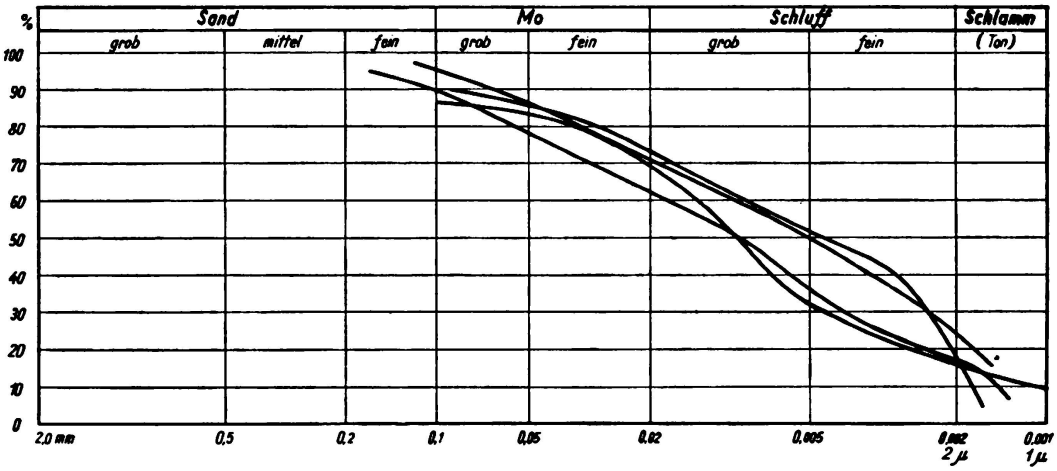


Fig. 32.

40. 13 girder bridges, Stettin Office. Spread foundations on partly very fine sand up to 12 m deep, mean foundation pressure 2.5 kg/cm². No settling and no damage.

41. Work No. 79, km 241.380, Hanover Office. Three-hinged arch of 14 m span, mean foundation pressure 2.7 kg/cm² (fig. 23). Subsoil sand layers of varying density, under the lefthand abutment somewhat clayey, therefore foundation on piles

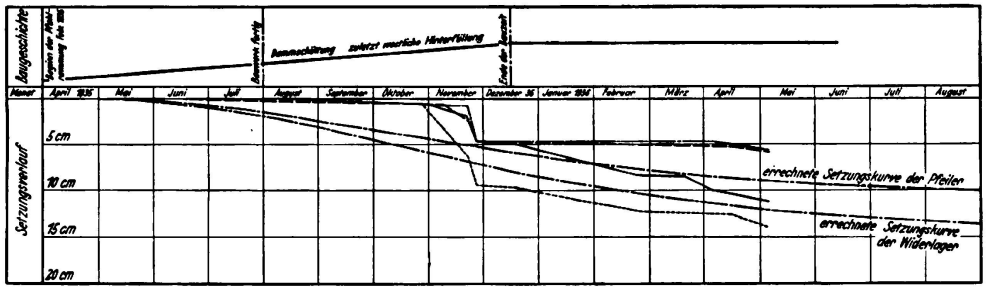


Fig. 33.

there. Completed April 1935, actual settlings western abutment 4 mm, eastern abutment (lefthand) 15 mm to March 1936. Settling stopped, the northern arch shows signs of cracks.

42. Work at km 7.167, Frankfurt-on-Main Office. Reinforced concrete frame with 19.55 m span, reinforced concrete rammed piles 10—11 m long, subsoil 5—10 m sand-gravel, under which stiff clay (in part sandy), mean foundation pressure 2.2 kg/cm². No settling and no damage.

43. Work at km 7.292, Frankfurt-on-Main Office. Reinforced concrete three-bay girder, central bay with suspended girder of 31.2 m span, side bays each 8.6 m.

Mean foundation pressure 2.1 kg/cm², side bays designed as frames with continuous slab between sheet piling. Subsoil 5—10 m sand-gravel, under which stiff clay (in part sandy), no settling and no damage.

44. Work at km 6.849, Frankfurt-on-Main Office. Reinforced concrete frame with

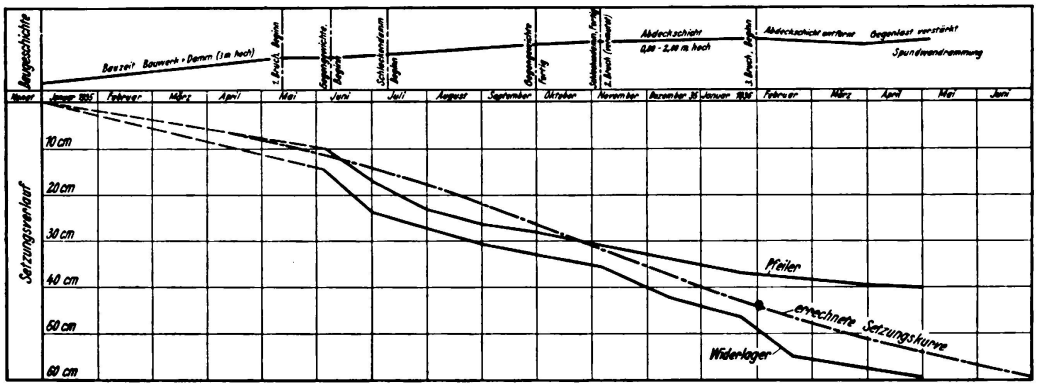


Fig. 34.

12.6 m span, spread foundations on 4—5 m sand-gravel, under which stiff clay (in part sandy) of great thickness: natural water content 15—21%, flow limit 25—50%, rolling limit 9—15%. Mean foundation pressure 2.2 kg/cm². No settling and no damage.

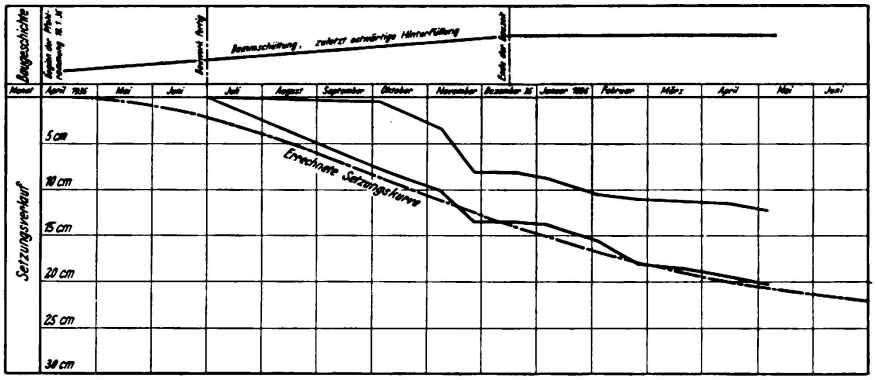


Fig. 35.

*IV. Summary and conclusions.*

In order to make things clearer, the essential data for a comprehensive judgement of the separate works are given in tabular form (tables 1—4). The soils in question may be practically classified in four groups, — clay and loess, silt, drift marl, sand and gravel (in part clayey). When the average settlings corresponding to these four groups are compared (table 5), — the separate values being, for the

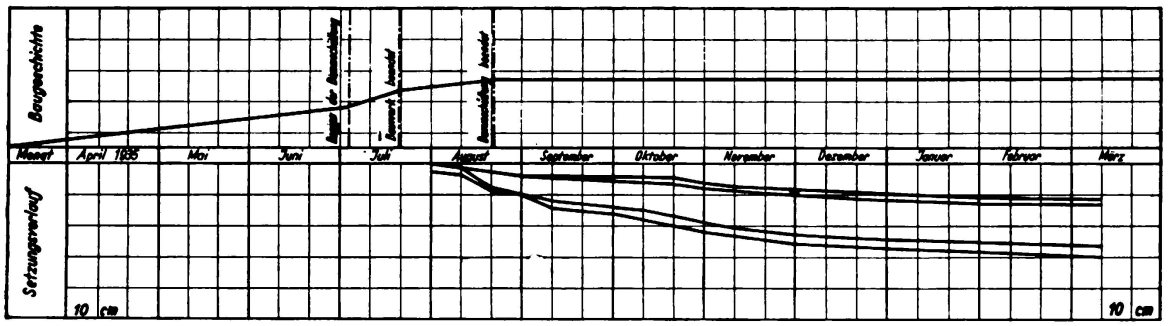


Fig. 36.

sake of simplicity, referred with the help of the theoretical settling curves quite roughly to the moment in which the greatest part of the movements is effected, — here also, in spite of the unequal influence, a number of factors such as thickness of layers and foundation pressure are found to bear a certain relation to each other. In order to prevent misunderstandings, however, it is necessary to call particular

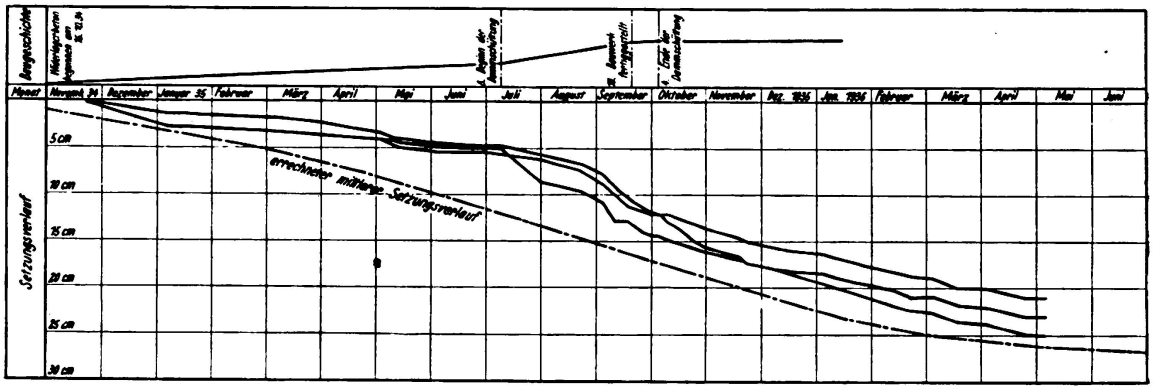


Fig. 37.

attention to the fact that the comparisons made in Table 5, and consequently also the conclusions deduced from them, refer solely to soil conditions found in Germany.

Of the 72 works on which observations have been made, about half rest on drift marl and about one third on sand-gravel beds of considerable thickness. As can

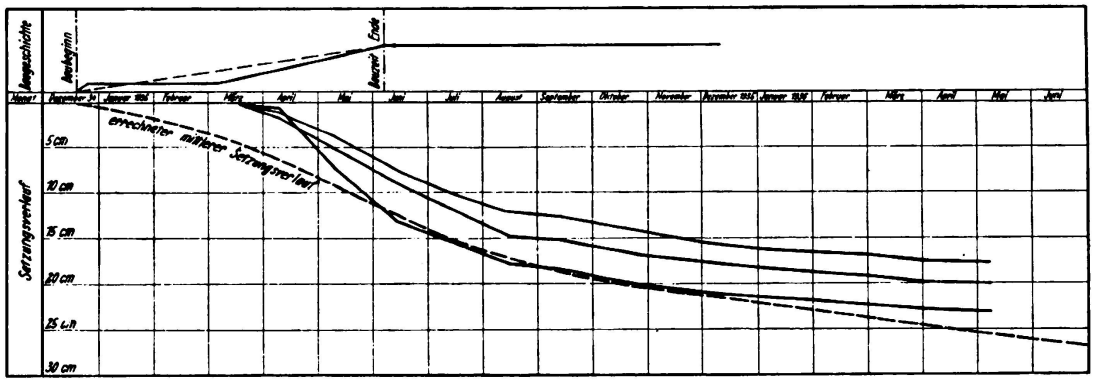


Fig. 38.

be seen from Table 5, the settlings amounted to 0—20 and 0—10 mm respectively for the two groups of soil mentioned. Control calculations have later shown that the factor of safety against the abutments and piers breaking through the foundation ground, with the maximum foundation pressures of 4.0 and 3.0 kg/cm² respectively, lies between 4 and 7. The slight settlings, together with the high factors of safety, would justify higher specific foundation pressures being adopted on beds of drift marl or sand-gravel. Assuming foundation pressures of 6 and 5 kg/cm², the factors of safety would still be 2 and 3 respectively, with only an inconsiderable increase in the settlings. Uniform settling with the adoption of considerably higher figures does not cause any damage; this is proved by the works built on clayey soils, in which settlings up to 200 m could be observed within a comparatively short time. Where damage has occurred, as for example outward inclination of the abut-

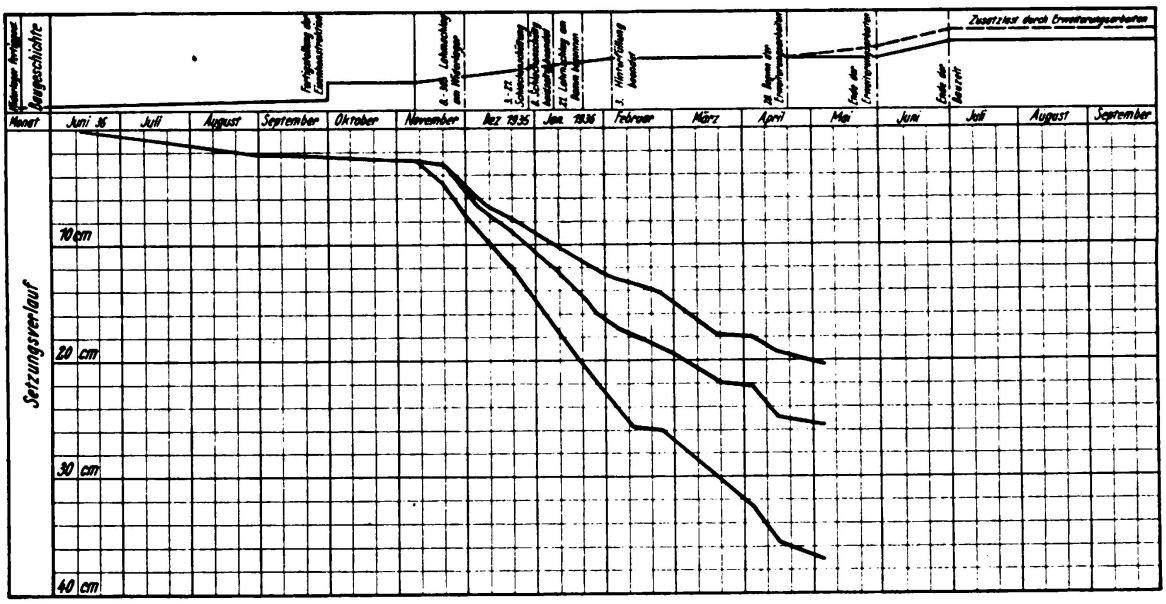


Fig. 39,

ments, it is without exception confined to cases where the embankment filling has been effected only after completion of the structure, or where the space to be filled between the abutment and embankment had been made very large (broad). The same holds essentially also for works resting on soft beds of silt, in so far as they are not caused to suffer through slides and irruptions of adjacent masses of earth in the embankment.

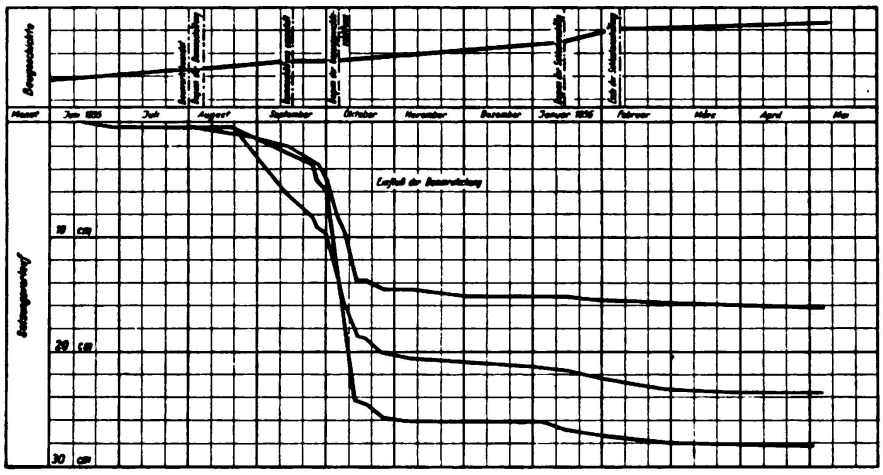

Fig. 40.

The greater part of the works is on spread foundations. Foundations on piles are confined cases where irregularities in settling were to be expected because of the irregular structure of the underground layers, or where the foundations had to be laid on soft siltlike layers.

As essential results of the present report, the following points deserve to be particularly noted: —

1. drift marl and sand-gravel beds of great thickness permit of higher loading than has hitherto been usual.
2. Embankment filling should be effected as soon as possible in order to prevent any irregular movements of the structure. The spaces to be filled in with earth behind the abutments after the structure has been completed should be kept as small as possible, when the structure rests on beds that are soft and not very permeable.

Table 1.

| No. | Foundation | Mean foundation pressure kg/cm² | Principal subsoil layer | Completed | Predicted settling in mm | Observed settling in mm | Remarks |
|---|---|---|---|---|---|---|---|
| 1 | Spread | 1.4 | Clay, stiff | June 1935 | — | Abutm. 54 pier 56 Apr. 1936 | Still settling |
| 2 | Spread | 2.4 | Clay, stiff | Dec. 1935 | — | Pier 52 Mar 1936 | Still settling |
| 3 | Spread | Abutm. 1.5 pier 1,0 | Siltlike clay, soft | Aug. 1935 | Abutm. 150 pier 60 | Abutm. 46 pier 25 | Settling stopped |
| 4 | Spread | 2.75 | Clayey silt, soft | Feb. 1936 | 95 | Av. 50 Apr. 1936 | Settling stopped |
| 5 | Spread | 1.1 | Sandy clay | Nov. 1935 | 2,20 | Av. 140 Apr. 1936 | Still settling |
| 6 | Spread | 1.5 | Clayey silt, soft | Dec. 1935 | — | Av. 280 Apr. 1936 | Still settling |
| 7 | Spread | 1.4 | Compact clay and silt like Clay | July 1935 | — | Abutm. 35 pier 70 Aug. 1935 | Still settling |
| 8 | Spread | 2.6 | Loess | June 1935 | — | Av. 40 Apr. 1936 | Settling stopping |
| 9 | Spread | 2.6 | Loess, sandy | Aug. 1935 | — | 23 Apr. 1936 | Settling stopping |
| 10 | Piles | Abutm. 1.1 pier 1.4 | Silt, siltlike clay. soft | Dec. 1935 | Abutm. 120 pier 90 | Abutm. 125 pier 60 Apr. 1936 | Still settling |

Table 2.

| No. | Foundation | Mean foundation pressure kg/cm² | Principal subsoil layer | Completed | Predicted settling in mm | Observed settling in mm | Remarks |
|---|---|---|---|---|---|---|---|
| 11 | Piles floating | 1.1 | Silt, soft | May 1936 | 470 | Av. 500 May 1936 | Still settling |
| 12 | Piles, floating | 1.5 | Silt, siltlike clay soft | Dec. 1935 | 200 | Av. 150 May 1936 | Still settling |
| 13 | Piles, floating | 1.5 | Silt, soft | Aug. 1935 | 250 | Av. 60 Mar. 1936 | Still settling |
| 14 | Piles, floating | 1.3 | Silt, soft | Oct. 1935 | 350 | Av. 230 May 1936 | Still settling |
| 15 | Piles, floating | 1.0 | Silt, soft | Nov. 1935 | 350 | Av. 200 May 1936 | Still settling |
| 16 | Piles, floating | 2.0 | Silt, soft | July 1936 | east abut. 900, west abut. 500 | Av. 300 Mai 1936 | Still settling |
| 17 | Spread | 1.8 | Silt | July 1935 | 350 | Av. 280 May 1936 | Still settling |
| 18 | Spread | 2.5 | drift marl, sandy clay | Dec. 1935 | 80—100 | 12 Dec. 1935 | Settling stopped |
| 19 | Spread | 3.0 | drift marl, sandy clay | Mar. 1936 | 10 | Av. 14 Mar. 1936 | Settling stopped |
| 20 | Spread | 3.0 | drift marl, sandy clay | Nov. 1935 | 40—60 | Av. 7 Jan. 1936 | Settling stopped |
| 21 | Spread | 3.0 | drift marl, sandy clay | Nov. 1935 | 20 | Av. 5 Jan. 1936 | Settling stopped |
| 22 | Spread | 3.0 | drift marl, sandy clay | Nov. 1935 | 20 | Av. 15 Jan. 1936 | Settling stopped |

Table 3.

| No. | Foundation | Mean foundation pressure kg cm$^2$ | Principal subsoil layer | Completed | Predicted settling in mm | Observed settling in mm | Remarks |
|---|---|---|---|---|---|---|---|
| 23 | Spread | 2.5 | drift marl, sandy clay | July 1935 | 60—80 | Av. 16 Jan. 1936 | Settling stopped |
| 24 | Spread | Abutm. 2.5 pier 3.0 | drift marl, sandy clay | Jan. 1935 | — | Av. 5 Aug. 1935 | Settling stopped |
| 25 | Spread | 2.5 | drift marl, sandy clay | Apr. 1935 | — | Av. 15 Aug. 1935 | Settling stopped |
| 26 | Spread | 2.0 | drift marl, sandy clay | Aug. 1934 | — | Av. 120 Aug. 1935 | Settling stopped |
| 27 | Spread | Abutm. 2.5 pier 3.0 | drift marl, clayey fine sand | Nov. 1934 | — | Av. 12 Aug. 1935 | Settling stopped |
| 28 | Spread | Abutm. 2.5 pier 3.0 | Clay, sand, drift marl | Nov. 1934 | — | Av. 10 Aug. 1935 | Settling stopped |
| 29 | Spread | 3.0 | drift marl, sandy clay | — | — | none | — |
| 30 | Spread | 2.5—4.0 | drift marl, sandy clay | — | — | none | — |
| 31 | Spread | 2.65 | drift marl, sandy clay | — | — | none | — |
| 32 | Spread | 2.2—2.5 | Loamy sand | — | — | 0—5 | Settling stopped |
| 33 | Spread | 3.0 | Sand, clayey silt | June 1935 | — | Av. 10 June 1935 | Settling stopped |
| 34 | Spread | 2.5 | Clayey sand | Aug. 1935 | — | Av. 4 Aug. 1935 | Settling stopped |

Table 4.

| No. | Foundation | Mean foundation pressure kg/cm² | Principal subsoil layer | Completed | Predicted settling in mm | Observed settling in mm | Remarks |
|---|---|---|---|---|---|---|---|
| 35 | Spread | Abutm. 2.0 pier 3.0 | Sand, slightly clayey | Sept. 1934 | — | Av. 5 Feb. 1935 | Settling stopped |
| 36 | Spread | Abutm. 1.5 — 1.7, pier 1.5—3.0 | Sand-gravel, pier I, clay, peat | Mar. 1936 | — | Abutm. 16 pier 15 pier I, 19 Apr. 1936 | Settling stoppel |
| 37 | Spread | Abutm. 1.4 pier 1.5 | Sand-gravel, part clayey | Aug. 1935 | — | Abutm. 20 to 100 pier 15 Apr. 1936 | Settling stopped |
| 38 | Spread | 2.5 | Sand | Feb. 1936 | 10 | 10 Febr. 1936 | Settling stopped |
| 39 | Spread | Outer pier 1.5, centr. pier 2.0 | Thin loam layer, sand, gravel | Oct. 1934 | — | Horiz. 45 Mar. 1935 | Settling stopped |
| 40 | Spread | 2.5 | Sand | — | — | none | — |
| 41 | Spread west abutm, piles east abutm. | 2.7 | Sand, part clayey | April 1935 | — | West abutm. 4 east abutm. 15 Mar. 1936 | Settling stopped |
| 42 | Piles | 2.1 | Sand-gravel, clay | — | — | none | — |
| 43 | Spread with sheet piling | 2.2 | Sand-gravel, clay | — | — | none | — |
| 44 | Spread | 2.2 | Sand-gravel, clay | — | — | none | — |

Table 5.

| Number of structures | Soil group | Mean foundation pressure in mm | Settling in mm |
|---|---|---|---|
| 9 | Silt | 1,1—2,0 | 200—1000 |
| 8 (11) | Clay, loess, loam etc. | 1,1—2,6 | 50—200 |
| 31 | drift marl, sandy and gravelly clay | 2,5—4,0 | 0—20 |
| 24 (21) | Sand, gravel | 1,5—3,0 | 0—10 |

## Vocabulary for illustration texts:

| Deutsch | English |
|---|---|
| **A** | |
| Abdeckschicht entfernt | top layer removed |
| Abdeckschicht ... hoch | top layer ... high |
| Aufschüttung | filling |
| **B** | |
| Baubeginn | beginning of construction |
| Baugeschichte | construction records |
| Bauwerk beendet<br>Bauwerk fertiggestellt | structure completed |
| Bauzeit, Bauwerk und Damm (3 m hoch) | construction time, structure and dam (3 m high) |
| Beginn der Dammschüttung | commencement of dam filling |
| Beginn der Pfahlrammung Februar 1935 | start of pile driving Feb. 1935 |
| Beginn der Erweiterungsarbeiten | commencement of extension work |
| Beginn der Gegengewichtsschüttung | commencement of ballasting |
| Beginn der Schlackenschüttung | commencement of cinder depositing |
| Bruch, Beginn | fracture, start |
| Bruch (vermutet) | fracture (suspected) |
| **D** | |
| Dammschüttung, zuletzt westliche Hinterfüllung | dam filling, western back filling last |
| Dammschüttung, zuletzt ostwärtige Hinterfüllung | dam filling, eastern back filling last |
| Dammschüttung beendet | dam filling completed |
| Dammschüttung eingestellt | dam filling interrupted |

| | |
|---|---|
| **E** | |
| Einfluß der Dammrutschung | influence of dam slipping |
| Ende der Bauzeit | end of construction time |
| Ende der Dammschüttung | completion of dam filling |
| Ende der Erweiterungsarbeiten | completion of extension work |
| Ende der Schlackenschüttung | completion of cinder deposits |
| Errechneter mittlerer Setzungsverlauf | calculated average values of subsidence |
| Errechnete Setzungskurve der Pfeiler | calculated curve of pier subsidence |
| Errechnete Setzungskurve der Widerlager | calculated curve of abutment subsidence |
| **F** | |
| fein | fine |
| Feinsand | fine sand |
| Fertigstellung der Eisenkonstruktion | completion of steel structure |
| **G** | |
| Gegengewichte, Beginn | counter weights, start |
| Gegengewichte fertig | counter weights, finished |
| Gegenlast verstärkt | counter weights increased (or strengthened) |
| Gelenk | hinge |
| Geschiebemergel (toniger Sand) | marl (clayey sand) |
| Grob | coarse (rough) |
| Grobsand und Feinkies | coarse sand and fine shingle |
| **H** | |
| Holzpfähle 8 m lang | wooden piles 8 m long |
| Hinterfüllung beendet | back filling completed |
| **K** | |
| Kies | shingle |
| **L** | |
| Lehm | clay |
| Lehmschlag am Widerlager | clay deposit at abutment |
| Lehmschlag am Damm begonnen | clay deposit for dam started |
| Löß, etwas sandig | loess, slightly sandy |
| Lößlehm | loess-clay |
| **M** | |
| Monat | month |
| mittel | average (or mean) |
| Mo (= Moorerde) | Mo = moor soil |
| **P** | |
| Pfeiler | pier |
| **S** | |
| Sand, etwas tonig | sand slightly clayey |
| Sandschichten in wechselnder Dichte | layers of sand in variable thickness |
| Sandschüttung | sand filling |
| Sand | sand |
| sandiger Schluff | sandy silt |
| Setzungsverlauf | run of subsidence |
| Schichten von Fein- und Mittelsand | layers of fine and medium grain sand |
| Schichten von Sand und Kies | layers of sand and shingle |
| Schlackendamm Beginn | cinder dam started |
| Schlackendamm fertig | cinder dam completed |
| Schlackenschüttung | cinder filling |
| Schlackenschüttung beidseitig beendet | cinder filling on both sides completed |
| Schlamm | mud |
| Schluff | silt |
| Schluff mit Feinsandeinlagerungen | silt mixed with fine sand |
| schluffiger Ton (weichplastisch) | sticky clay (plastic and soft) |
| steifer Ton, z. T. sandig | stiff clay partly sandy |
| Spundwandrammung | shut pile ramming |

| | |
|---|---|
| T | |
| Ton | clay |
| toniger Sand und Kies | clayey sand and shingle |
| toniger Schluff | clayey silt |
| Torf (Moorerde) | peat |
| W | |
| Widerlagerbeton begonnen am Widerlager | concreting of abutment started on abutment |
| Widerlager fertiggestellt | abutment completed |
| Z | |
| Zusatzlast durch Erweiterungsarbeiten | supplementary load due to extensions. |

## Summary.

The author describes the soil conditions for a large number of new structures which were built in connection with the new Reich Motor Car Road system. He compiled the measured subsidences and compares the measured values with those predicted.

# VIII 3

## Report on Dynamic Soil Tests.

# Bericht über die dynamischen Bodenuntersuchungen.

## Rapport sur l'auscultation dynamique des terrains.

Geh. Regierungsrat Dr. Ing. A. Hertwig,
Professor an der Technischen Hochschule Berlin.

### Foreword.

Static load tests on soil under directly imposed loads or under pressure by hydraulic presses are admittedly unsatisfactory in various respects. The results depend to a very great extent upon the area of the surface loaded. Even the early tests made by *Engesser*[1] (1) showed that for the same degree of loading per unit of surface the amount of subsidence increased with the area subjected to loading. *Engesser*'s theorem was subsequently proved by the test results obtained by *Kögler* (2, 3, 4) and others. For a given surface area the amount of subsidence has a minimum value that increases rapidly when the area is decreased but more slowly when the area becomes larger. So far, however, the tests carried out have not employed surface ares of more than about 1 m². It is extremely difficult to draw conclusions from such tests by extending them to loaded surfaces of sizes encountered during practical building operations. A further drawback of the static load test lies in the fact that the effect of loading does not penetrate very deep. In this connection *Kögler* and others have shown that its effect extends to a depth equivalent to about five or six times the diameter of the surface loaded. Thus, in these loading tests it is as often as not impossible to make any allowance for deeper layers of soil which under certain circumstances can exert a very considerabler influence on the amount of subsidence, so that it is easy to arrive at false conclusions from test loading.

With a view to obviating these drawbacks, the 'Degebo' — Deutsche Forschungsgesellschaft für Bodenmechanik (German Research Institute for Soil Mechanics) — has for the past seven years been elaborating processes for dynamic soil tests.

### § 1. Description of apparatus.

On the soil to be tested is placed a machine capable of exerting on the soil beneath it forces running sinoidally and in any desired direction. These machines are of extremely simply construction; they function on the principle of eccentric masses rotating in opposite directions on two shafts (Fig. 1). Sinoidal forces

[1] The numbers design the conforming number of the index.

acting vertically to the surface of the ground, as well as forces and turning moments acting in any desired direction can be produced with them. These oscillators are manufactured by Messrs. Losenhausenwerk, Düsseldorfer Maschinenbau-Aktien-Gesellschaft, Düsseldorf-Grafenberg. The weight of the machine, the magnitude of the centrifugal forces and the number of revolutions of the shafts can be altered.

The waves set up under strip or point loading in the homogeneous, elastic half-space extending to infinity have been investigated by *Rayleigh* and *Lamb* (7, 8). Progressive thrust waves, compression waves and surface waves are caused, whose speed of propagation is as 1.7 : 1 : 0.9 respectively. These waves are observed almost exclusively in macroseismics. The waves produced by the machine just described, which has a given mass and a finite ground area, have recently been the object of strict mathematical research by *H.* and *E. Reissner* (36). We shall refer to this work in due course. Simplified assumptions are here made for the practical application of the oscillations produced in the soil for the purpose of determining the properties of the latter.

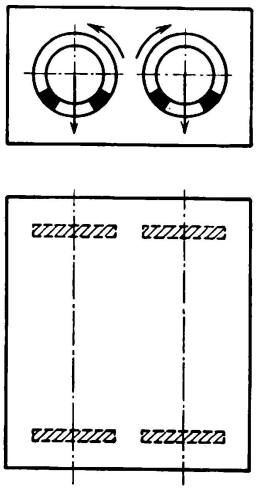

Fig. 1.

The arrangement of masses for vertical agitation.

In a number of the tests the machine and a certain portion of the ground is considered as an oscillating mass element standing on a more or less elastic base, namely, the soil to be examined. In the second group of tests the waves emanating from the machine are investigated.

## § 2. The machine on an elastic base.

When the oscillator placed on the ground is agitated by vertical, periodic forces, the machine can as a first approximation be considered as a mass element vertically unrestrained. The ground exerts a linear rebound action and a shock-absorbing power which, as a first approximation, can be valued as proportional to the velocity. Now the whole action of movement is governed by the linear differential equation with fixed coefficients:

$$M\frac{d^2x}{dt^2} + b\frac{dx}{dt} + cx = P\sin\omega t,$$

or when divided by M:

$$\frac{d^2x}{dt^2} + 2\lambda\frac{dx}{dt} + \alpha^2 x = \beta\sin\omega t.$$

In this equation M is the oscillating mass,

$b \frac{dx}{dt}$ the shock-absorbing force, and

cx the elastic rebound action,

P sin $\omega t$ the periodic agitation force whose rotary frequency is $\omega$.

In the test the rotary frequency is now allowed to assume all possible values. The amplitudes x of the machine are recorded by a vibrograph affixed to the machine. Further, the phase displacement between the position of the eccentric mass and the oscillating machine is recorded, the indications of the vibrograph continuously giving the position of the eccentric masses as well. Thirdly, the energy imparted to the machine is measured.

A test of this kind shows that the amplitudes x of the oscillating mass element rise from O to maximum value as the number of rotations increases, and fall again asymptotically towards a definite value if the rotations are increased still further. The record of the amplitudes therefore contains a point of resonance when the frequency of the agitating agent coincides with the natural frequency $\alpha$ of the undamped oscillation of the mass element. This resonance point is also apparent in the record of imparted energy and that of phase displacement (Fig. 2—5).

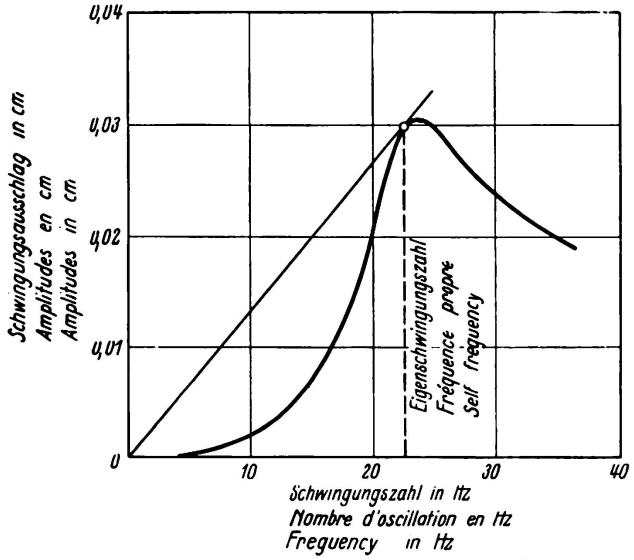


Fig. 2.
Amplitudes of the moving mass on the ground in dependence of the frequency.

The curves recorded in the test for amplitude, energy and phase can be used in calculating the constants $\alpha$ and $\lambda$ in the differential equation of the oscillating concentrated mass. The evaluation process, which cannot be given in detail here, is described in the 'Veröffentlichung der Deutschen Forschungsgesellschaft für Bodenmechanik', Heft 1 (Publication of the German Research Institute for Soil Mechanics, No. 1) (14). As amplitudes, imparted energy and phase are recorded on different instruments, the accuracy of the values $\alpha$ and $\lambda$ can also be determined. The mean deviation of the $\alpha$ figures varies between 3 and 5%; that of the damping figure $\lambda$, is considerably greater. The reason for this lack of accuracy cannot be gone into here.

The natural frequency figure $\alpha = \sqrt{\frac{c}{M}}$ depends upon the elastic properties

of the soil. The results of a long series of tests on soils of the most widely differing natures are arranged in Table I in the order of increasing $\alpha$. In the third column of the Table will be found the loads per unit of surface. A comparison between the two columns reveals that there is a relation between the value $\alpha$ and the admissible loading. The values of $\alpha$ rise in accordance with admissible loading, so that $\alpha$ can be used as an immediate standard of measurement for the loading to which the ground is subjected. The use of $\alpha$ to determine the carrying property of the soil is more advantageous than the determination of admissible loading by static load tests, in that when establishing the value of $\alpha$ experimentally many much larger portions of soil are involved than in static testing, so that the influence of deeper layers also becomes evident. Furthermore, with this method the size of the surface under load does not play such a decisive part as in the static testing method. Of course in the dynamic test, too, only such values of $\alpha$ can be immediately compared as have been obtained with a

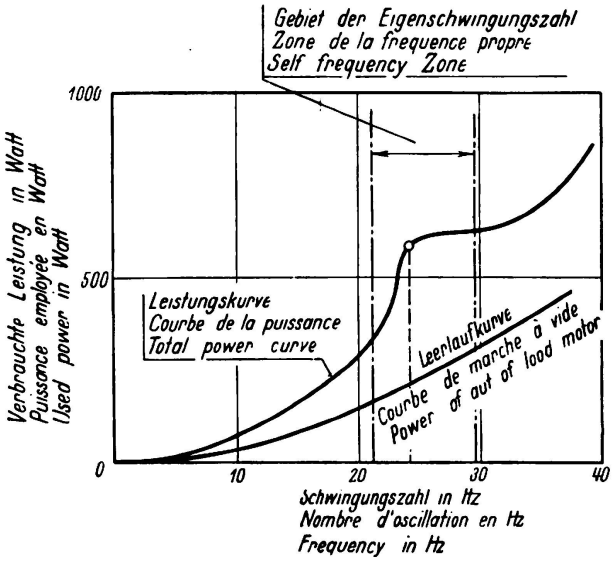


Fig. 3.
Power in dependence of frequency.

standard apparatus, i. e. with a machine of definite weight, ground area and centrifugal force. There is, however, a possibility of making a mutual comparison between results given by machines of other constants.

The damping value $\lambda$ is dependent on the one hand upon the internal friction of the soil, and on the other upon the deformation energy exerted to produce non-elastic, permanent subsidence. If the internal friction and the deformation energy are great, the damping is also great. But since these two circumstances, friction and permanent subsidence, have an influence upon the damping, it cannot of course be concluded that soils of great shock-absorbing power must reveal great permanent subsidences, for a soil with great internal friction can also possess great shock-absorbing power without being subject to great permanent subsidences.

Fig. 5 shows the action of subsidence as it occurred in a test, independently of the frequency of agitation. If this compressive action is brought into relation with the amplitude curve, it will be found that for very many soils the subsidences at first increase, slowly, grow rapidly when the resonance zone is reached,

and beyond this zone again increase but slowly. The permanent subsidences occuring in non-cohesive soils are mainly caused by the collapse of unstable arrangements of granules with regard to each other. When the ground is agitated, the friction between the oscillating particles of soil decreases so much in the resonance zone that the arrangements of particles, blocked by static loading, collapse, until finally they attain maximum compactness during the process of oscillation.

It is therefore possible to predict with a good degree of reliability the behaviour of the ground under dynamic loading and vibration, by considering the value obtained for the shock-absorbing properties of the soil, and the amount of subsidence.

In the case of strongly cohesive soils by dynamic loading of the ground cannot of course give adequate information as to the influence of time on the compressions. For this further investigations will naturally be required — laboratory

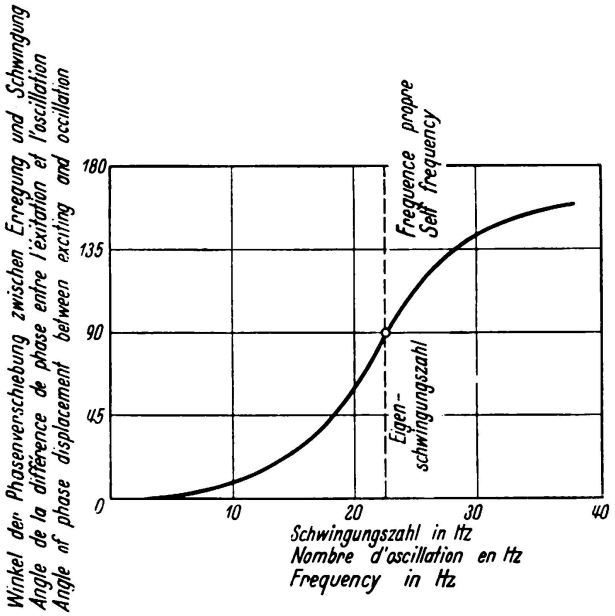


Fig. 4.
Phase displacement between agitation and oscillation in dependence of the frequency.

tests on cohesive soils, carried out on undisturbed specimens by the well known processes. But even for non-cohesive soils it is advisable to supplement the dynamic tests by investigating undisturbed specimens and ascertaining the size-distribution of the granules, the degree of porosity and the compactability of the soil.

## § 3. Speed of continuous surface waves.

The nature of the waves produced by the machine has not yet been fully explained. It is, however, possible to carry out the following measurements: A seismograph is used to record, at sufficiently close intervals along a straight line emanating from the oscillator, the amplitudes of a small surface area of the ground approximating a surface point, and at the same time the position of the eccentric weight in the oscillator. If, now, simultaneously with the position of the eccentric mass we now follow, say, that of a wave crest, which can easily

be found in the various records at a sufficiently short distance from the points of measurement, it will be seen that this wave crest is propagated at a certain rate. For it a graphic time-table (Fig. 6) can be drawn up similar to a railway time-table. In homogeneous ground this table yields a straight line (Fig. 6b) at an angle to the time axis. The tangent of its angle of incline reveals the speed of propagation. If the wave enters soil of a different density during its progreß, this rate curve gives a different speed; where there is a transition from one type of ground to another the rate curve is suddenly bent (see Fig. 6a).

These tests have been carried out on the most widely-differing kinds of ground and the results noted in Col. 1 of Table I appended. It will be noticed that in this Table the speeds are also arranged in order of magnitude, rising from 80 m/sec to 1100 m/sec. The propagation speed of these waves is thus — just like the constant of elasticity of the soil established above — a standard of measurement for the quality, i. e. the carrying capacity, of the ground. This standard is an even more sensitive one than the elastic constant $\alpha$ found above.

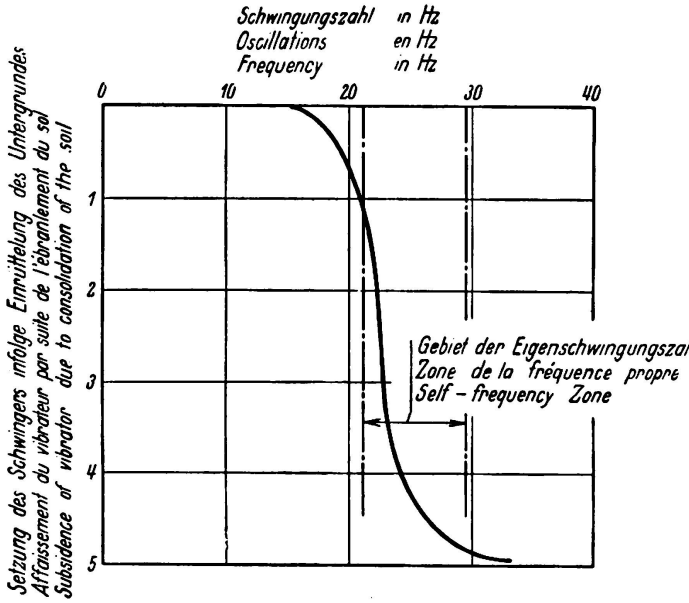


Fig. 5.
Subsidence of swinging mass due to shaking of the soil in dependence of the frequency.

If, now, the machines are placed at different points on the piece of landwhere soil properties are to be measured at the surface, and the propagation speeds measured in various directions, a map can be drawn up giving the surface properties of the ground (Fig. 7).

By measuring simultaneously the waves produced in the same soil by impact as caused by drop-weights or explosions, a conclusion may be arrived at concerning the nature of the waves set up by oscillation. Impact waves show much greater speeds and are generally referred to as compressive waves. The waves of far lower propagation speed produced by the oscillator and measured at the surface are therefore transversal or Rayleigh waves in homogenous half-space. It is a task for contemporary research workers to determine the exact character of these waves.

On recording the amplitude curve of a surface point, it will be seen that sinoidal agitation force gives a purely sinoidal amplitude diagram as well. It

is only in the immediate proximity of the machine that this sinoidal form is sometimes disturbed, other and secondary periodic forces of a different frequency from that of the rotating eccentric mass exerting an influence upon it. As Fig. 8 shows, the amplitude decreases rapidly as the distance from the oscillator grows larger, the relation forming more or less an exponential curve. This kind of decrease has been observed by quite a number of investigators (37, 38, 39).

Various types of soil possess various degress of absorption. Available measurements would seem to indicate that absorption is dependent upon wave-lenght, and is greater for short than for long waves.

Propagation speed, too, is frequently found to depend on wave-length (dispersion), although further investigation is necessary if the questions of absorption and dispersion are to be fully understood.

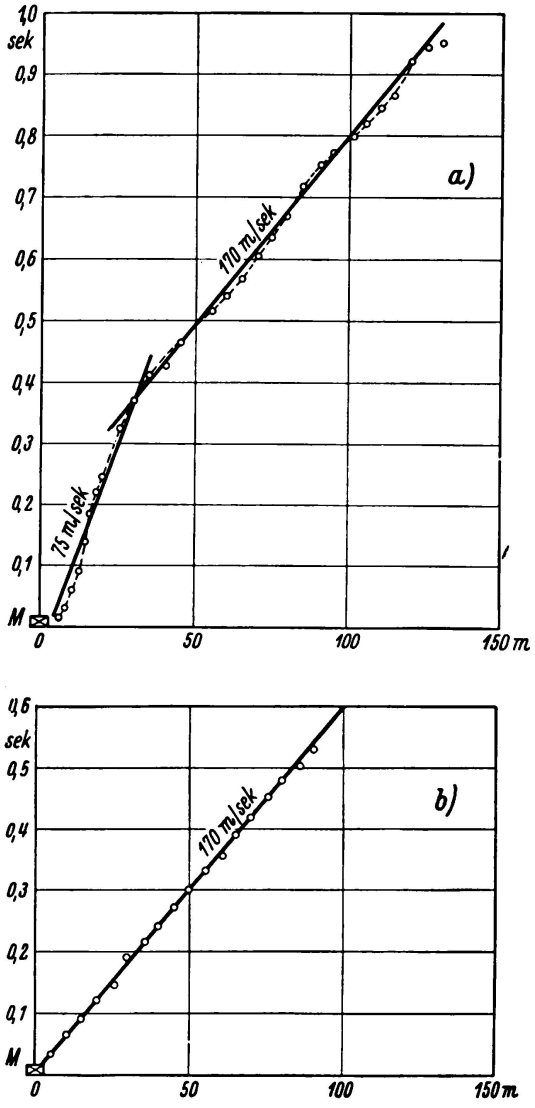


Fig. 6.
Time curve of the elastic waves caused in the soil by the swinging mass
a) in stratified ground,
b) in homogeneous ground.

## § 4. The waves in stratified soil.

If, at a certain depth below the surface, the upper layer terminates in a plane parallel to the surface and gives way to a soil of different texture, and if in

this case the absorption of the waves in the top layer is greater than in the layer below, then the rate curve (Fig. 6) also reveals a sudden kink, the speed for the top layer appearing first in the neighbourhood of the machine. The speed for the deeper-lying layer is revealed at a greater distance. Here the surface wave has already been absorbed and the oscillation of the deeper layer appears at the surface. This interpretation of the rate curve is confirmed by other investigations carried out on top and deeper layers.

The separate branches of the rate curve are not straight lines but reveal slightly curved sinoidal lines placed on top of the straight lines. Their significance has been investigated in the 'Degebo' Publications, No. 4 (15). Even in the rate curve the speed gives an indication of the character of the deeper layer.

If the amplitudes of the points lying on a straight line emanating from the oscillator are further observed, it will be found that, as already mentioned, they

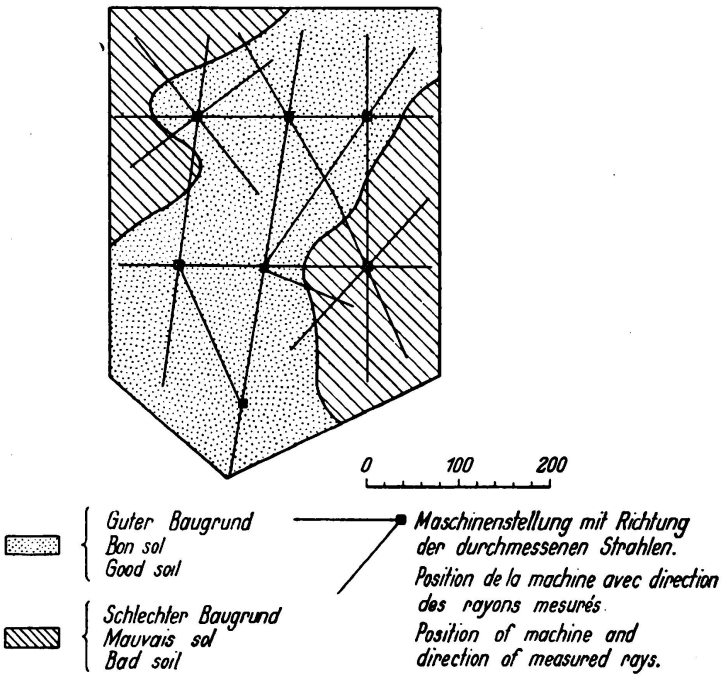


Fig. 7.

Result of a dynamic soil test. Determination of limits between good and bad soil.

decrease at an approximately exponential rate in homogeneous soil as the distance from the oscillator increases. In ground composed of layers, on the other hand, a steady decrease does not occur, but at certain places the amplitudes again appear as definite maxima. There can be various reasons for such maxima. When the individual layers are perfectly homogeneous, these maxima are only to be explained by interference between the waves of the upper and lower layer, or by the overlapping of waves thrown back at the dividing surface. If the maxima are determined along all possible straight lines emanating from the oscillator, they will lie in concentric circles about the latter if the soil is homogeneous and the plane separating the layers parallel to the surface. Making certain assumptions as to the flow of these waves, as is done in seismics when

examining subterraneous deposits, it is now possible to ascertain the depth of the plane separating the two layers by observing how far distant the interference rings lie. If the dividing plane is not parallel to the surface, ellipse-like, con-focal curves are formed instead of concentric circles. Distorted curves may also appear if the ground round about the machine is not homogeneous. It can be determined which of the two cases, non-homogeneity or a sloping plane of separation, has to be dealt with by taking measurements along a straight line in a direction away from the machine, and vice versa, measuring towards the machine.

When investigating the internal structure of the ground with the aid of the dynamic process, the wave-length employed naturally plays a very important part. Fig. 8a—b shows the course of the amplitudes for two measurements taken at the same place, one with a wave-length of 15 m and the other with a

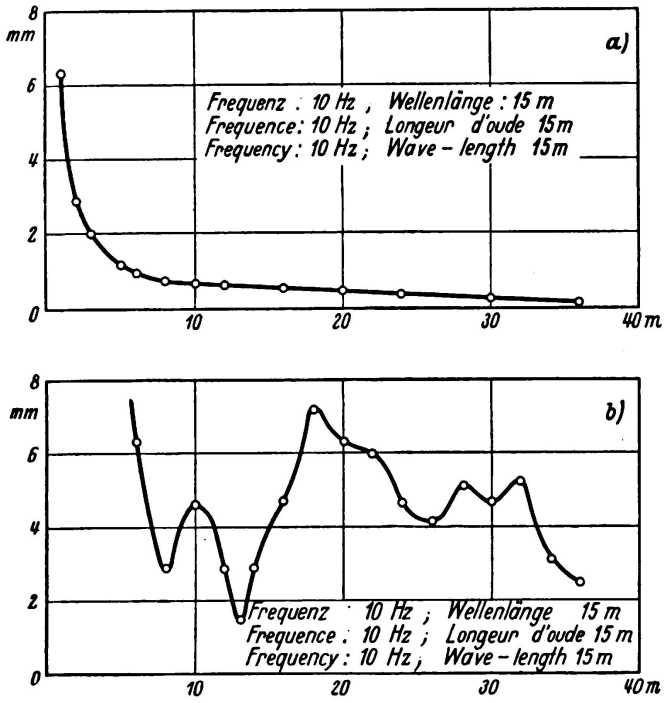


Fig. 8.
Amplitudes of soil oscillation in dependence on the distance from the agitator
a) for long waves,
b) for short waves.

wave-length of 7.5 m. The first curve runs fairly smoothly, the second reveals a large number of maxima and minima. Here symptoms of deflection become apparent; if the wave-lengths are not in the right proportion to the various differently composed portions of the ground, the waves are deflected around these irregularities. This fact is also of importance when waves are to be screened in the ground.

## § 5. Application.

The application of the process has already been referred to in the preceding paragraphs. A few examples taken from actual practice will now be briefly considered.

### 1) Determining the $\alpha$ values and compressions.

On ground where borings and superficial examination had led to the assumption of a good degree of regularity of the sub-soil, it was necessary, in view of

the dynamic demands to be made upon it, to predict the subsidences that might be expected at the various foundation sites, as uneven subsidence of the separate foundation elements might have extremely bad effects. The foundation plan of the projected building and the points where the machine was placed are shown in Fig. 9. At these points the applied energy curves, the amplitude curves and the subsidence were measured. The figures for $\alpha$ fluctuated between 21.7 and 24 Hz, the subsidences between 7 and 3 mm. The examinations were carried out with a standard apparatus of 1 m² base area, 2700 kg weight and equal eccentricity. The subsidences cover all dynamic loading applied during a certain period. Tests for compactness carried out in the laboratory with undisturbed soil specimens confirmed the irregularities revealed by the $\alpha$ figures and the subsidences. On the basis of the data so obtained, and taking into consideration the size of the ground area of the foundations, admissible loading was calculated

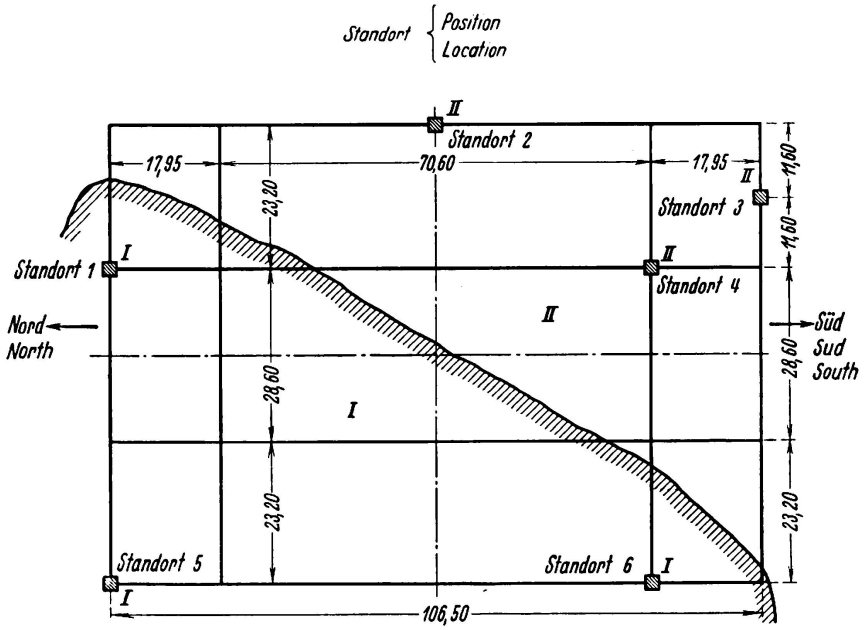


Fig. 9.

Layout for a dynamic soil test. Positions of agitator on the site plan of proposed building. The shaded line indicates the boundary between good and bad ground.

for each pier to give the same amount of subsidence for all. The admissible pressures for the one groups of foundations was 2 kg/cm², for the other 2.5 kg/cm². For sites of smaller foundation area it is sufficient to determine the $\alpha$ figures and the subsidences, making allowance for damping; these factors will give adequate information as to the regularity of the sub-soil. Investigation of undisturbed soil specimens in the laboratory is necessary for the pre-calculation of subsidence in the case of cohesive soil, and even with non-cohesive soit it is desirable.

When constructing the foundations of turbines at the present time it is the custom to calculate the natural frequency of the machines on their elastic foundations of two-dimensional frame constructions, it being understood that

the whole of the body, through its foundation slab, rests on solid ground. In this case it is assumed that the elastic yield of the ground can be disregarded in relation to the deformations of the frame foundation. This assumption, however, is not always fulfilled. Thus, if under certain circumstances the elastic yield of the ground has to be considered when calculating frequency even for turbines, in the case of block foundations it is quite impossible to proceed without a

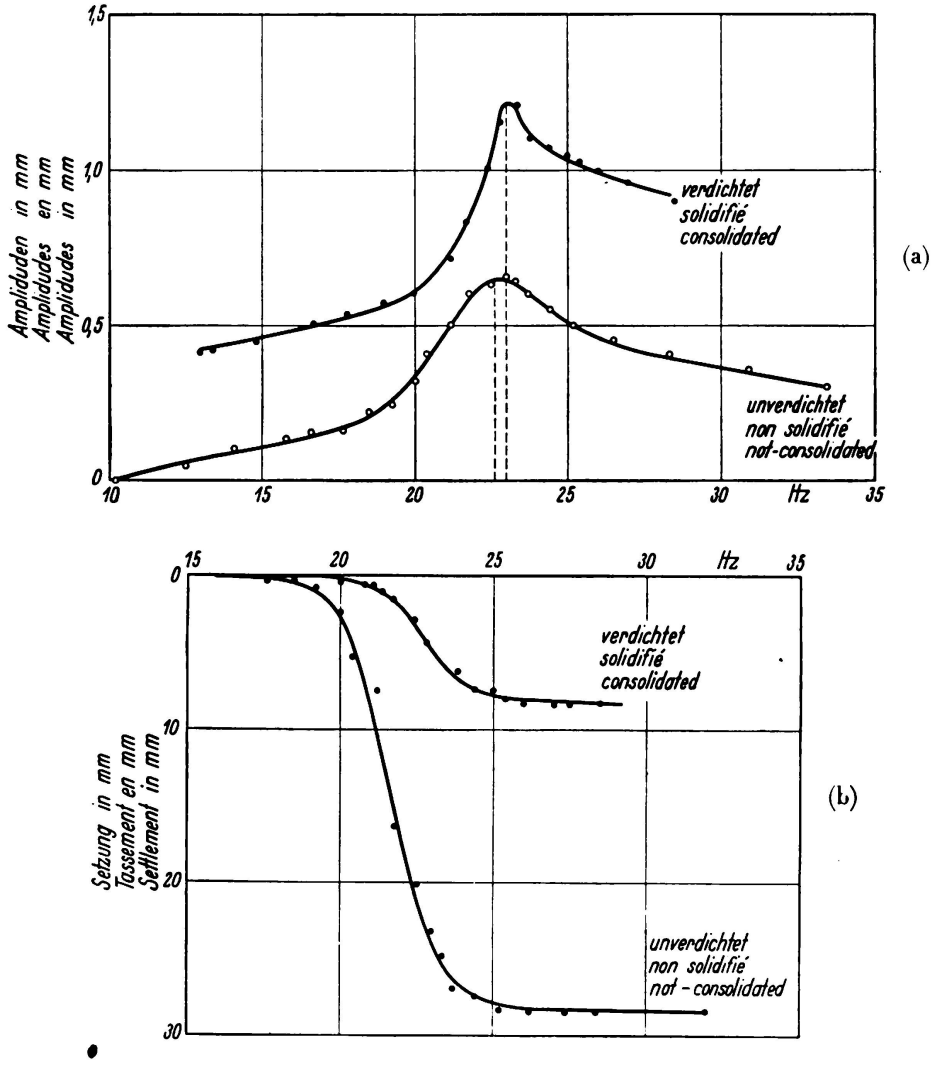


Fig. 10.

a) Amplitudes and
b) Subsidence of agitator in dependence on the frequency before and after consolidation.

knowledge of this yield. Here the machine and the foundation block together form a rigid body supported by an elastic base on the ground. The natural frequencies of the six degrees of freedom of the rigid body depend upon the distribution of its mass and the elastic constants of the ground. The $\alpha$ values, oscillating mass of ground and also elastic constants have been determined several times for such foundations by means of the above process. In view of the symmetry mostly possessed by the body, the problem can be treated as a two-dimensional one, so that only an elastically supported plate with two or

three degrees of freedom — according to its other symmetrical properties — need be calculated (35).

Practical cases treated till now have given extremely good coincidence between precalculation and the natural frequencies subsequently measured. The latter are also obtained with the aid of an oscillator and by recording the resonance curves in the manner explained. If the instruments available are delicate enough, it is possible to record the resonance curves of the amplitudes even for machines and foundations of several thousand tons' weight with an oscillator of 2000 kg centrifugal force.

The effect of artifical compacting can be tested by subsequently measuring only the $\alpha$ values and the subsidences. Fig. 10a—b illustrates amplitude curves and subsidence curves, as recorded for an artificially compacted dam before and after compacting. Compacting increased the $\alpha$ figure from 22.6 to 23.0 (Fig. 10a), i. e. but very slightly, whereas subsidence dropped from 28 mm to 8 mm (Fig. 10b). The subsidence curves show the course already mentioned. Subsidence takes place mainly within the resonance zone. The amplitude curve of the uncompacted soil greatly differs from that of the compacted soil. The resonance peak in compacted soil becomes much more pointed, a sign that internal damping has decreased. In the loosely arranged soil a greater portion of energy is consumed during oscillation than in the soil that has become more dense and elastic.

### 2) Determining the speeds.

If it is a question of examining the building site on a large tract of land, the various properties can be successfully determined by speed measurements, the propagation speeds being obtained at various places in various directions along straight lines (Fig. 7). If the ground is perfectly uniform and uncompacted, the same speed will be ascertained from every point and in every direction. If, however, the ground is irregular, there will be kinks in the rate curves (Fig. 6b). In Fig. 7 is shown a site plan drawn up for the various kinds of ground on the basis of these measurements. It has already been mentioned that the kink in a rate curve also occurs for ground composed of different soil layers. It can be decided which of the two cases is the one in question by comparing the measurements taken at the various points shown in Fig. 7.

The method of determining propagation speeds can also be successfully applied in practice for the solution of various other problems. The compacting of earth dams for roads and barrages, for instance, is an important question at the present time. One case is that of two railway dams built about twelve years ago of sand from the Mark district of Germany; one of these was subjected only to atmospheric influences during this period of twelve years, since no traffic passed over it, the other being under regular railway traffic the whole time. Propagation speed measurements at the borrowing pit and on each of the dams gave very informative differences. The dam not used for traffic gave a figure of 180 m/sec, well below that of the propagation speed of the natural ground, viz. 230 m/sec at the borrowing pit. Consolidation raised the propagation speed of the dam under traffic to 340 m/sec. Unfortunately, the speed for the new-built dam is not known. On the basis of other measurements, however, it can be

estimated at its most unfavourable figure as one-half the speed of the natural ground. The preceding results show that when an earth dam is allowed to lie idle, its consolidation is but very slowly influenced by atmospheric action, and that the latter can never cause the same degree of density as is produced by vibration.

Speed measurements have also proved reliable for testing the effects of the various artificial methods of attaining consolidation in dams, e. g. washing, rolling, tamping, vibrating, etc. The periodical "Die Straße" (Nr. 18, 1935) published a report on tests of this nature.

The examination of built-up earthen road dams and of roads as such also comes within the range of the speed measuring process. In general it will be found that the effect of a concrete road slab, for instance, on a dam consists in an increase of average propagation speed from the slab and the sub-grading. Only in one single case was it found that, slab and sub-grading oscillated as a uniform body. The construction in question was a gravel dam with an extremely

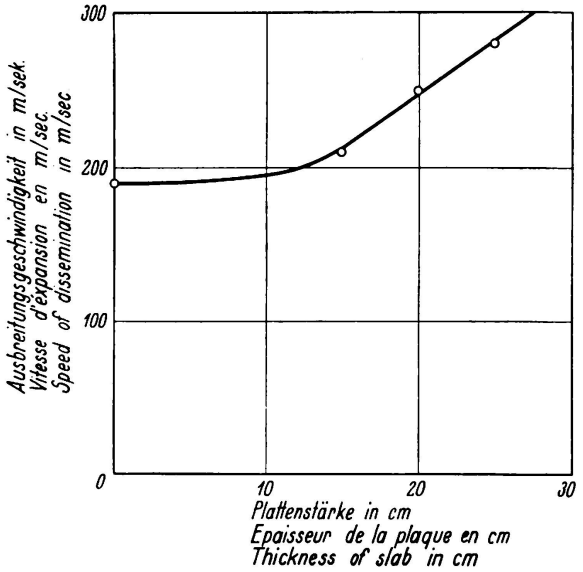


Fig. 11.
Rate of propagation of elastic waves in a road dam carrying concrete road slabs, in dependence on the thickness of the slabs.

favourable grain distribution, arranged in layers of about 30 cm and compacted by rolling and tamping. At the gravel pit from which the material was taken the elastic waves in the gravel had a propagation speed of 420 m/sec; in the dam itself, treated as described, a propagation speed of 560 m/sec was recorded. After a concrete surfacing of 25 cm thickness had been applied, an examination of the whole dam with a wave-length of 22 m revealed no alteration of propagation speed. At other places the speed of the waves in built-up ground was 125 m/sec; in the dam with a surface of 25 cm the propagation speed was 270 m/sec. From these observations it must be concluded that in the first case the dam and its concrete surfacing oscillated as a uniform whole, while in the second instance the concrete, resting on a more or less elastic base, undergoes vibrations due to bending. Finally, measurements were also taken to test the influence of the thickness of the surfacing for the same base. Fig. 11 illustrates the increase in propagation speed for increasing thickness of the surfacing, the base remaining the same. If sufficient experience and measurement results were available, it would most likely be possible to ascertain the minimum thickness

required for a given speed in the dam alone. Of course the substructure of the dam also affects the total result; for the sake of simplicity this influence was not taken into consideration in the above.

### 3) The examination of stratified soil.

If it is desired to employ in a reliable manner the interferences occuring in soils composed of layers for the calculation of the thickness of these layers, it has hitherto been necessary to make various and rather arbitrary assumptions concerning the setting up of these interferences. In a few cases one or the other theory leads to correct results. In other cases, especially when there are more than two layers, the results of calculation are still very uncertain. In this connection further progress can only be made when more light has been thrown on the question of the various kinds of waves produced. The necessary investigation work has now been taken in hand, and its results and their practical applications will be reported on in due course.

## Conclusion.

After six years of research work, including numerous theoretical and practical tests, we have come to the conclusion that the dynamic examination of soil is a valuable process. Of course this process alone cannot reveal all the properties of the ground. As has been stated in the preceding, cohesive soils in particular require the application of other well-known methods, such as those elaborated by *Terzaghi* (20, 40) and his disciples, for determining the influence of time on cohesive soils.[2]

The measurements hitherto made of amplitude and output curves, etc., and the greatly simplified theory of the oscillating concentrated mass with one degree of freedom, have enabled satisfactory coincidence to be attained and the significance of many phenomena to be interpreted. The work by *Erich Reissner* (36) on the stationary, axial-symmetrical oscillation, caused by a vibrating mass, of a homogeneously elastic half-space, particularly in relation to dynamic soil tests', which will shortly appear in Issue 5 of the Veröffentlichungen der Deutschen Forschungsgesellschaft für Bodenmechanik (Publications of the German Research Institute for Soil Mechanics), has further proved the justification of the simplified theory.

## Reference Works.

[1] *Engesser:* Theorie des Baugrundes (Theory of Building Ground), Zentralbl. d. Bauverw. 1893, p. 306.

[2] *Kögler:* Über Baugrund-Probebelastungen (Test Loading of Building Ground). Bautechnik 1931, Issue 24.

[3] *Preß:* Baugrundbelastungsversuche. Bautechnik 1930, Nr. 42; 1931, N° 50; 1932, Nr. 30.

[4] *Görner:* Über den Einfluß der Flächengröße auf die Einsenkung von Gründungskörpern (The Influence of Surface Area on the Subsidence of Foundations). Zeitschr. f. Geologie und Bauwesen 1932, N° 2.

---

[2] At the present time dynamic soil tests are being carried out by the Seismos Society for Soil Testing, Hanover. This concern possesses both instruments and experience in having carried out many soil tests for mineral deposits on the Mintrop process, and the material may also be used for dynamic soil tests.

[5] *Aichhorn:* Über die Zusammendrückung des Bodens infolge örtlicher Belastung (Compression of the Soil due to Local Loading). Geologie und Bauwesen 1932, N° 1.

[6] *Kögler* and *Scheiding:* Druckverteilung im Baugrunde (Distribution of Pressure in Building Ground). Bautechnik 1928, Nr. 15, 17; Bautechnik 1929, N° 18, 52.

[7] *Lord Rayleigh:* The Theory of Sound. London 1894/6.

[8] *H. Lamb:* Phil. Trans. (A) Vol. 203, 1904. Proc. Roy. Soc. A 93, London 1917.

[9] *E. Pfeiffer:* Handbuch der Physik IV, Chap. 4, Elastokinetik.

[10] *G. Abgenheister:* Handbuch der Physik IV, Chap. 8, Seismik.

[11] *H. Martin:* Handbuch der Experimentalphysik XVII, 1, Schwingungslehre (Theory of Oscillation).

[12] *A. E. H. Love:* Probl. of Geodynamics. Cambridge 1911.

[13] *O. Fröhlich:* Druckverteilung im Baugrund (Distribution of Pressure in Building Ground). Jul. Springer, Vienna 1934.

[14] Veröffentlichung der Deutschen Forschungsgesellschaft für Bodenmechanik (Publication of the German Research Institute for Soil Mechanics), Issue 1. Jul. Springer, 1933.

[15] Veröffentlichung der Deutschen Forschungsgesellschaft für Bodenmechanik, Issue 4. Julius Springer, 1936.

[16] *A. Hertwig:* Die dynamische Bodenuntersuchung (The Dynamic Testing of Soil). Bauingenieur, 12, 1931.

[17] *A. Hertwig:* Baugrundforschung (Building Site Research). Zeitschr. d. V. D. I. 77, 1933.

[18] *A. Hertwig* and *H. Lorenz:* Das dynamische Bodenuntersuchungsverfahren (The Dynamic Process of Soil Investigation). Bauingenieur 16, 1935.

[19] *H. Lorenz:* Neue Ergebnisse der dynamischen Baugrunduntersuchung (New Results of Dynamic Investigations of Building Sites). Zeitschr. d. V. D. I. 78, 1934.

[20] *W. Loos:* Praktische Anwendung der Baugrunduntersuchungen (Practical Application of Building Ground Investigations). Jul. Springer, 1935.

[21] *P. Müller:* Druckverteilung und Einsenkungen im Erdreich (Distribution of Pressure and Subsidences in Soil). Bautechnik 12, 1934.

[22] *P. Müller:* Tragfähigkeit und Formänderungswiderstand des Bodens (Carrying Capacity and Resistance to Deformation of Soil), Bautechnik 13, 1935.

[23] *R. Köhler:* Zeitschr. f. Geophysik 10, 1934.
[24] *R. Köhler:* Nachr. Geo. Wiss. II Göttingen 1934, Nr. 2.
[25] *R. Köhler:* Zeitschr. techn. Phys. 16, 1935.
[26] *R. Köhler* and *A. Ramspeck:* Zeitschr. techn. Phys. 14, 1933.
[27] *A. Ramspeck:* Zeitschr. Geophys. 10, 1934.
[28] *G. A. Schulze:* Zeitschr. Geophys. 11, 1935.
} Seism. Publ., Geophys. Inst., Göttingen University.

[29] *A. Ramspeck:* Dynamische Bodenuntersuchungen an der Reichsautobahn Stuttgart—Ulm (Dynamic Soil Examinations on the Stuttgart—Ulm State Motor Road). Die Straße 18, 1935.

[30] *A. Ramspeck:* Dynamische Untersuchung von Straßendecken (Dynamic Investigation of Road Decking). Die Betonstraße 11, 1936, Nr. 2.

[31] *R. Müller* and *A. Ramspeck:* Verdichtung geschütteter Dämme (Consolidation of Built-up Dams). Die Straße 18, 1935.

[32] *F. Meister:* Die dynamischen Eigenschaften von Straßen (The Dynamic Properties of Roads). Diss. Stuttgart, publ. M. Boerner, Halle, 1935.

[33] *K. Schwien:* Über die Ausbreitung von Erschütterungen (The Diffusion of Shock Effects). Diss. Hannover 1932.

[34] *Hort, Martin, Geiger:* Zur Frage der Schutzwirkung eines Grabens gegen Erschütterungen (The Protective Action of a Ditch against Shock Effects). Schalltechnik 2, 1932.

[35] *R. Rausch:* Berechnung von Maschinenfundamenten als elastisch gestützte schwingende Scheiben (Calculation of Machinery Foundations as Elastically Supported, Oscillating Plates). Bauingenieur 11, 1930, Issue 13—14, Z. d. V. D. I. 75, 1931.

[36] *E. Reißner:* Über die stationäre, achsialsymmetrische, durch eine schüttelnde Masse erregte Schwingung eines homogenen elastischen Halbraumes, insbesondere in Beziehung zu dynamischen Bodenuntersuchungen. Dissertation, Charlottenburg. (To be published shortly).

[37] *L. Mintrop:* Über die Ausbreitung der von den Massendrucken einer Großgasmaschine erzeugten Bodenschwingungen (The Diffusion of Soil Vibrations caused by the Mass Action of Big Gas Engines. Dissertation, Göttingen 1911.

[38] *A. Heinrich:* Über die Ausbreitung von Bodenschwingungen in Abhängigkeit von der Beschaffenheit des Untergrundes (The Diffusion of Soil Vibrations in Dependence on the Structure of the Sub-soil). Dissertation, Breslau 1930.

[39] *G. Bornitz:* Über die Ausbreitung der von Großkolbenmaschinen erzeugten Bodenschwingungen in die Tiefe (The Downward Diffusion of Soil Vibrations caused by Largepistoned Engines). Jul. Springer, Berlin 1931.

[40] *v. Terzaghi:* Erdbaumechanik (Soil Mechanics). Leipzig 1935.

## Tables.

| No. | Kind of Soil | Diffusion speed | Natural frequency $a$ | Adm. compression of soil kg/cm² |
|---|---|---|---|---|
| 1 | 3 m moor on sand | 80 m/sec | 4.0 Hz. | — |
| 2 | Powder sand | 110 „ | 19.3 „ | 1.0 |
| 3 | Tertiary period clay, moist | 130 „ | 21.8 „ | — |
| 4 | Loamy sand, fine-grained | 140 „ | 20.7 „ | — |
| 5 | Moist medium-coarse sand | 140 „ | 21.8 „ | 2.0 |
| 6 | Jurassic clay, moist | 150 „ | — | — |
| 7 | Old deposit of sand and cinders | 160 „ | — | — |
| 8 | Medium-coarse sand and sub-soil water | 160 „ | — | 2.0 |
| 9 | Medium-coarse sand, dry | 160 „ | 22.0 „ | 2.0 |
| 10 | Loamy sand on marl shingle | 170 „ | 22.6 „ | 2.5 |
| 11 | Gravel with larger stones | 180 „ | 23.5 „ | 2.5 |
| 12 | Loam, moist | 190 „ | 23.5 „ | — |
| 13 | Marl shingle | 190 „ | 23.8 „ | 3.0 |
| 14 | Fine sand with 30% medium-coarse sand | 190 „ | 24.2 „ | 3.0 |
| 15 | Loam, dry, with limestone pieces | 200 „ | 25.3 „ | — |
| 16 | Medium-coarse sand, undisturbed | 220 „ | — | 4.0 |
| 17 | Marl | 220 „ | 25.7 „ | 4.0 |
| 18 | Diluvian loess, dry | 260 „ | — | — |
| 19 | Gravel below 4 m sand | 330 „ | — | 4.5 |
| 20 | Coarse shingle, compact | 420 „ | 30.0 „ | 4.5 |
| 21 | Variegated sandstone (deteriorated) | 500 „ | 32.0 „ | ²/₃ adm. compressive stress |
| 22 | Medium-hard keuper sandstone | 650 „ | — | |
| 23 | Variegated sandstone (non-deteriorated) | 1100 „ | — | |

## Summary.

The dynamic testing of subsoils has been developed in two directions. In the first instance a certain spring constant is determined; whose value increases in different soils in about the same way as the permissible soil pressure found by experience. A second procedure is based on the rate of propagation of forced elastic waves, which can be used as a scale for the bearing capacity of the soil. The measurements allow at the same time to determine the subsidence as function of the agitator frequency which allows the prediction of subsidence in case of static and dynamic loading. The dynamic procedures in use have still the disadvantage of pure static trial loading.

# VIII 4

## Limits of Equilibrium of Earths and Loose Materials.

## Grenzzustände des Gleichgewichtes in Erd- und Schüttmassen.

## Etats limites de l'équilibre dans les masses de terre et de dépôt.

Dr. M. Ritter,
Professor an der Eidg. Technischen Hochschule, Zürich.

In the following report we shall establish the conditions which must be fulfilled by the internal stresses of a noncohesive mass of earth or other loose material when the mass is at the so-called limit of equilibrium. We shall confine our observations to two-dimensional states of stress, on the fundamental assumption that the stresses constantly vary with the place under consideration. Applying the classic law of friction, we find the limit of equilibrium at any point through which a rupture surface passes, i. e. a surface in which the resultant stress q forms the frictional angle ρ with the surface normal.

As early as 1857 *Rankine* analysed the classic state of stressing, now called after him, in the interior of a laterally unlimited mass of earth of even surface, using the hypotheses mentioned. *Winkler, Mohr, Weyrauch, Lévi* and others subsequently elaborated this theory. *Boussinesq* and *Résal*[1] extended *Rankine*'s theory to other surface conditions and attempted to establish the state of stressing behind a retaining wall when the direction of earth pressure deviates from that demanded by *Rankine*'s theory. This problem, particularly in conjunction with *Coulomb*'s theory of earth pressure, eventually led to numerous discussions in technical publications. In 1893 *F. Kötter* published the general differential equation for the pressure in a curved rupture surface[2]. Although quite a number of engineers subsequently treated earth pressure problems under the assumption of curved friction surfaces, the relation has not, as far as we know, been practically applied. In 1924 H. Reissner[3] expressed his views on the problem of earth pressure in an extensive work and discussed the difficulties offered by the analysis of the general limit condition under consideration of the dead weight of the mass of earth. More recently *A. Caquot*[4] has worked out the theory as a whole and

---

[1] *J. Résal:* Poussée des terres (Earth Pressure), Vol. 2, Paris 1903.

[2] *H. Müller-Breslau:* Erddruck auf Stützmauern (Earth Pressure on Retaining Walls), Stuttgart 1906.

[3] *H. Reissner:* Zum Erddruckproblem (The Problem of Earth Pressure). Sitzungsberichte der Berliner Mathematischen Gesellschaft, 1924.

[4] *A. Caquot:* Equilibre des massifs à frottement interne (Equilibrium of solid bodies with internal friction), Paris 1934.

applied it in solving a number of practical problems. Apart from its importance in calculating retaining walls, its principal use lies in determining the carrying capacity of foundation strips at the limit of equilibrium — a problem to which *Rankine* had already tried to find a solution. Now that light has been thrown by *K. Terzaghi*[5] on the principle of cohesion for masses of earth or loose material, calculation can also be extended in certain cases to include cohesive soil as well. Thus, Caquot elaborates the formula for the carrying capacity of a foundation strip to cover soil with so-called apparent cohesion.

*1. Principles.*

On the assumption that the stresses in a mass of soil vary from point to point, the angle $\rho'$, formed by the stress $q'$ of any surface element forms with its normal, is a continuous function of the angle $\varphi$ of the surface element in respect to a fixed direction. The angle $\rho'$ attains its highest value $\rho$ in the rupture surfaces; thus the latter are defined by the fundamental relation

$$\frac{d\rho'}{d\varphi} = 0. \tag{1}$$

In conjunction with the conditions necessary for equilibrium, this relation suffices to determine both the relative position of the rupture surfaces in respect to the main stresses, and the main stress ratio that must be present in a limiting state of equilibrium.

If $\sigma_1$ and $\sigma_2$ denote the main stresses, the conditions necessary for equilibrium in an infinitely small prism of earth having a length = 1 (see Fig. 1), then

$$q \sin \rho' = (\sigma_1 - \sigma_2) \sin \varphi \cos \varphi$$
$$q \cos \rho' = \sigma_1 \cos^2 \varphi + \sigma \sin^2 \varphi,$$

hence

$$\operatorname{tg} \rho' = \frac{(\sigma_1 - \sigma_2) \operatorname{tg} \varphi}{\sigma_1 + \sigma_2 \operatorname{tg}^2 \varphi}. \tag{2}$$

Fig. 1.

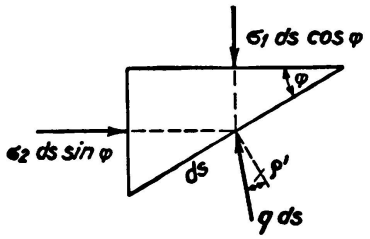


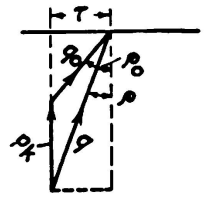


Fig. 2.

The maximum $\rho' = \rho$ is created in accordance with Eq. 1 for

$$\frac{d\rho'}{d\varphi} = \frac{d \operatorname{tg} \rho'}{d \operatorname{tg} \varphi} = \frac{(\sigma_1 - \sigma_2)(\sigma_1 - \sigma_2 \operatorname{tg}^2 \varphi)}{(\sigma_1 + \sigma_2 \operatorname{tg}^2 \varphi)^2} = 0; \tag{3}$$

which first of all gives

$$\sigma_1 = \sigma_2 \operatorname{tg}^2 \varphi \tag{3a}$$

and Eq. 2 yields for the rupture surfaces

$$\operatorname{tg} \rho = -\operatorname{cotg} 2\varphi.$$

[5] *K. Terzaghi:* Erdbaumechanik (Soil Mechanics), Vienna 1925.

Thus we have $\varphi = 45^\circ + \frac{\sigma}{2}$ ; the rupture surfaces form with the surface on which $\sigma_1$ acts, the angles $\pm (45^\circ + \frac{\sigma}{2})$, which means that they intersect below the angle $90^\circ - \rho$.

The ratio (3a) is therefore transformed into

$$\sigma_2 = \sigma_1 \operatorname{tg}^2 \left(45^0 - \frac{\rho}{2}\right); \tag{4}$$

this relation between the two main tensions must be present at every point belonging to a friction surface, i. e. to every point at the limit of equilibrium. The pressure q at the friction surface can readily be expressed in terms of $\sigma_1$ or $\sigma_2$, and amounts to

$$q = \sigma_1 \operatorname{tg} \left(45^0 - \frac{\rho}{2}\right). \tag{5}$$

The relations we have established may easily be extended to *cohesive soil*, on the assumption that apparent cohesion, as so designated by *Terzaghi*, is present. This is created by the pressure of capillary water, which compacts the material and subjects it to a state of spatial stressing having the universal compressive stresses $p_k$ which exceed the other stresses. The angle of friction $\rho$ remains as long as the state of stressing is considered to include the compressive stresses $p_k$. The law of friction now becomes

$$\tau = (\sigma + p_k) \operatorname{tg} \rho = p_k \operatorname{tg} \rho + \sigma \operatorname{tg} \rho. \tag{6}$$

Even Coulomb had calculated in principle with this law, introducing a coefficient of cohesion and writing the law of friction as $\tau = c + \sigma \operatorname{tg} \rho$.

As the compressive stresses $p_k$ are self-stresses and maintain equilibrium in some part of the mass of soil, it is necessary, when the stresses $\sigma_1$, $\sigma_2$ and q are brought into relation with external forces, to exclude the stresses $p_k$. Eq. 4 therefore becomes the following for cohesive materials:

$$\sigma_2 + p_k = (\sigma_1 + p_k) \operatorname{tg}^2 \left(45^0 - \frac{\rho}{2}\right),$$

hence

$$\sigma_2 = \sigma_1 \operatorname{tg}^2 \left(45^0 - \frac{\rho}{2}\right) - p_k \left[1 - \operatorname{tg}^2 \left(45^0 - \frac{\rho}{2}\right)\right]. \tag{7}$$

After deduction of the normal stressing $p_k$, the compression q at the rupture surface becomes (Fig. 2)

$$q_0 = q \frac{\sin \rho}{\sin \rho_0}, \quad \text{where} \quad \operatorname{tg} \rho_0 = \frac{\operatorname{tg} \rho}{1 - \frac{p_k}{q \cos \rho}}. \tag{8}$$

At the rupture surface there thus arises an apparent (greater) angle of friction $\rho_0$, while the angle $45^\circ + \frac{\sigma}{2}$ between rupture surface and main stressing is maintained.

The easiest way of assessing the practically possible values of $p_k$ is by considering the vertical walls of excavations, which, as is well known, often hold without shoring to a considerable height h. At the surface of such a wall $\sigma_1 = \gamma h$ and $\sigma_2 = 0$, hence according to Eq. 7 the material must be subject to a capillary compressive stress of

$$p_k = \gamma h \frac{1}{\operatorname{tg}^2\left(45^0 + \frac{\rho}{2}\right) - 1} \tag{9}$$

Compressive stresses $p_k$ of from 0.3 to 0.5 kg/cm$^2$ are frequently to be observed in gravel sand containing clay.

*2. Compressive stresses at the rupture surface.*

We shall now proceed to establish *F. Kotter*'s equation for compressive stressing at a curved rupture surface in a particularly simple form especially intended for engineers[1]. We shall consider an infinitely small prism of earth lying at a curved rupture surface AC at a distance s from the surface C (cf. Fig. 3). Let the prism have a length = 1 vertically to the plane of the figure, and let the one surface $1 - 2 = ds \cdot 1$ lie in the rupture surface, the other surface 2 — 3 being turned an angle of $d\varphi$. On the surface 1 — 2 acts the compressive stress q ds at the angle of friction $\rho$, on surface 2 — 3 the compressive stress q' ds, also at the angle of friction $\rho$ (cf. Eq. 1). The condition necessary for equilibrium as regards turning around the axis o in the surface 1 — 3 is

$$q\,ds \cdot \frac{ds}{2}\cos(\rho - d\varphi) = q'\,ds \cdot \frac{ds}{2}\cos(\rho + d\varphi);$$

from which we get

$$q' = q\frac{\cos(\rho - d\varphi)}{\cos(\rho + d\varphi)} = q\frac{\cos\rho\cos d\varphi + \sin\rho\sin d\varphi}{\cos\rho\cos d\varphi - \sin\rho\sin d\varphi}$$

or when $\cos d\varphi = 1$ and $\sin d\varphi = d\varphi$

$$q' = q(1 + 2\operatorname{tg}\rho \cdot d\varphi). \tag{10}$$

The dead weight of the earth prism creates an infinitely small moment of a higher order and therefore does not come under consideration. We now add to the surface 1 — 3 the congruent prism 1 — 3 — 4 having its 1 — 4 surface in the rupture surface. Now the compressive stress (q + dq) ds acts on the 1 — 4 surface at the angle of friction $\rho$, the compressive stress q'' ds on the surface 3 — 4 also — in accordance with Eq. 1 — at the angle of friction $\rho$. The prism 1 — 2 — 3 — 4 has a dead weight of $\gamma\,ds^2\,d\varphi \cdot 1$, wherein $\gamma$ denotes the specific weight of the earth. We can readily eliminate q'' by introducing the condition necessary for maintaining equilibrium against displacement in the direction of the axis a — a perpendicular to the stress q''. This condition is

$$(q + dq)\,ds\,d\varphi - q(1 + 2\operatorname{tg}\rho\,d\varphi)\,ds\,d\varphi = \gamma\sin(\varphi - \rho)\,ds^2\,d\varphi$$

[6] *M. Ritter:* The theory of earth pressure on retaining walls. Schweizerische Bauzeitung 1910. These elucidations were confined to non-cohesive material.

and yields *F. Kötter*'s differential equation

$$\frac{dq}{ds} - 2q \operatorname{tg}\rho \cdot \frac{d\varphi}{ds} = \gamma \sin(\varphi - \rho). \tag{11}$$

Integration gives us

$$q = \gamma e^{2\varphi \operatorname{tg}\varphi} \int_0^s e^{-2\varphi \operatorname{tg}\rho} \sin(\varphi - \rho)\, ds + q_a,$$

in which C denotes the compressive stress at the point C. If the rupture surface is plane, $d\varphi/ds$ disappears and we get

$$q = \gamma s \sin(\varphi - \rho) + q_a. \tag{12}$$

In the case of a cohesive material $q_o$ and $\rho_o$ can be calculated from q and $\rho$ with the aid of Eq. 8; here it should be noted that $\rho_o$ varies along the rupture surface as the relation $p_k/q$ changes. This fact makes the application of the equation more difficult.

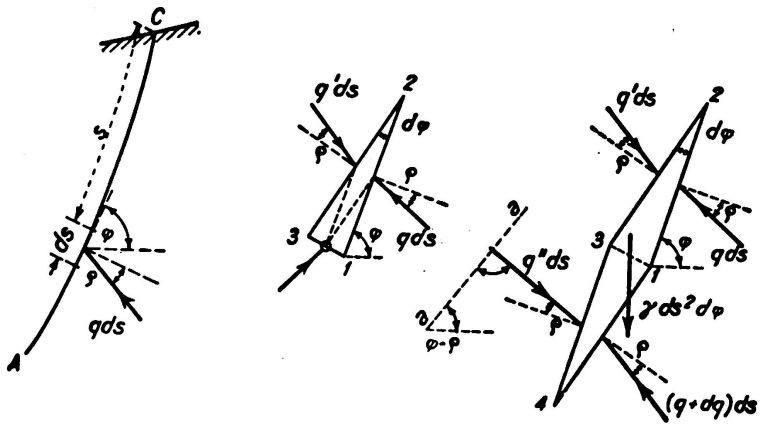


Fig. 3.

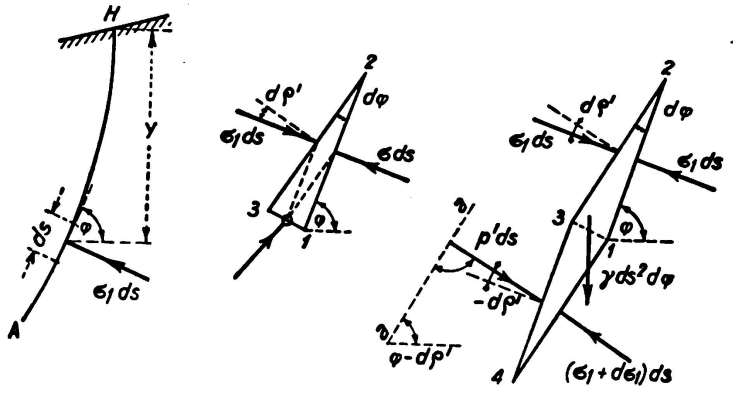


Fig. 4.

*2. The principal stresses.*

For the principal stressing $\sigma_1$ or $\sigma_2$ a relation can be established, in the same manner as for the compressive stress q at the rupture surface, permitting the ready calculation of $\sigma_1$ and $\sigma_2$ at any depth below the surface. A H in Fig. 4 is a principal stress surface whose tangents may take the direction of

the principal stress $\sigma_2$. Let us consider the infinitely small prism of earth 1 — 2 — 3, having a length = 1 and one surface of which, 1 — 2 = ds · 1, lies in the principal surface A H and forms the angle $d\varphi$ with the surface 2 — 3. On the surface 1 — 2 acts the principal stress $\sigma_1$, on the surface 2 — 3 the stress p, which is only distinguished from $\sigma_1$ by an infinitely small magnitude of the second order. The principal stresses, as is known, being maximum values, on the principal surface we have $d\sigma/d\varphi = 0$. It should be noted that p does not act normally to the surface 2 — 3, but at an angle $d\rho'$, which can easily be calculated. From Eq. 12, for a prism of earth with an angle $\varphi$ of any size, we get

$$\frac{d\rho'}{d\varphi} = \frac{(\sigma_1 - \sigma_2)(\sigma_1 - \sigma_2 \operatorname{tg}^2 \varphi)}{(\sigma_1 + \sigma_2 \operatorname{tg}^2 \varphi)^2};$$

by turning the surface ds. 1 in the principal plane, i. e. by making $\varphi = 0$, the following is obtained:

$$\left(\frac{d\rho'}{d\varphi}\right)_{\varphi=0} = 1 - \frac{\sigma_2}{\sigma_1} = 1 - \operatorname{tg}^2\left(45^0 - \frac{\rho}{2}\right). \tag{13}$$

To the surface 1 — 3 we now add the congruent prism 1 — 3 — 4, whose surface 1 — 4 lies in the principal surface A H and is subjected to the main stressing $\sigma_1 + d\sigma_1$, while the compressive stress $p'ds$ acts on the surface 3 — 4 at an angle of $-d\rho'$ (it is easy to realise that $d^2\rho'/d\varphi^2$ disappears when $\varphi = 0$). The dead weight of the prism 1 — 2 — 3 — 4 is $\gamma\, ds^2 d\varphi \cdot 1$. The condition necessary to prevent displacement in the direction of the axis a — a, inclined at an angle of $\varphi - d\rho'$ and perpendicular to p', is expressed:

$$(\sigma_1 + d\sigma_1)\, ds\, (d\varphi - d\rho') - \sigma_1\, ds\, d\rho' - \sigma_1\, ds\, (d\varphi - 2\, d\rho') = \gamma\, ds^2\, d\varphi \sin(\varphi - d\phi;)$$

from which is obtained:

$$\frac{d\sigma_1}{ds} = \frac{\gamma \sin\varphi}{1 - \frac{d\rho'}{d\varphi}} = \gamma \operatorname{tg}^2\left(45^0 + \frac{\rho}{2}\right) \sin\varphi. \tag{14}$$

The integration, beginning from the surface, yields

$$\sigma_1 = \gamma \operatorname{tg}^2\left(45^0 + \frac{\rho}{2}\right) \cdot \int_0^s \sin\varphi\, ds = \gamma \operatorname{tg}^2\left(45^0 + \frac{\rho}{2}\right) \cdot y + \sigma_{a1}, \tag{15}$$

in which $\sigma_{a1}$ denotes the main stressing $\sigma_1$ (caused by surcharge) at the surface. Eq. 15 implies that the main stress $\sigma_1$ set up at the depth y by the weight $\gamma$, corresponds to the compressive stress of a liquid of $\gamma \operatorname{tg}^2\left(45^0 + \frac{\rho}{2}\right)$ specific weight.

In corresponding manner it is possible to calculate the main stress $\sigma_2$. The condition necessary for equilibrium in the infinitely small prism of earth is in this case

$$\frac{d\sigma_2}{ds} = \frac{\gamma \sin\varphi}{1 + \frac{d\rho'}{d\varphi}};$$

in which we have to introduce

$$\left(\frac{d\rho'}{d\varphi}\right)_{\varphi=90^0} = \operatorname{tg}^2\left(45^0+\frac{\rho}{2}\right)-1$$

By integration we obtain

$$\sigma_2 = \gamma \operatorname{tg}^2\left(45^0-\frac{\rho}{2}\right)\cdot y + \sigma_{a2}, \tag{16}$$

$\sigma_{a2}$ representing the main stress $\sigma_2$ at the surface.

For cohesive soil Eq. 15 is written

$$\sigma_1 + p_k = \gamma \operatorname{tg}^2\left(45^0+\frac{\rho}{2}\right)\cdot y + (\sigma_{a1}+p_k).$$

Eq. 15 and also Eq. 16 thus remain in the sense that the compressive stresses $p_k$ vanish. The influence of cohesion is expressed in the alteration of $\sigma_{a1}$ in accordance with Eq. 7.

*4. Carrying capacity of the foundation strip.*

The relations developed in Pars. 2 and 3 permit the calculation of the greatest possible loading of a foundation strip, compatible with equilibrium. The loading in this case is that which, when rupture surfaces form, causes the soil to be laterally displaced and the foundation block to subside. Let us assume that the foundation lies at a depth h below the surface, that its width is 2b and its length such that the problem can be treated as a two-dimensional stress problem. Fig. 5 shows roughly the approximate character of the state of

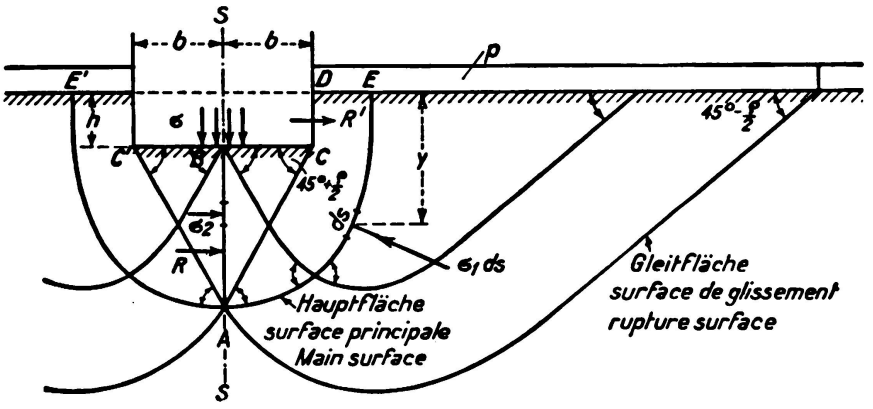


Fig. 5.

stressing at the limit of equilibrium. The specific compressive stress of the foundation we shall designate with $\sigma$, and we shall assume that outside the foundation there also acts a surface stress p.

For reasons of symmetry the plane s — s is a principal surface in the sense of Par. 3, so that in accordance with Eq. 16 the horizontal principal stress

$$\sigma_2 = \gamma \operatorname{tg}^2\left(45^0-\frac{\rho}{2}\right)\cdot y + \sigma \operatorname{tg}^2\left(45^0-\frac{\rho}{2}\right). \tag{17}$$

acts at the depth y. The rupture surfaces must form the angle $45^0 - \frac{\sigma}{2}$ with the principal surface s — s, and the angle $45^0 + \frac{\sigma}{2}$ with foundation slab.

Below the foundation, therefore, within the form C A C′, there prevails the classic Rankine state of stressing with plane rupture surfaces, and

$$z = b \operatorname{tg}\left(45^0 + \frac{\rho}{2}\right). \tag{18}$$

Outside the rupture surfaces A C and A C′ the system of stresses is more complicated; as seen in Fig. 5, curved rupture surfaces are created, a group of them cutting the free surface at an angle of $45^\circ - \frac{\rho}{2}$, since the surface on which p acts represents a principal surface. The principal surface of the stresses $\sigma_1$, which passes through A, cuts this group of rupture surfaces at an angle of $45^\circ + \frac{\rho}{2}$, thus forming in section with the plane of the figure the curve E A E′ which, for reasons of symmetry, possesses a horizontal tangent at A and cuts the free surface vertically at E and E′.

Although the form of the principal surface E A E′ is not quite definite, it is easy to calculate the principal stressing $\sigma_1$ from Eq. 15, for $\sigma_1$ does not depend on the form of the surface, but soleley on the depth y. According to Eq. 4, at the surface we get the relation

$$p = \sigma_{a1} \operatorname{tg}^2\left(45^0 - \frac{\rho}{2}\right),$$

from which it is necessary to withdraw $\sigma_{a1}$ and introduce it into Eq. 15. Accordingly, at the depth y

$$\sigma_1 = \gamma \operatorname{tg}^2\left(45^0 + \frac{\rho}{2}\right) \cdot y + p \operatorname{tg}^2\left(45^0 + \frac{\rho}{2}\right). \tag{19}$$

We analyse the compressive stress $\sigma_1 \, ds \cdot 1$ into its horizontal components $\sigma_1 \, ds \sin\varphi = \sigma_1 \, dy$ and its vertical components $\sigma_1 \, ds \cos\varphi$. The condition for equilibrium in the body of earth A B C D E necessary to prevent horizontal displacement then yields the foundation pressure $\sigma$ at the limit of equilibrium.

This condition is

$$R + R' = \int_0^{h+z} \sigma_1 \, dy. \tag{20}$$

The resultant R in the surface A B ensues from Eq. 17 by integration —

$$R = \frac{1}{2} \gamma z^2 \operatorname{tg}^2\left(45^0 - \frac{\rho}{2}\right) + \sigma z \operatorname{tg}^2\left(45^0 - \frac{\rho}{2}\right).$$

To obtain the resultant R′, however, Eq. 18 has to be used, giving us

$$R' = \frac{1}{2} \gamma h^2 \operatorname{tg}^2\left(45^0 + \frac{\rho}{2}\right) + p h \operatorname{tg}^2\left(45^0 + \frac{\rho}{2}\right).$$

The sum of the horizontal forces at the curved main surface A E is

$$\int_0^{h+z} \sigma_1 \, dy = \int_0^{h+z} \gamma \operatorname{tg}^2\left(45^0 + \frac{\rho}{2}\right) y \, dy + \int_0^{h+z} p \operatorname{tg}^2\left(45^0 + \frac{\rho}{2}\right) dy$$

$$= \frac{1}{2} \gamma (h+z)^2 \operatorname{tg}^2\left(45^0 + \frac{\rho}{2}\right) + p (h+z) \operatorname{tg}^2\left(45^0 + \frac{\rho}{2}\right).$$

If these expressions are introduced into Eq. 20 and z is expressed, in accordance with Eq. 18, in terms of b, we obtain the foundation pressure $\sigma$ at the limit of equilibrium, namely,

$$\sigma = \frac{1}{2}\gamma b\left[\mathrm{tg}^5\left(45^0+\frac{\rho}{2}\right)-\mathrm{tg}\left(45^0+\frac{\rho}{2}\right)\right]+(\gamma h+p)\,\mathrm{tg}^4\left(45^0+\frac{\rho}{2}\right). \quad (21)$$

The first summation represents the carrying capacity when the foundation is placed directly on a free surface. The second term, which expresses the influence of the depth of the foundation when the surface is subjected to loading, has already been deducted by Rankine himself and is to be found in most manuals. For soil with cohesive properties $\sigma' + p_k$ must be inserted in Eq. 21 instead of $\sigma$, and $p + p_k$ instead of p. This yields the increased foundation pressure $\sigma'$ at the limit of equilibrium

$$\sigma' = \sigma \mp p_k\left[\mathrm{tg}^4\left(45^0+\frac{\rho}{2}\right)-1\right]. \quad (22)$$

The employment of the principal surfaces in calculating the carrying capacity $\sigma$ and $\sigma'$ respectively offers the advantage that the form of the principal surfaces outside the zone A C C′ need not be exactly known. Besides which one can also try to use the rupture surface A F passing through A to determine the stressing. *A. Prandtl, H. Reissner* and *A. Caquot* (l. c.) for $h = 0$ and disregarding the weight $\gamma$, deduced that

$$\sigma = p\,\mathrm{tg}^2\left(45^0+\frac{\rho}{2}\right)\cdot e^{\pi\,\mathrm{tg}\,\rho} \quad (23)$$

which for cohesive soil (by writing $\sigma' + p_k$ instead of $\sigma$ and $p + p_k$ instead of p) becomes

$$\sigma' = \sigma + p_k\left[\mathrm{tg}^2\left(45^0+\frac{\rho}{2}\right)e^{\pi\,\mathrm{tg}\,\rho}-1\right]. \quad (24)$$

These relations were arrived at by taking as a basis the state of stressing sketched in Fig. 6, for which the condition of a continuous form of the stresses is fulfilled. In the regions A C C′ and C F G Rankine's states of stressing, with plane surfaces, are assumed, while in the zone A C F continuous transition is obtained by using the *Résal* state of stressing, in which one set of rupture lines is represented by a group of rays, and the other (which crosses it at an angle of $90^\circ - \rho$), by logarithmic spirals. It is then easy to recognise that the compressive stresses, at the rupture surface A G pass through the point C, and that the angle A C G is a right angle. The moment equation for the point C of the earth body A B C J G then gives us directly the relations 23 and 24. However, the author finds this basis of calculation, which leads to very much higher limit loads than Eq. 21, extremely unsure. For, firstly, it is by no means proved that the state of stressing shown in Fig. 6 (in itself possible and not contradictory) correspond to the minimum values of $\sigma$ and $\sigma'$ respectively. Furthermore, it is not possible to extend the calculation in order to take the dead weight $\gamma$ of the soil into account, since the equilibrium of forces at the element C M N is upset if the compressive stresses at the surfaces C M and C N are determined according to Eq. 12 and the dead weight is taken into account in the calculation.

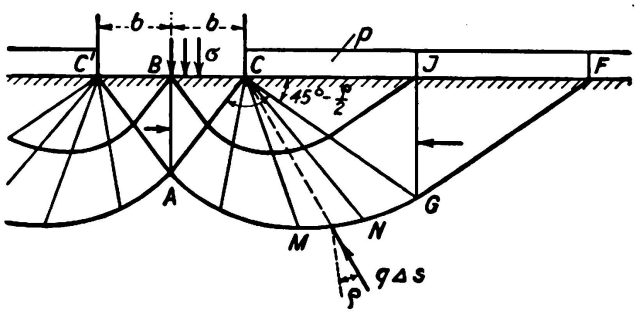


Fig. 6.

*5. Earth pressure on retaining walls.*

The general relations given in sections 2 and 3, permit the calculation of the earth pressure E acting at any angle, i. e. at the angle of incidence $\rho'$ ($\rho' < \rho$) as given by Coulomb, on the face A B of a retaining wall (cf. Fig. 7). The

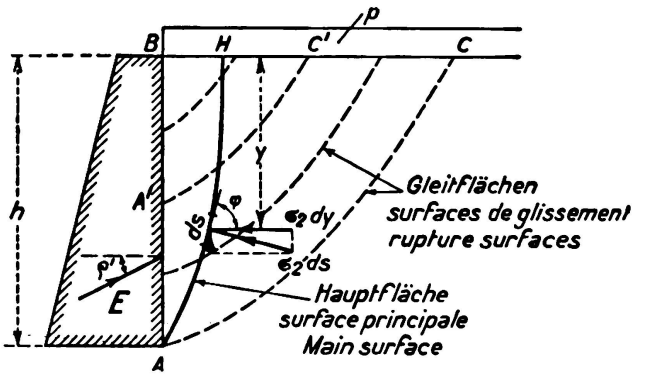


Fig. 7.

hypothesis of plane rupture surfaces, for an arbitrary arrangement, of the direction of E, leads of course to contradictions in the equilibrium of forces in the slipping earth prism, for which reason *H. Müller-Breslau, H. Reissner* (l. c.) and others found it necessary to calculate with curved rupture surfaces. The main problem — the ascertaining of the form of the rupture surfaces requiring the greatest earth pressure E to ensure equilibrium — has not been solved up to the present time.

In the following we shall confine our attention to horizontal ground and vertical retaining wall. The rupture surfaces A C, A′ C′, of unknown shape, are cut at an angle of $(45^\circ - \frac{\rho}{2})$ by the main surface A H, which is acted upon by the main stresses $\sigma_2$, calculable from Eq. 16. Thus at a depth of y we have

$$\sigma_2 = \gamma \operatorname{tg}^2\left(45^0 - \frac{\rho}{2}\right) \cdot y + p \operatorname{tg}^2\left(45^0 - \frac{\rho}{2}\right),$$

in which p is an evenly distributed surcharge. We analyse $\sigma_2$ ds into its horizontal component $\sigma_2 \, ds \sin\varphi = \sigma_2 \, dy$ and its vertical component $\sigma_2 \, ds \cos\varphi$. The equilibrium of forces against displacement of the earth body A B H in a horizontal direction gives us

$$E \cos\rho' = \int_A^H \sigma_2 \, dy = \gamma \operatorname{tg}^2\left(45^0 - \frac{\rho}{2}\right) \cdot \int_0^h y \, dy + p \operatorname{tg}^2\left(45^0 - \frac{\rho}{2}\right) \cdot \int_0^h dy,$$

whence
$$E = \left(\frac{1}{2}\gamma h^2 + p\,h\right)\frac{tg^2\left(45^0 - \frac{\rho}{2}\right)}{\cos\rho'}. \tag{25}$$

With this formula, which is based on the curved form of rupture surfaces, we can obtain perceptibly higher earth pressures than with Coulomb's earth pressure formula, which assumes plane rupture surfaces.

If the question is one of cohesive soil, $p + p_k$ should be written in Eq. 25 instead of p, and $p_k\,h$ introduced for $E' \cos\rho'$. From this is obtained

$$E' = E - p_k\,h\,\frac{1 - tg^2\left(45^0 - \frac{\rho}{2}\right)}{\cos\rho'} \tag{26}$$

The relations 25 and 26 are based on the assumption that the limit of equilibrium has been reached in all points of earth body A B C. Whether this state creates the greatest earth pressure, or whether the case in which only one rupture surface is formed is more unfavourable, cannot be determined by the author.

## Summary.

For the limit of equilibrium in which every point of the earth body belongs to a (curved) rupture surface, the differential equations for compressive stress at the rupture surface and at the main surface (main stresses) are deduced and integrated. These equations, established for non-cohesive and cohesive soil, are applied in the calculation of the carrying capacity of a strip of foundation, and in the establishment of the earth pressure on a retaining wall, assuming curved rupture surfaces.

Leere Seite
Blank page
Page vide